ASSESSING THE COMPONENTS OF THE eIF3 COMPLEX AND THEIR PHOSPHORYLATION STATUS

By

Adam Richard Farley

Dissertation

Submitted to the Faculty of the

Graduate School of Vanderbilt University

in partial fulfillment of the requirements

for the degree of

DOCTOR OF PHILOSOPHY

in

Biochemistry

December, 2011

Nashville, Tennessee

Approved:

Professor Andrew J. Link

Professor Richard M. Caprioli

Professor David K. Cortez

Professor Bruce D. Carter

Professor Katherine L. Friedman

ACKNOWLEDGEMENTS

I would like to think my mentor and teacher, Dr. Andrew Link, for his guidance and support during this dissertation work. Dr. Link has provided valuable insight into the world of science and what is necessary to solve difficult problems. The experience I have gained through work at the bench, producing scientific communications, and teaching others mass spectrometry has proven to be both exciting and rewarding. I am sure my graduate experiences in Dr. Link's laboratory will continue to shape my scientific future.

I also want to thank Dr. Elizabeth Link for her continual commitment to editing and reviewing publications that I was lucky enough to take part in. The help of previous lab members, Dr. David Powell, Dr. Vince Gerbasi, Dr. Morgan Sammons, as well as Jennifer Jennings, Connie Weaver, Dexter Duncan, and Jill McAfee was wonderful. I wish the best of luck and give thanks to Chris Browne and Parimal Samir for taking up the role of graduate student after me. I must also show my appreciation to all the students of the Proteomics courses at Cold Spring Harbor Laboratory. Their questions pushed me to gain a deeper understanding of the science that I have been involved in than I would have otherwise considered.

The professors whose classrooms I have been a part of while at Vanderbilt deserve much credit for pushing me to explore and ask hard questions about science. They have truly made my graduate career in the classroom a very enjoyable experience. I hope to pass on what I have learned to future generations of scientists. I want to thank the biochemistry department and its faculty and staff for guidance and instruction during my time here.

I want to issue a heart felt thank you to all my family and friends for their support during my graduate career. Even though your questions about what I was doing or when it would be finished may have been taxing, your support was greatly needed and appreciated. Finally, I would like to thank my wife, Leah, and our three young daughters, Gemma, Lillian, and Isabella. I hope one day to inspire them as much as they have me.

TABLE OF CONTENTS

LIST OF TABLES

Table **Page**

LIST OF FIGURES

Figure **Page**

ABBREVIATIONS

(E)-3-(2,3,4,5-Tetrabromophenyl)acrylic acid (TBCA)
3-[(2,4,6-Trimethoxyphenyl)methylidenyl]-indolin-2-one (IC261)
5,6-Dichloro-1-b-D-ribofuranosylbenzimidazole (DRB)
casein kinase 2 complex (CK2)
casein kinase I inhibitor (D4476)
casein kinase II inhibitor (DMAT)
casein kinase II inhibitor 1 (TBB)
collision induced dissociation (CID)
cross correlation score (Cn)
doubling time (t_{dub})
eIF4e binding protein (4E-BP)
electron capture dissociation (ECD)
electron transfer dissociation (ETD)
electrospray ionization (ESI)
epidermal growth factor (EGF)
eukaryotic initiation factor (eIF)
fused silica capillary (FSC)
high pressure liquid chromatography (HPLC)
higher energy c-trap dissociation (HCD)
immobilized metal affinity chromatography (IMAC)
isotope coded protein labeling (ICPL)
isotope tags for relative or absolute quantification (iTRAQ)
liquid chromatography (LC)
mass spectrometry (MS)
matrix assisted laser desorption ionization (MALDI)
messenger RNA (mRNA)
molecular weight (MW)
multidimensional peptide identification technology (MudPIT)
multifactor complex (MFC)
multistage activation (MSA)
not detected (nd)
O-linked β-N-acetylglucosamine (O-GlcNAc)
posttranslational modification (PTM)
protein abundance factor (PAF)
pulsed Q dissociation (PQD)
quadrupole-TOF (Q-TOF)
reverse phase (RP)
ribosomal RNA (rRNA)
RNA recognition motif (RRM)
strong annion exchange (SAX)
strong cation exchange (SCX)
sulfometuron methyl (SM)
tandem affinity purification (TAP)

tandem mass spectrometry (MS/MS)
tandem mass tags (TMT)
TAP negative control (TAP-cntrl)
thin layer chromatography (TLC)
time of flight (TOF)
transfer RNA (tRNA)
two-dimensional gel electrophoresis (2D-GE)

CHAPTER I

INTRODUCTION

This dissertation investigates the identity of proteins that interact with the eukaryotic translation initiation factor eIF3 and the posttranslational modifications that regulate eIF3's activity or function. Of the three process involved in translation, initiation of protein synthesis is the most complex and actively studied since research has found this process to be aberrant in human cellular development disorders, diseases, and cancer (Van Der Kelen et. al., 2009; Jackson et. al., 2010). A key to understanding the process of translation initiation is comprehensive knowledge of how the proteins involved in this process interact with each other and protein posttranslational modifications that modulate their function and activity. These key protein-protein interactions and posttranslational modifications can serve to dynamically regulate eukaryotic translation initiation and thereby control the global rate of protein synthesis within a cell. To this end, the hypothesis of my thesis is that for the essential and conserved eukaryotic translation initiation factor eIF3, there are unexpected and unidentified eIF3 protein-protein interactions and protein phosphorylations that regulate its function and activity in the process of translation initiation. As such, I specifically targeted affinity-tagged components of eIF3 to identify copurifying proteins. Novel

interacting partners were validated with reciprocal protein isolations and mass spectrometry analysis. The acquired mass spectrometry data was used to identify unexpected posttranslational modifications. The presence of a copurifying protein kinase with eIF3 supported my identification of novel eIF3 phosphorylation sites.

Phosphorylation and other posttranslational modifications are chemical alterations to proteins that play a dynamic role in attenuating their biological functions. Elucidating the nature of phosphorylations present on components of eIF3 could have implications in how this complex is regulated within cells. Autoradiography of ^{32}P-labeled affinity purified eIF3 reveals that components of the initiation complex are indeed phosphorylated *in vivo*. My proteomics data and *in vitro* kinase assays support the argument that the yeast Casein Kinase 2 complex (CK2) selectively targets eIF3. Mass spectrometry analysis of affinity purified and phosphoprotein enriched eIF3 allowed me to localize specific phosphorylation events to specific residues on components of eIF3. I specifically targeted a triply phosphorylated species of Nip1, a core component of eIF3, by generating point mutants lacking the identified sites of phosphorylation. Growth rate assays revealed that the strains harboring *nip1* mutations for the identified phosphorylation sites exhibit a marked increase in their doubling times.

Mechanisms of Protein Synthesis

The central dogma of molecular biology holds that genes composed of DNA are transcribed into RNA molecules that are in turn decoded into proteins (Crick, 1958; Crick, 1970). The decoding process that messenger RNA (mRNA) undergoes to produce polypeptides is termed translation. The translation of mRNAs is an essential cellular process and the machinery driving this process is composed primarily of proteins, RNAs, and individual amino acids. The assembled macromolecular machinery facilitating translation is the ribosome. An additional subset of proteins, translation factors, serves to regulate the function of the ribosome in translation. The ribosome is composed of two subunits named according to their sedimentation coefficients. In eukaryotes these two subunits consist of the 40S and 60S complexes. The 40S complex contains 33 individual proteins as well as the 18S RNA (Dinman, 2009). The 60S subunit is comprised of 46 proteins with 3 separate ribosomal RNA molecules (rRNA), 5S, 5.8S and the 28S (Dinman, 2009). Short RNA molecules termed aminoacyl transfer RNAs (tRNAs) transfer a specified amino acid to the nascent polypeptide chain during translation. These tRNAs contain a three base segment known as the anticodon that base pairs with the corresponding three base codon on the translating mRNA (Jackson et. al., 2010). Each individual tRNA uniquely attaches to one of the 20 amino acids. For active translation to occur, the 40S and 60S ribosomal subunits join together on an mRNA molecule through the concerted effort of the essential translation factors to form the 80S ribosome.

Protein translation can be deconstructed into three distinct phases, initiation, elongation, and termination. The first step in this process, initiation, consists of the events leading to the formation of the 80S ribosome primed with methionyl tRNA base paired at the AUG start codon. The essential and highly conserved process of eukaryotic translation initiation is mediated by interactions of numerous multi-subunit eukaryotic initiation factors (eIFs) with the ribosome, mRNA, and tRNAs (Figure 1-1). In the first step, a ternary complex consisting of eIF2 bound to GTP and Met-tRNA is recruited to the 40S ribosomal subunit to form the 43S pre-initiation complex (Kimball, 1999; Unbehaun et. al., 2004). *In vitro* experiments suggest that this interaction is promoted by the initiation factors eIF1, eIF1A, and eIF3 (Asano et. al., 2000; Asano et. al., 2001; Valasek et. al., 2002; Valasek et. al., 2003; Olsen et. al., 2003; Nielsen et. al., 2004; Singh et. al., 2005). In the next step, eIF4F, which is composed of factors eIF4A, eIF4E, and eIF4G (Hernandez and Vazquez-Pianzola, 2005) facilitates interaction of the 43S pre-initiation complex with the 5' cap structure of the mRNA producing the 48S pre-initiation complex. Efficient formation of the 48S pre-initiation complex is also dependent on eIF3 (Hinnebusch et. al., 2004). The 40S complex scans the mRNA from the 5' end for the start codon in a process mediated by eIF1 and eIF1A (Maag et. al., 2005). Once the Met-tRNAi anti-codon pairs with the AUG codon, eIF2-bound GTP is hydrolyzed in a reaction stimulated by eIF5 (Das and Maitra, 2000). The GTP hydrolysis triggers the release of the bound eIFs and the joining of the 60S subunit to create the 80S ribosome (Das and Maitra, 2001).

At this point, the 80S complex accepts the next aminoacyl-tRNA in the A site of the ribosome and the process of translation elongation begins.

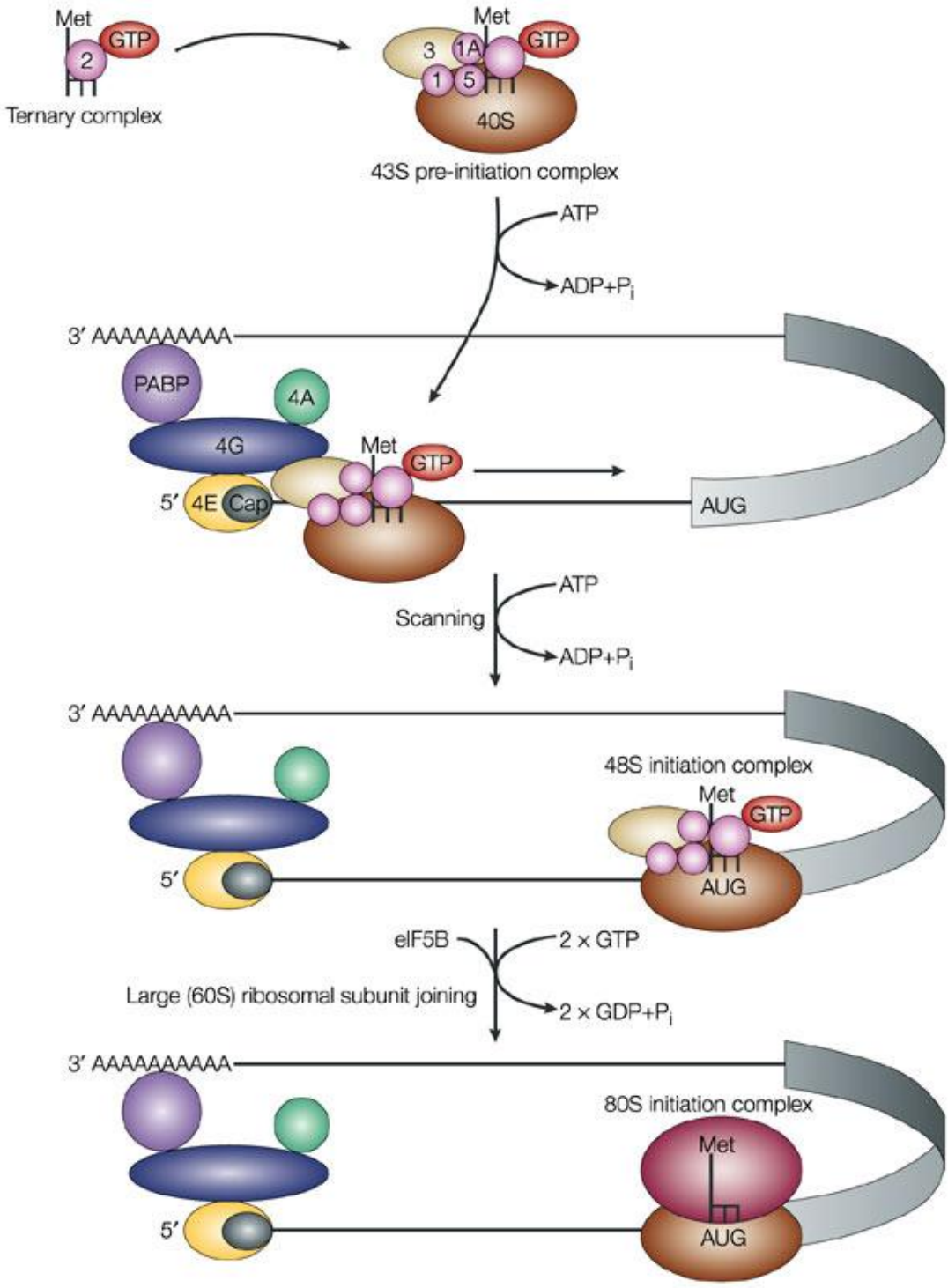

Figure 1-1 Translation Initiation in Eukaryotic Cells. Adapted from Gebauer, *et. al.* Nat Rev Mol Cell Biol. 2004, 5(10):827-35

Elongation is the process by which the ribosome decodes polypeptide information from the codons of the mRNA to produce the nascent polypeptide by utilizing the ribosome's peptidyl transferase activity. The ribosome scans down the template mRNA and base pairs the appropriate anticodon of a charged aminoacyl-tRNA with the cognate mRNA codon. The 23S rRNA within the 60S subunit catalyzes peptide bond formation (Jackson et. al., 2010). The process of elongation is mediated by two key proteins. eEF1A is responsible for delivering cognate aminoacyl-tRNAs to the A-site of the ribosome. Once in position, the nascent peptide chain is transferred to the amino acid of the A-site aminoacyl-tRNA. The second factor, eEF2 is involved in translocating both mRNA and tRNA from the A-site to the P-site following peptidyl transfer. eEF2 then promotes the transfer of deacylated tRNA from the P-site to the E-site. Yeast and various other fungi possess an additional elongation factor, eEF3, which is required for elongation and contains ribosome stimulated ATPase activity. eEF3 interacts with both ribosomal subunits and facilitates eEF1A-mediated cognate aminoacyl tRNA binding to the ribosomal A-site.

The final step in the process of translation is termination and involves recognition of the stop codon, mRNA release and dissociation of the 80S ribosome into 40S and 60S subunits. When a UAA, UAG or UGA stop codon enters the A-site, the release factor eRF1 recognizes the stop codon (Kisselev et. al., 2003). eRF3 then hydrolyzes the ester bond of the P-site peptidyl-tRNA (Alkalaeva et. al., 2006). eRF1 is composed of three distinct functional domains.

Domain 1 is believed to recognize stop codons in the A-site of the ribosome (Song et. al., 2000). Domain 2 interacts with the peptidyl transferase center of the ribosome to trigger peptidyl-tRNA hydrolysis by eRF3 (Frolova et. al., 1999). The final domain is thought to mediate eRF3 binding to eRF1 (Ito et. al., 1998).

In eukaryotes, the regulated translation of mRNAs, or translational control, is a major regulatory mechanism involved in all biological processes, including development (de Moor et. al., 2005), response to stress (Hinnebusch, 2005; Holcik and Sonenberg, 2005; Clemens, 2005), signaling (Parsa and Holland, 2004; Shmulevitz et. al., 2005), plasticity (Sutton, 2005), immune response (Lindemann, 2005; Beretta, 2004), and cell growth (Kuersten and Goodwin, 2003; Gebauer and Hentze, 2004). Defects in protein synthesis and translational control are major factors in diseases, including fragile-X syndrome (Denman et. al., 2004) and several different cancers (Bjornsti and Houghton, 2004; Ruggero and Sonenberg, 2005). Multiple drug therapies are being developed and used to treat human diseases that focus on the translation machinery (Meric and Hunt, 2002). One example is the chemotherapeutic drug rapamycin, which targets the TOR signaling pathway involved in regulating translation (Calkhoven et. al., 2002; Tee et. al., 2005).

Specific regulatory events, namely protein phosphorylation of eIFs serve to both increase and decrease their activities within cells. Phosphorylation of the eIF2α subunit of eIF2 blocks the exchange of GDP for GTP by eIF2B. This prevents the formation of the 43S preinitiation complex and inhibits protein

synthesis (Hinnebusch, 1997). Phosphorylation of eIF4 has been shown to correlate with increased translation rates (Sonenberg, 1997). In addition, phosphorylation of the eIF4E binding protein (4E-BP) inhibits its ability to bind eIF4E and results in an increase in translation rates (Figure 1-1) (Gingras et. al., 2001). Dephosphorylation of 4E-BP has been shown to occur under nutrient starvation and cellular stress (Gingras et. al., 2001).

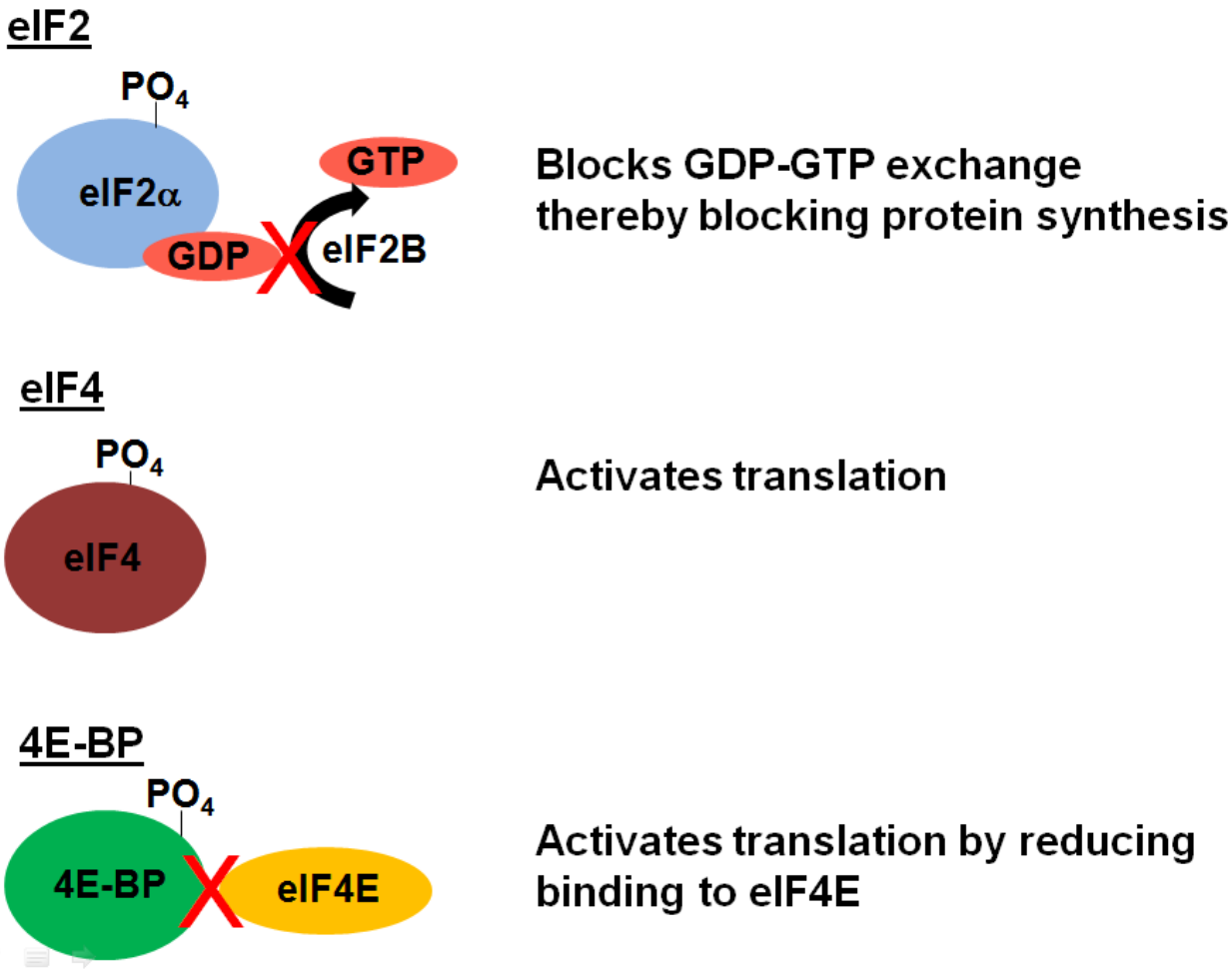

Figure 1-2. Phosphorylation of eIFs altering their activity levels. Previous investigations have established that eIF3 activity is regulated in response to cellular stimuli.

The role of the eIF3 complex

Translation initiation in eukaryotes is dependent on the concerted actions of a multitude of eIFs (Figure 1-1). At least 12 different eIFs function to interact with Met-tRNA, mRNA, and the ribosomal subunits to form pre-initiation complexes and recognize the AUG start codon on mRNA (Hinnebusch, 2005). eIFs are regulated by a variety of cellular responses to control gene expression (Hinnebusch, 2000). One of the first eIFs to be identified was eIF3, but until recently, its functional roles remained unknown. eIF3 has been implicated to have a role in the assembly of the ternary complex composed of eIF2, GTP, and Met-tRNA (Valasek et. al., 2002). eIF3 also recruits the ternary complex along with the 40S ribosomal subunit to form the 43S preinitiation complex and further functions to scan along the mRNA for AUG start codon recognition. Table 1-1 shows the compositional variation of eIF3 among a variety of organisms

Subunit Name	Gene Name	Human MW	*S. cerevisiae* MW	*S. pombe* MW	Wheat MW	*A. thaliana* MW
eif3a	*RPG1*	170	110	107	116	114
eif3b	*PRT1*	116	90	84	83	82
eif3c	*NIP1*	110	93	104	107	105
eif3d	*MOE1*	66	none	63	87	66
eif3e	*INT6*	48	none	57	45	51
eif3f	*CSN6*	47	none	33	34	32
eif3g	*TIF35*	44	33	31	36	33
eif3h		40	none	40	41	38
eif3i	*TIF34*	36	39	37	41	36
eif3j	*HCR1*	35	30	31	none	none
eif3k		28	none	none	25	25
eif3l		none	none	none	60	60

Table 1-1. The composition of eIF3 in various organisms.

eIF3 in the budding yeast *S. cerevisiae* is composed of five core proteins, Rpg1, Nip1, Prt1, Tif34, and Tif35, all of which are essential genes (Phan et. al., 1998) (Figure 1-3). The largest of these proteins, Rpg1, was initially identified as a required protein for yeast to pass through G1 phase (Kovarik et. al., 1998). Rpg1 was identified as part of eIF3 due to its homology with a subunit of the mammalian eIF3. A study of Rpg1 has shown that deletion of the N-terminal domain impairs 40S subunit binding (Nielsen et. al., 2006). Prt1 was initially identified in yeast as required factor for translation initiation and cellular proliferation (Hanic-Joyce et. al., 1987). It has also been shown that the N-terminal domain of Prt1 contains a RNA recognition motif that mediates a protein-protein interaction with Hcr1. This is unique in that the RNA binding domain of Prt1 has dual functionality as a protein binding domain (Valasek et. al., 2001). Both the RNA binding domain and the Hcr1 interaction are necessary for eIF3 to bind the 40S ribosome. In addition, mutations in Prt1 reduce eIF3's ability to bind Met-tRNA (Phan et. al., 1998). When both Rpg1 and Prt1 are separately depleted in yeast, recruitment of the mRNA to the 40S subunit is greatly impaired (Jivotovskaya et. al., 2006). Nip1, initially identified as a nuclear transport protein, has since been shown to be part of the eIF3 complex (Gu et. al., 1992; Valasek et. al., 2000). Studies have determined that Nip1 interacts with ribosomal 40S subunit proteins Rps0A and Rps10A and may directly contact the solvent-exposed side of the 40S subunit (Valasek et. al., 2003). Mutations in Nip1 cause faulty AUG start codon selection (Valasek et. al., 2004). Tif34 and

Tif35 have been shown to promote the linear scanning of mRNA (Cuchalova et. al., 2010).

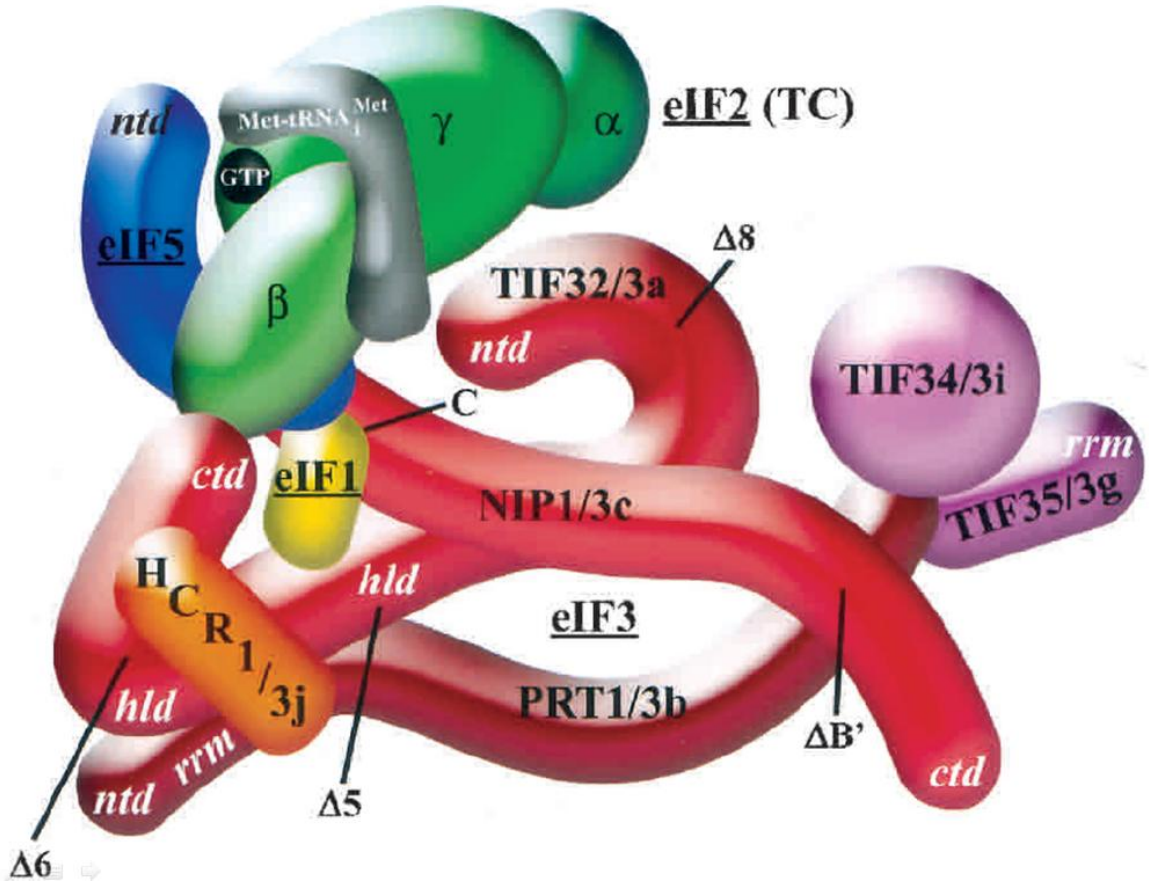

Figure 1-3. The multifactor complex (MFC). Through the concerted action of eIFs and associated proteins, the MFC functions to form the 48S preinitiation complex. Adapted from Valasek, *et al.*, Genes and Development, 2003, 17:786-799.

Proteomic analysis of protein complexes

A comprehensive understanding of protein synthesis control mechanisms is absolutely essential to understanding both normal and disease-altered cellular processes. Identification of all the proteins involved in translation will be a key step towards dissecting the molecular mechanisms of eukaryotic protein synthesis. Mapping the interactions and posttranslational modifications of these proteins will provide insights into their biochemical functions and regulation. The identification of novel translation initiation factors and regulatory modifications may lead to new molecular targets for therapeutic intervention in a number of human diseases. Given the high percentage of genes in the genomes of sequenced organisms are uncharacterized, I hypothesize that unexpected proteins are associated with eukaryotic eIF3 translation complexes. To identify novel protein interactions, I performed a systematic and targeted tandem affinity purification (TAP) purification and mass spectrometry analysis. Several studies have reported the results of large-scale, systematic affinity purifications of yeast proteins of various functions and processes followed by mass spectrometry analysis (Gavin et. al., 2002; Ho et. al., 2002; Krogan et. al., 2004; Gavin et. al., 2006). In contrast to there earlier studies, my focused project used replicate analysis and semi-quantitative approaches to quantify the abundance of identified proteins from the mass spectrometry analysis of the affinity purified protein complexes.

Of the techniques currently available for determining protein interaction networks, mass spectrometry-based (MS) proteomics is perhaps the most powerful. The term proteomics refers to the analysis of all the proteins in a biological sample including posttranslational modifications and alternatively spliced variants of proteins (Wilkins et. al., 1996). Since this term was coined in 1995, it has evolved to include protein expression, function, structure, and sub-cellular localization (Graves and Haystead, 2002; Pandey and Mann, 2000; Aebersold and Mann, 2003). The key instrument utilized in proteomics today is the mass spectrometer. The developments in the technology and methodology associated with this instrumentation have improved dramatically in the past 25 years (Qoronfleh, 2006). Some of these advents include both electrospray ionization (ESI) and matrix assisted laser desorption ionization (MALDI) to generate charged species for MS analysis, as well as new MS instrumentation with a marked increase in sensitivity, resolution, and accuracy. The great complexity of the proteome necessitates additional technology to resolve protein mixtures prior to mass spectrometry. This was originally approached using two-dimensional gel electrophoresis to separate proteins based upon molecular weights and isoelectric points. However, this technique is slow, inconsistent, and limited by the physical properties of the proteins analyzed but allows the analysis of intact proteins (Zhou and Johnston, 2004). Another two-dimensional method uses isoelectric focusing to fractionate proteins based on their isoelectric points. The fractions are then collected and can be subjected to another round of separation based on another dimension using reverse phase separation or size

exclusion. A similar approach is the basis of Proteome Discovery's GELFREE system. In this approach proteins are fractionated using a SDS-PAGE gel for the first dimension which can be further fractionated for more comprehensive separations. To circumvent the problems associated with 2D gels, new techniques have been developed that utilize chromatographic separations of whole proteins or peptides from proteolytically digested proteins.

Two methods are typically used to generate protein and peptide ions for MS analysis. The first, electrospray ionization (ESI), generates ions from a liquid stream passed through a voltage difference. This technique easily adapts to online liquid chromatography (LC). The ions generated by ESI are multiply charged, thereby serving to increase the mass range of the MS instrument and enabling the use of quadrupole mass analyzers. It was shown in 1989 that a triple quadrupole instrument could be used to fragment the multiply charged ions of intact peptides generated by ESI (Hunt et. al., 1989). From this fragment information, it is possible to generate spectra that can be analyzed to yield amino acid sequence information. This development promoted work that combined tandem mass spectrometry (MS/MS) with online LC through ESI to generate peptide sequence information on complex peptide mixtures (Covey et. al., 1991). However, LC-ESI is best suited to small, acidic peptides and is restricted by the online nature of the chromatography. Tandem spectra are typically generated in a data-dependent manner on the most intense ions reaching the detector. The data dependency arises in that the instrument generally selects an n^{th} most intense ion from the initial precursor scan for fragmentation and subsequent

detection in the tandem mass spectrum. As a result, only a subset of available spectra is generated for every data-dependent cycle. Additionally, co-elution of peaks in the chromatography will cause suppression of the less intense signal and loss of data. There also exists a finite time to gather data as a peak is eluted from the chromatography column.

The second major method for ionization, MALDI, involves mixing peptides with a matrix material, typically cinnamic acid derivatives (Gobom et. al., 2001). The matrix serves to absorb energy in the form of electromagnetic radiation applied to the matrix-sample mixture. The absorbed energy causes the ionization of the sample-matrix which then passes to the mass analyzer. MALDI was originally utilized in the field of proteomics for peptide mass fingerprint analysis of digested proteins. This ionization technique is best suited to large, basic peptides as opposed to those generated by ESI, and MALDI produces singly charged ions that have greatly simplified spectra. Since MALDI requires an offline method of separating peptides it was easily amenable to 2D-gel based applications. The offline nature of generating MALDI samples allows this approach to overcome some of the temporal limitations associated with online LC methods.

The traditional liquid chromatography-based (LC) separation for MS/MS analysis involves strong cation exchange (SCX), strong anion exchange (SAX), or reverse phase (RP) in a single dimension. The dimensionality of the chromatography refers to the steps used to separate peptides. For example, a 2-

D separation would consist of using a reverse phase material to separate based upon hydrophobicity and then a SAX resin to fractionate based upon charge. Only separating proteins or peptides in one-dimension causes an abundant overlap of elution peaks in the chromatogram leading to obscuring and subsequent signal loss. To circumvent this problem, the multidimensional peptide identification technology (MudPIT) method was developed (Link et. al., 1999). MudPIT consists of a biphasic column containing a SCX section followed by RP material. This 2D configuration, when combined online with ESI-MS/MS, resulted in the most complete proteome characterization of the yeast *S. cerevisiae* at its time with the identification of 1,484 proteins (Washburn et. al., 2001). It is now possible to add an additional dimension to the MudPIT analysis to further fractionate complex samples (Washburn, 2002).

Proteomic analysis of posttranslational modifications

Protein posttranslational modifications (PTMs) perform essential roles in the biological regulation of a cell (Rucker and McGee, 1993). PTMs are enzymatic, covalent chemical modifications of proteins that typically occur after translation from mRNAs. Chemical modifications of proteins are extremely important because they potentially change a protein's physical or chemical properties, conformation, activity, cellular location, or stability. In fact, most proteins are altered by the addition or removal of a chemical moiety on either the functional group of an amino acid or the protein's N- or C-terminus. Some PTMs can be added and removed dynamically as a mechanism for reversibly

controlling protein function. Over 420 types of protein modifications have been identified and curated in the UNIPROT database to date (www.uniprot.org). The most commonly identified PTMs to date include phosphorylation, sumoylation, ubiquitination, nitrosylation, methylation, acetylation, sulfation, glycosylation, and acylation (Table 1-2).

PTM	Nominal Mass shift (Da)	Stability	Proposed biological function
Phosphorylation			Cellular signaling processes, enzyme activity, intermolecular interactions
pSer, pThr	+80	Very labile	
pTyr	+80	Moderately labile	
Glycosylation			
O-linked	203, >800	Moderately labile	Regulatory elements, O-GlcNAc
N-linked	>800	Moderately labile	Protein secretion, signaling
Proteinaceous			
Ubiquitination	>1,000	Stable	Protein degradation signal
Sumoylation	>1,000	Stable	Protein stability
Nitrosative			
Nitration, nTyr	+45	Stable	Oxidative damage
Nitrosylation, nSer, nCys	+29	Stable	Cell signaling, enzyme activity
Methylation	+14	Stable	Transcription
Acetylation	+42	Stable	Histone regulation, protein stability
Sulfation, sTyr	+80	Very labile	Intermolecular interactions
Deamidation	+1	Stable	Intermolecular interactions, sample handeling artifact
Acylation			Membrane tethering, intermolecular interactions, cell localization signals
Farnesyl	+204	Stable	
Myristoyl	+210	Stable	
Palmitoyl	+238	Moderately labile	
Disulfide bond	-2	Moderately labile	Protein structure and stability
Alkylation ,aCys	+57	Stable	Sample handeling
Oxidation, oMet	+16	Stable	Sample handeling

Table 1-2. Common PTMs encountered in mass spectrometry. Included are their associated mass shifts, predicted MS stability and proposed biological functions.

Vast amounts of scientific effort have gone toward identifying PTMs and elucidating their biological functions. Perhaps the best studied cases involve eukaryotic histones and the myriad of PTMs that are associated with transcriptional regulation (Berger, 2007; Fuchs et al., 2009; Issad and Kuo, 2008; Olsson et al., 2007; Reid et al., 2009). Histones associate with chromosomal DNA to form nucleosomes that bundle together to form chromatin fibers. The histone code hypothesizes that chromatin–DNA interactions are regulated by combinations of histone PTMs (Jenuwein and Allis, 2001; Strahl and Allis, 2000). The acetylation of lysine was first discovered in histones and is correlated with actively transcribed genes (Roth et al., 2001). Combinations of methylation, acetylation, ADP ribosylation, ubiquitination, and phosphorylation of histone tails function to regulate specific gene expression programs (Godde and Ura, 2008).

One of the most ubiquitous PTMs, phosphorylation, is the focus of many biochemical investigations. It has been estimated that 30% of the human proteome is phosphorylated (Cohen, 2001; Hubbard and Cohen, 1993). For example, tyrosine kinases and phosphatases transduce signals from ligand-bound receptors on the cell surface to downstream targets in the insulin/IGF-1 signaling pathway (Taniguchi et al., 2006). Classic approaches to detecting PTMs on proteins involved Edman degradation and thin-layer chromatography (TLC). However, these methods are hampered by the requirement of significant amounts of starting material and an inability to identify rare or substoichiometric PTMs. Because most PTMs result in a concomitant change in the mass of the modified protein, methods that can detect changes in molecular mass, namely

mass spectrometry-based proteomics, are now routinely utilized to identify PTMs. Some PTMs, such as phosphorylation or methylation, increase the mass of a protein, while other PTMs, like signal peptide cleavage or disulfide bond formation, decrease the mass. Depending on the mass spectrometry instrument used, the proteomic approaches have the advantage of high sensitivity and can determine molecular masses to an accuracy of less than 1 part per million (<1 ppm) (Makarov et al., 2006; Lu et al., 2008; Scigelova and Makarov, 2006).

Instrument manufacturers and academic researchers are constantly improving instrument technologies and developing new methods to identify PTMs (Garcia et al., 2007). For example, recent advances in the field include such developments as electron transfer dissociation (ETD) and electron capture dissociation (ECD) for the chemical fragmentation of peptides and dynamic detectors capable of accurately measuring masses of undigested proteins (Coon et al., 2004; Mikesh et al., 2006; Pitteri et al., 2005; Syka et al., 2004). Enrichment strategies to selectively isolate proteins or peptides with a desired PTM can be coupled with mass spectrometry-based proteomic techniques. These enrichment techniques can alleviate the problems created by rare modifications. Among the variety of affinity enrichment strategies available, there are two major categories. First are approaches that use antibodies to recognize a specific PTM or uniquely modified peptide. For example, antiphosphotyrosine antibodies are used to enrich for peptides with phosphotyrosine residues (Blagoev et al., 2004; Rush et al., 2005; Zhang et al., 2005). Second, there exist emerging technologies to enrich for PTMs based on the chemical affinity of a

modification for an immobilized resin. Such techniques include immobilized metal affinity chromatography (IMAC) for phosphorylations and lectin chromatography for glycosylations (Ito et al., 2009).

Another widely used proteomic technique useful in the identification of PTMs is two-dimensional gel electrophoresis (2D-GE). PTMs can alter the isoelectric point and electrophoretic mobility of a protein in a 2D-gel experiment. When such a change is detected between different cell types or growth conditions, the protein can be isolated and sequenced to identify its PTMs. For example, the differential phosphorylation of a protein will alter its isoelectric point and may cause charge heterogeneity. The differentially phosphorylated protein will appear as a train of 2D spots with different isoelectric points but with similar molecular weights. This pattern is sometimes referred to as ‘‘pearls-on-a-string.’’ Specific protein staining methods for revealing protein PTMs have been devised over the years (Ge et al., 2004; Patton, 2002). These include fluorescent methods for the direct detection of phosphoproteins and glycoproteins in gels (Ge et al., 2004; Steinberg et al., 2001; Schulenberg et al., 2003). For these 2D spots, the proteins can be in-gel digested, and the recovered peptides can be analyzed by mass spectrometry to identify, validate, and map the expected PTMs (Hayduk et al., 2004; Steinberg et al., 2003). However, the 2D-GE approaches to identifying PTMs are not trivial since the recovery and analysis of the modified peptides are often problematic.

Multiple tools now exist in proteomics to quantify the absolute or relative abundance of proteins and their specific PTMs (Paoletti and Washburn, 2006). *In vivo* and *in vitro* labeling methods have been developed to use mass spectrometry for quantifying PTMs and precisely measuring their changes during cellular events (Goodlett et al., 2001; Gygi et al., 1999; Oda et al., 1999; Ong et al., 2002; Ross et al., 2004; Zhang et al., 2005). Quantitation can be crucial in determining the biological significance of a given PTM, since simply identifying the presence of a modification will not provide sufficient biological information to model its importance. A study by Matthias Mann and coworkers performed in HeLa cells found that 14% of the identified phosphorylation sites were modulated at least two fold by epidermal growth factor stimulation, demonstrating the importance of quantifying PTMs (Olsen et al., 2006).

There are, however, several limitations that must be considered when using mass spectrometry-based proteomics to identify PTMs. Some PTMs, such as phosphorylation of serine, tyrosine and threonine, and either O-linked or N-linked glycosylation, are labile, and maintaining the modification during sample preparation can be difficult. If ineffective separation techniques are used, unmodified peptides or proteins can mask the modified form during the mass spectrometry analysis. The detection of substoichiometric PTMs is especially difficult when the majority of the protein molecules may be unmodified. Proteins are typically digested into peptides, and the peptides are directly analyzed. Modification of a given peptide with labile groups such as in phosphorylation, sulfation, and glycosylation can reduce its ionization efficiency, thereby

compromising the mass spectrum and preventing sequence determination. Alternatively, there can be ambiguity as to which amino acid is modified, since many peptides contain multiple potential amino acid targets for the PTM. In addition, when using collision induced dissociation (CID) to fragment peptides containing labile PTMs such as phosphorylation and glycosylation, the labile group undergoes a β-elimination reaction to generate a neutral loss fragment (Figure 1-2). This pathway is more energetically favorable than fragmentation at the amide bonds. The resulting mass spectrum often fails to generate enough sequencing ions to unambiguously identify the peptide or modified amino acid. Finally, the detection of rare PTMs can be challenging, and identification often requires highly sensitive mass spectrometry methods or PTM enrichment strategies.

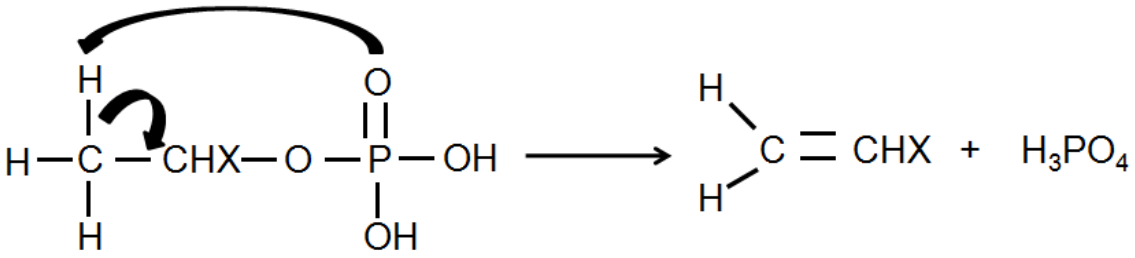

Figure 1-4. β-elimination of H_3PO_4. Labile functional groups added to amino acid side chains can undergo the more energetically favorable elimination reaction to generate an alkene and phosphoric acid. X=H for serine and X=CH_3 for threonine.

Phosphorylation

The reversible phosphorylation of serine, threonine, and tyrosine residues is probably the most heavily studied PTM. Protein phosphorylation signaling networks mediate cellular responses to a variety of stressors, growth factors, cytokines, and cellular interactions. Phosphorylation also influences a multitude of cellular processes such as proliferation, proteolysis, apoptosis, migration, transcription, and protein translation (White, 2008). Phosphorylation events have the ability to force conformational changes in a protein's structure that can either activate or deactivate the protein's enzymatic activity. Phosphate groups are polar in nature and when added to residues, decrease the hydrophobicity of their environment. In eukaryotic cells, reversible protein phosphorylation occurs primarily on serine, threonine, and tyrosine side chains. However, *S. cerevisiae* lack tyrosine kinases and phosphorylation is primarily restricted to serines and threonines. Aberrant regulation of protein kinases and phosphatases has been implicated in cancer, autoimmune diseases, metabolic disorders, and infectious diseases (Blume-Jensen and Hunter, 2001; Gatzka and Walsh, 2007; Sirard et al., 2007; Taniguchi et al., 2006). Single phosphorylation events can have dramatic implications on cellular processes. For example, the dephosphorylation of eIF4E-binding protein is triggered by nutrient deprivation, environmental stress, or infection with some picornaviruses and results in a marked increase in eIF4E binding activity and an inhibition of translation (Gingras et al., 2001).

The traditional method of identifying phosphorylation sites involves growing cells with 32P-labeled ATP or phosphoric acid. The phosphoproteome incorporates the radioactive phosphate from the growth medium. The radioactive proteins are detected using such techniques as 2D-GE or high-performance liquid chromatography (HPLC). The fractionated proteins are then isolated and hydrolyzed. The resulting phosphopeptides are separated on TLC plates and subsequently sequenced by Edman degradation. However, these techniques are time consuming, require large amounts of relatively pure phosphoproteins, and necessitate the use of significant amounts of radioactive material (McLachlin and Chait, 2001). Because of these drawbacks, mass spectrometry-based proteomics has quickly emerged as the preferred technique for identifying phosphorylations.

A proteomic study comparing *Escherichia coli*, *Lactococcus lactis*, and *Bacillus subtilis* found that nearly every enzyme in the glycolytic pathway, which mediates carbon metabolism, was phosphorylated on various serine, threonine, and tyrosine residues (Soufi et al., 2008). Interestingly, they also found that the detected consensus sites of phosphorylation appear far more evolutionarily conserved than the primary sequence (Soufi et al., 2008). A separate study investigating the mouse liver phosphoproteome identified many of the phosphorylation sites previously annotated in the Swiss-Prot mouse database (Pan et al., 2008). However, more than half of the identified sites were novel, suggesting that there are still many more phosphorylation sites yet to be identified in the mouse phosphoproteome (Pan et al., 2008).

Mass spectrometers have the ability to identify specific sites of phosphorylation within complex protein mixtures. This approach does present problems that are often faced in other proteomic applications, including limited sample amounts, complex samples, and a wide dynamic range of protein concentrations within the sample (White, 2008). To compound the difficulty of these experiments, phosphorylation is often substoichiometric, and therefore the phosphopeptide is at a lower concentration than the other peptides from the same protein. The large population of unmodified peptides suppresses the mass spectrometric response to the phosphopeptides. This phenomenon can lead to a lack of detectable signal for the phosphopeptides of interest (McLachlin and Chait, 2001). Suppression artifacts can be minimized by reducing the fraction of unmodified peptides relative to the PTM variants using any of a variety of enrichment strategies. One such enrichment strategy applicable to identifying phosphorylations is the use of strong cation exchange (SCX) resin to selectively isolate phosphopeptides. It has been found that, with a pH of less than 2.6, tryptic phosphopeptides are not retained by the SCX particles (Beausoleil et al., 2004). This is likely due to their more anionic nature afforded by the phosphate group. The flow through of the SCX column can be subsequently fractionated with a reverse phase (RP) column and subjected to mass spectrometry analysis (Lim and Kassel, 2006). The separation of the phosphorylated peptides from their unmodified counterparts helps alleviate the problem of suppression during mass spectrometry as discussed above. This enrichment strategy has the advantage of being applicable to both off-line and on-line fractionation approaches. One

negative aspect of this approach is that it relies on the inability of the SCX resin to bind the phosphopeptides, as opposed to other strategies that bind the phosphorylated residues and thereby positively enrich for them selectively.

Immobilized Metal Affinity Chromatography (IMAC) is the most widely utilized method for selectively isolating phosphopeptides from complex mixtures of digested proteins. This method typically utilizes a metal chelating agent to bind trivalent metal cations, such as Fe3+ or Ga3+ (Sykora et al., 2007). The charged resin is subsequently used to bind the phosphorylated peptides. The resin with bound phosphopeptides is washed with a rinse solution, typically an acetic acid solution, to remove unmodified peptides. The phosphopeptides can then be eluted with phosphate buffer or a high pH solution either directly onto a RP column for desalting and subsequent mass spectrometric analysis or off-line for further enrichment or manipulation. The IMAC approach does present some complications, however. If multiply phosphorylated peptides are present in abundance, they can overwhelm the IMAC resin and result in the loss of singly and doubly phosphorylated species. Additionally, other acidic peptides will have an affinity for the IMAC column and will be enriched along with the phosphorylated peptides. This problem is exacerbated by exceedingly complex peptide mixtures such as whole cell extracts. In an attempt to avoid this problem, many investigators methyl esterify the acidic residues and the C-terminus using a chemical reduction procedure (Ficarro et al., 2002). However, studies have found that the methyl esterification reaction is not quantitative (Cirulli et al., 2008). Thus, the peptide of interest is present as modified, partially modified and

unmodified versions. The complexity of the mixture is increased, and the relative amount of a given peptide is actually reduced (Cirulli et al., 2008).

An approach analogous to IMAC is the use of titanium dioxide (TiO2) as a substitute for the metal chelating resin (Larsen et al., 2005; Pinkse et al., 2004; Thingholm et al., 2006). Just as the phosphate groups of the modified peptides have affinity for the trivalent metal used in IMAC, they also have an affinity for the titanium dioxide molecules under acidic conditions (Larsen et al., 2005; Pinkse et al., 2004; Thingholm et al., 2006). By shifting to a high pH buffer, the phosphopeptides can be eluted from the TiO2 material. This approach has the advantage of requiring less column preparation time and fewer rinse cycles than the IMAC resin. Studies have shown that, although these two methods use the same principle of affinity, they are complementary in that distinct phosphopeptides are detected by each of the two approaches (Cantin et al., 2007). IMAC is characterized by a higher affinity for multiply phosphorylated peptides while titanium dioxide preferentially binds singly phosphorylated species (Bodenmiller, et al., 2007). This highlights the utility of using both approaches in a single investigation to obtain maximal coverage of the phosphoproteome.

Another method for phosphopeptide enrichment employs chemically introduced affinity tags at the sites of phosphorylation (Goshe et al., 2001; Oda et al., 2001). One such method uses an alkaline environment to remove H_3PO_4 from phosphoserine or phosphothreonine residues in a β-elimination reaction (McLachlin and Chait, 2003; Oda et al., 2001). A dithiol group is then added to

the double bond in a Michael-like addition reaction. The thiol is then treated with an alkylating reagent linked to a biotin group. The resulting biotinylated peptides can then be enriched using avidin column chromatography (McLachlin and Chait, 2003). One difficulty of this approach is the recovery of the tagged species can be problematic due to the high affinity of biotin for avidin. Also, this method enriches for phosphoserine and phosphothreonine, not phosphotyrosine. O-linked β-N-acetylglucosamine (O-GlcNAc) modifications are also susceptible to β-elimination followed by Michael addition and can therefore compete with phosphorylations for enrichment (Wells et al., 2002). Finally, under the alkaline environment of the β-elimination reaction, unwanted side reactions can occur that have unanticipated affects on peptide mass. These side reactions can make it difficult to identify the peptides downstream during mass spectrometry.

During mass spectrometry, specific chemical properties of phosphoproteins must be taken into account. Phosphorylation is a labile addition to S and T amino acids. Traditional fragmentation methods result in the preferential neutral loss of H_3PO_4 or HPO_3 from phosphoserine and phosphothreonine residues prior to fragmentation along the peptide backbone. The vast majority of the population undergoes β-elimination reaction, leaving only a fraction remaining to fragment along the backbone (Bennett et al., 2002; Lee et al., 2001; Ma et al., 2001). The resulting mass spectrum contains fewer sequencing ions, and these ions are generally lower in intensity. Therefore, there is a low signal-to-noise ratio, which hampers interpreting the peptide sequence.

Although capable of losing the phosphate group, phosphotyrosine seldom generates the intense neutral loss ions that are seen for peptides containing phosphoserine or phosphothreonine residues. Some mass spectrometers that use electron transfer dissociation (ETD) or electron capture dissociation (ECD) avoid this neutral loss problem and can yield spectra suitable for both sequence analysis and phosphoresidue determination. This alternative fragmentation method will be discussed further when considering the various instrument types used in the proteomic identification of PTMs. On the other hand, neutral loss artifacts can be used to the advantage of the investigator. The neutral loss signature is a conspicuous indicator that the peptide contains a site of phosphorylation. The neutral loss peak observed in the mass spectrum is generally of high intensity due to its preferential formation. Therefore, if a loss of 98 m/z (H_3PO_4) or 80 m/z (HPO_3) for a +1 charged peptide is observed from the precursor ion, one can infer the presence of a phosphoserine or phosphothreonine reside within the sequence of the peptide. Modern mass spectrometers can monitor for this mass loss. An ion trap mass spectrometer can isolate the neutral loss species and initiate another round of fragmentation (MS3 scan) (Beausoleil et al., 2004; Gruhler et al., 2005; Olsen and Mann, 2004; Ulintz et al., 2009). This additional analysis step can result in additional sequence coverage to aid in identifying the phosphopeptides and mapping the PTM to a specific amino acid. An alternative approach to an MS3 scan is ‘‘Pseudo MSn’’ or multistage activation (MSA) for phosphopeptide fragmentation in an ion trap mass spectrometer (Schroeder et al., 2004). The method induces CID of the

neutral loss product from the MS/MS scan of the phosphopeptide. The product ions from the neutral loss ions along with the initial MS/MS product ions are trapped together resulting in a composite spectrum. In MSA, the neutral loss product ions are converted into a variety of structurally informative fragment ions, which show improved scores in database search algorithms (Schroeder et al., 2004; Ulintz et al., 2009).

Phosphorylation introduces a negative charge onto the peptide, and this also can affect analysis by mass spectrometry. The negative charge can reduce the mass spectrometer response when operated in positive-ion mode (McLachlin and Chait, 2001). This diminished response results in poor quality spectra and makes identifying the phosphopeptide more difficult. Furthermore, this increased negative charge can reduce proteolysis during preparation of protein mixtures prior to mass spectrometry. As a caveat, Hanno Steen and coworkers found no evidence for decreased ionization/detection efficiencies when selectively investigating phosphopeptides using electrospray ionization (ESI) (Steen et al., 2006). As an alternative, a precursor ion scanning technique pioneered by Steve Carr and coworkers can be employed to avoid some of the problems generated by performing MS in the positive-ion mode (Carr et al., 1996). Tandem mass spectrometry is performed in negative-ion mode, and phosphorylated residues generate characteristic fragments of 79 Da for PO_3 or 63 Da for PO_2. When one of these events is detected in the precursor ion scan, MS/MS is performed on the precursor ion (Zappacosta et al., 2006). This approach can be more sensitive than positive mode mass spectrometry for detecting phosphopeptides (Carr et

al., 1996). However, negative-mode spectra are difficult to interpret and not widely studied (Witze et al., 2007). One interesting approach combines both positive-ion mode and negative-ion mode in the same experiment. Precursor ion scanning is performed in the usual negative ion mode, the instrument's polarity is switched, and MS/MS fragmentation spectra are obtained in the positive-ion mode (Carr et al., 1996). Although identifying sites of phosphorylation is challenging, many proteomic techniques are available that can be customized for characterizing these critically influential PTMs.

Protein and PTM quantitation

When investigating the biological significance of PTMs, it is often advantageous to know the relative or absolute abundance of a specific modification or group of PTMs. This allows for the direct comparison of the modification of interest across varied biological samples. An example is comparing the abundance of a PTM in cells or tissues obtained from a normal versus a disease state. Quantifying these changes can lead to insights into the role of PTMs in a myriad of processes from cell growth to diseases and apoptosis. A range of methods are available to quantify PTMs. Traditional methods utilize 2D-GE and differential staining to identify differences in the level of protein expression among samples. However, this approach has a low resolution and sensitivity, and differences in the ability of some proteins to stain can lead to artifacts (Ong and Mann, 2005). The 2D-GE approach is most amenable to abundant protein species (Anderson and Anderson, 1998). More

recently, mass spectrometry-based approaches have alleviated some of the problems posed by gel-based approaches. These methods include protein or peptide labeling strategies, tagging approaches and differential proteomic methods using spectral counting (Gygi et al., 1999; Ong et al., 2002; Washburn et al., 2001). While these methods are more widely applied to quantifying protein changes among samples, they can also be used to quantify changes in PTMs from different biological samples.

Quantitative measurements can either be absolute, in terms of concentration or copy number per cell, or relative, in terms of fold change among differentially treated samples. Absolute concentrations are more difficult to obtain, but are more informative and can be used to derive relative measurements. LC-MS/MS experiments allow the plotting of signal intensities as a peptide elutes from the chromatographic column over time. The area under this curve for any given species is directly related to the abundance of the peptide and allows for label-free quantitation. However, the physiochemical properties of peptides such as hydrophobicity, charge, and size vary widely and can lead to differences in the mass spectrometer's detector response. In addition, co-elution of other peptides and variations in elution conditions can be problematic for quantitative investigations. Protein abundance estimates using this method can vary by a factor of 3–5-fold from the true abundance (Ong and Mann, 2005).

A set of chemical tagging strategies for protein quantitation utilizes the reactivity of the peptide N-terminus and the epsilon-amino group of lysine

residues. Isotope-coded protein labeling (ICPL), isotope tags for relative and absolute quantification (iTRAQ), and tandem mass tags (TMT) are all approaches that were developed to exploit the reactivity of amines to specific chemical groups (Ross et al., 2004; Schmidt et al., 2005; Thompson et al., 2003). The most recognized of these approaches, iTRAQ, incorporates isobaric tags that fragment in the tandem mass spectrometer to generate unique reporter ions at m/z values of 113–121 (Ong et al., 2004). The peak areas of the low mass-fragment ions are integrated to determine the quantification values.

Mass spectrometers such as quadrupoles, TOF, and Orbitrap instruments that have the inherent ability to detect low m/z fragment ions are typically used for iTRAQ experiments. Commercially available kits allow examination of up to eight states in one single experiment. Since the labeled peptides are isobaric, they should behave similarly in chromatographic separations and reveal quantitative differences in their fragmentation spectra. Using the iTRAQ approach, different samples are isolated under different conditions, trypsin digested, and labeled with the iTRAQ reagents. Samples are then combined and analyzed in a single MS/MS experiment. As with other MS-based approaches, sufficient peptide separation is crucial since coeluting peptides of similar mass can contribute to the observed reporter ion series and interfere with the quantification. Ion trap mass spectrometers are typically not useful for iTRAQ analysis because the reporter ions generated from the fragmentation of the iTRAQ tags are lost with the lower 1/3 of the MS/MS data. The use of pulsed q-dissociation (PQD) was introduced to alleviate this problem but has found limited

use in proteomics (Bantscheff et al., 2008; Cunningham et al., 2006; Griffin et al., 2007).

Using the iTRAQ approach, it is possible to compare the degree of phosphorylation of the proteome under different conditions. Studies performed by Forest White and coworkers used antiphosphotyrosine antibodies followed by IMAC enrichment and iTRAQ labeling to investigate the effect of epidermal growth factor (EGF) stimulation on the phosphorylation state of cells over time (Zhang et al., 2005). This study probed four time points (0, 5, 10, and 30 min) in a single analysis. They were able to quantify relative changes in the phosphorylation of 78 sites on 58 proteins (Zhang et al., 2005). This experimental approach highlights the utility of combining enrichment for PTMs with quantitation to gain additional insight into the biology of cells. It is difficult to determine what fraction of a peptide population is phosphorylated under certain conditions. This is because the unphosphorylated counterpart will behave differently in its MS detector response. So while it is feasible to compare unmodified forms and other unmodified forms or different phosphorylated forms of the same peptide under different conditions, it is not reliable to compare modified versus unmodified forms based on the ratio of reporter ion peaks generated.

Isotope labeling and tagging strategies can be tedious, cumbersome, and expensive. In addition to the chromatographic peak integration method discussed previously, other label-free quantitation methods exist that can be applied to quantifying PTMs. These methods typically involve some form of spectral

counting and normalization for protein length (Washburn et al., 2006). It is debatable whether these methods are truly quantitative, and as a result, these methods are more commonly referred to as differential proteomic techniques. The spectral counting methods are based on the principle that, as the abundance of a protein increases in a given sample, more MS/MS spectra are isolated for peptides derived from that protein. Relative quantitation is inferred by comparing the number of spectra collected for a particular protein between experiments. The utility of this approach is questionable because it does not directly measure any physical property of the peptide and assumes a linear response for every protein (Bantscheff et al., 2007). As previously mentioned, the physiochemical properties of peptides vary widely in a sample digest and their resulting chromatographic and MS detector behavior can vary greatly. These methods provide a larger dynamic range than labeling and tagging procedures and are most applicable when investigating large or global protein changes among samples. However, the uncertain linear response among peptides and the potentially poor accuracy of spectral counting approaches limits their widespread use (Old et al., 2005).

Summary

Translation is a conserved, essential process in all living organisms and involves a myriad of biological factors. Translation initiation is a key process to study as it has been implicated in the involvement of aberrant cellular states. I focused my efforts on studying the eukaryotic translation initiation factor eIF3 in *S. cerevisiae*.

I hypothesize that there are unexpected and unidentified eIF3 protein-protein interactions and protein phosphorylations that regulate its function and activity in the essential process of translation initiation. Chapter 2 of the thesis focuses on the identification of novel eIF3 interacting proteins. I utilized a proteomic approach to elucidate previously uncharacterized protein-protein interactions between eIF3's components and other members of the yeast proteome. Chapter 3 deals with determining which amino acid residues among the components of eIF3 are phosphorylated. I utilized radiolabeling and mass spectrometry to attempt to first identify phosphoproteins and then localize the phosphorylations to specific side chains. Chapter 4 investigates the utility of using pulsed-Q disassociation to identify and quantify proteins using the iTRAQ system. This is a technique that, if it would have been more successful, would have allowed me to apply quantitative techniques to my study of the eIF3 complex. The final chapter summarizes the findings and suggests a model for what I discovered pertaining to the phosphorylations and interactions of eIF3. This chapter also speculates as to future work and may be conducted to further the knowledge of the nature and function of eIF3.

CHAPTER II

eIF3 INTERACTS WITH FUN12, HCR1 AND CK2 IN *S. CEREVISIAE*

Abstract

The eukaryotic initiation factor 3 (eIF3) is an essential, highly conserved multi-protein complex that is a key component in the recruitment and assembly of the translation initiation machinery. To better understand the molecular function of eIF3, I examined its composition and phosphorylation status in the budding yeast *Saccharomyces cerevisiae*. I hypothesized that an optimized affinity purification protocol tailored for maximum recovery of the eIF3 complex will also yield novel identifications of proteins interacting with eIF3 core subunits. The yeast eIF3 complex contains five core components: Rpg1, Nip1, Prt1, Tif34, and Tif35. In work described here, liquid chromatography coupled with tandem mass spectrometry analysis of affinity purified eIF3 complexes showed that several other initiation factors (Fun12, Tif5, Sui3, Pab1, Hcr1, and Sui1) and the Casein Kinase 2 complex (CK2) co-purify with the core eIF3 subunits. Reciprocal affinity purifications of tagged Fun12 and Sui3, two previously uncharacterized interactions, validated that core components of eIF3 also copurify with these two proteins. These results implicate that the interaction of eIF3 with Fun12 links the formation of the pre-initiation complex with the binding of the 60S ribosome and

the termination of translation initiation. Our finding that Pab1 interacts with the eIF3 complex suggests a link between eIF3 and the efficient formation of the 48S pre-initiation complex. The observation that CK2 consistently copurifies with components of eIF3 and the important role of phosphorylation in a wide array of biological processes led us to examine whether it can catalyze the phosphorylation of components of the eIF3 complex.

Introduction

A key player in the assembly and function of the 48S pre-initiation complex is the multi-protein eIF3 complex. While the mammalian eIF3 complex contains eleven subunits, much of what is known about the mechanisms of eIF3 function have been characterized in studies of the five-subunit eIF3 complex in *S. cerevisiae* (Hinnebusch et. al., 2004). The yeast eIF3 subunits Rpg1, Nip1, Prt1, Tif34, and Tif35 are homologs of the human eIF3 subunits eIF3a, eIF3c, eIF3b, eIF3i, and eIF3g, respectively (Table 1-1) (Browning et. al., 2001). Yeast Hcr1 is homologous to human eIF3j, but does not appear to be a core eIF3 component (Valasek et. al., 2001). The eIF3 complex, as well as eIF1, eIF5, and the eIF2 ternary complex, have been identified as part of a multifactor complex (MFC) that mediates the assembly of the 48S pre-initiation complex (Hinnebusch et. al., 2004; Asano et. al., 2001) (Figure 1-4). Within eIF3, Rpg1 and Hcr1 interact with Prt1 *via* an N-terminal RNA recognition motif (RRM) (Valasek et. al., 2001), which mediates protein-protein interactions despite the name. These interactions are crucial for the structural integrity of the eIF3 complex and its stable

association with the MFC and 40S ribosome complex (Valasek et. al., 2001). Nip1 and Prt1 play key roles in both the assembly and maintenance of the 48S pre-initiation complex (Hinnebusch et. al., 2004). Nip1 interacts directly with eIF1 and eIF5, suggesting that it coordinates in conjunction with eIF1, Met-tRNAi, and eIF5 to function in both AUG start codon recognition and eIF2-GTP hydrolysis (Valasek et. al., 2003; Valasek et. al., 2004). The smallest of the eIF3 subunits, Tif34 and Tif35, have recently been shown to promote the linear scanning of mRNA (Cuchalova et. al., 2010). The RNA recognition motif of eukaryotic translation initiation factor 3g (eIF3g) is required for resumption of scanning of posttermination ribosomes for reinitiation on GCN4 and together with eIF3i stimulates linear scanning (Cuchalova et. al., 2010).

Materials and Methods

Yeast strains

TAP-tagged yeast strains used in this study have been previously described (Ghaemmaghami et. al., 2003).

Purification eIF3 Components

The eIF3 complex was purified using a previously described protocol from TAP-tagged yeast strains grown to early stationary phase ($O.D._{600}$ 2-4) in YPD medium (Powell et. al., 2004; Link et. al., 2005). For identifying the protein composition of eIF3, 2 L cultures of strains expressing TAP-tagged alleles of *RPG1, NIP1, PRT1,* and *TIF5* were analyzed. BY4741, the parental strain for the TAP clones, was used as a negative control since it lacks any affinity tagged

gene. For analysis of the association of Casein Kinase 2 (CK2) with eIF3, a TAP-tagged allele of CKB2 was used for a similar purification. For validation experiments, TAP-tagged FUN12 and Pab1 strains were used.

Mass spectrometry analysis of purified proteins

Purified proteins were identified using two different methodologies. In one approach, proteins were separated by 10% acrylamide SDS-PAGE. Stained bands were excised and in-gel trypsin digested, and purified proteins were identified using reversed-phase LC-MS/MS analysis (Powell et. al., 2003; Powell et. al., 2004). In the second approach, components of eIF3 were identified directly in solution with Multidimensional Protein Identification Technology (MudPIT) using an LTQ linear ion trap (Thermo Electron, Inc) (Link et. al., 1999; Sanders et. al., 2002; Powell et. al., 2004). Protein samples were reduced with 1/10 volume of 50 mM DTT at 65°C for 5 min, cysteines were alkylated with 1/10 volume of 100 mM iodoacetamide at 30°C for 30 min, and proteins were trypsinized with modified sequencing grade trypsin at ~25:1 subtrate:enzyme ratio (Promega, Madison, WI) at 37°C overnight. A fritless, microcapillary (100 µm-inner diameter) column was packed sequentially with the following: 9 cm of 5 µm C_{18} reverse-phase packing material (Synergi 4 µ Hydro RP80a, Phenomenex), 3 cm of 5 µm strong cation exchange packing material (Partisphere SCX, Whatman) and 2 cm of C_{18} reverse-phase packing material. The trypsin-digested samples were loaded directly onto the triphasic column equilibrated in 0.1% formic acid, 2% acetonitrile, which was then placed in-line

with an LTQ linear ion trap mass spectrometer (Thermofisher, Inc.). An automated six-cycle multidimensional chromatographic separation was performed using buffer A (0.1% formic acid, 5% acetonitrile), buffer B (0.1% formic acid, 80% acetonitrile) and buffer C (0.1% formic acid, 5% acetonitrile, 500 mM ammonium acetate) at a flow rate of 300 nL/min. The first cycle was a 20-min isocratic flow of buffer B. Cycles 2-6 consisted of 3 min of buffer A, 2 min of 15-100% buffer C, 5 min of buffer A, followed by a 60-min linear gradient to 60% buffer B. In cycles 2-6, the percent of buffer C was increased incrementally (from 15, 30, 50, 70 to 100%) in each cycle. During the linear gradient, the eluting peptides were analyzed by one full MS scan (200-2000 *m/z*), followed by five MS/MS scans on the five most abundant ions detected in the full MS scan while operating under dynamic exclusion.

Mass Spectrometry Data Analysis

To process and analyze the mass spectrometry data, the program *extractms2* was used to generate an ASCII peak list and identify +1 or multiply charged precursor ions from native *.RAW mass spectrometry data files (Jimmy Eng and John R. Yates III, unpublished). Tandem spectra were searched with no protease specificity using SEQUEST-PVM (Sadygov et. al., 2002) against the SGD yeast_orfs database containing 6,000 entries with a static modification of +57 on C (addition of a carbamidomethyl group). For multiply charged precursor ions ($z \geq +2$), an independent search was performed on both the +2 and +3 mass of the parent ion. Data were processed and organized using the BIGCAT software

analysis suite (McAfee et al., 2006). A weighted scoring matrix was used to select the most likely charge state of multiply charged precursor ions (Link et al., 1999; McAfee et al., 2006). From the database search, tryptic peptide sequences with SEQUEST cross-correlation scores (Cn) $\geq$ 1.5 for +1 ions, $\geq$ 2 for +2 ions, and $\geq$ 2 for +3 ions were considered significant and used to create a list of identified proteins.

A protein abundance factor (PAF) representing relative protein abundance, was calculated for each identified protein by normalizing the total number of non-redundant spectra that correlated significantly with each cognate protein to the molecular weight of the protein and multiplying by 10^4 (Powell et. al., 2004).

Identification of Phosphorylated Components of eIF3

TAP-Rpg1 and an unlabeled strain were metabolically labeled with ^{32}P-orthophosphate at early stationary phase in rich media. eIF3 was purified, the protein components were separated by SDS-PAGE, and phosphorylation was detected by autoradiography. Prominent bands corresponding to the molecular weight of eIF3 components were identified by mass spectrometry analysis of the corresponding bands excised from the unlabeled eIF3 complex analyzed in parallel.

Results

In Vivo Interaction of eIF3 Components

The goals of this study were to identify comprehensively the composition of the *S. cerevisiae* eIF3 complex and dissect the sites of *in vivo* phosphorylation. To this end, I first established an approach for high-quality purification of the eIF3 complex using epitope tags and tandem affinity purification (TAP). This approach enables the efficient recovery of proteins present at low cellular concentrations under native conditions (Rigaut et. al., 1999). I used individually TAP-tagged yeast strains in which the fusion proteins are driven by native promoters, avoiding overexpression (Gavin et. al., 2002; Ghaemmaghami et. al., 2003). eIF3 complexes were purified in duplicate from four different yeast strains, each expressing a different TAP-tagged protein (Rpg1, Nip1, Prt1, or Tif5) (Browning et. al., 2001). To control for purification of non-specific proteins, three independent extracts were prepared and analyzed in parallel from an isogenic untagged yeast strain (BY4741). The isolated eIF3 complexes and control purifications were trypsin-digested in solution, and the proteins were identified using the 2-D LC-MS/MS mass spectrometry approach termed Multidimensional Protein Identification Technology (MudPIT) (Fig. 1B) (Link et. al., 1999 ;Sanders et. al., 2002; Fleischer et. al., 2006). To estimate the relative abundance of each protein, a Protein Abundance Factor (PAF) was calculated using the acquired mass spectrometry data (Powell et. al., 2004). A PAF is a label-free, semi-quantitative measure of a protein's relative abundance and is

based on the fact that a protein's abundance is directly related to the frequency at which its peptides are selected for MS/MS analysis.

Figure 2-1

A

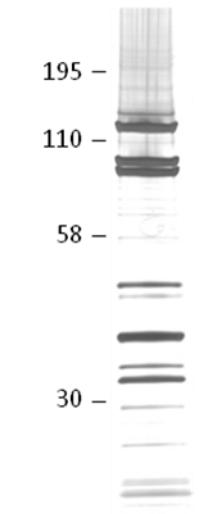

B

	Yeast Protein	Locus	MW	TAP-Rpg1	TAP-Nip1	TAP-Prt1	TAP-cntrl
eIF3 Subunits	Rpg1	YBR079C	110	6.9 (1.0)	6.6 (1.21)	8.3 (1.02)	nd
	Nip1	YMR309C	93	5.2 (0.75)	5.5 (1.0)	6.6 (0.81)	nd
	Prt1	YOR361C	88	7.0 (1.02)	5.3 (0.98)	8.1 (1.0)	nd
	Tif34	YMR146C	39	8.5 (1.23)	7.7 (1.41)	8.5 (1.05)	nd
	Tif35	YDR429C	30	6.2 (0.90)	1.5 (0.48)	7.2 (0.90)	nd
Associated Initiation Factors	Tif5	YBR041W	45	7.1 (1.02)	1.5 (0.28)	2.9 (0.04)	nd
	Sui1	YNL244C	12	4.9 (0.71)	nd	nd	nd
	Hcr1	YLR192W	29	4.1 (0.60)	1.6 (0.31)	0.7 (0.09)	nd
	Fun12	YAL035W	113	0.9 (0.13)	0.4 (0.07)	0.1 (0.01)	nd
	Pab1	YER165W	64	1.2 (0.17)	nd	nd	nd
	Sui2	YJR007W	35	nd	nd	0.4(0.05)	nd
	Sui3	YPR237C	32	0.3 (0.04)	0.3 (0.06)	0.3 (0.04)	nd
	Gcd11	YER025W	56	0.06(0.01)	nd	0.5(0.06)	
CK2 Subunits	Cka1	YIL035C	45	0.2 (0.03)	nd	nd	nd
	Cka2	YOR061C	39	0.3 (0.04)	nd	0.5 (0.06)	nd
	Ckb1	YGL019W	32	0.3 (0.04)	nd	nd	nd
	Ckb2	YOR029C	29	0.3 (0.04)	nd	nd	nd

Figure 2-1. Purification and mass spectrometry identification of eIF3 components. The eIF3 complex was isolated from *S. cerevisiae* by tandem affinity purification (TAP). Complexes and control extracts were prepared in duplicate or triplicate from strains expressing affinity tags specific for three core eIF3 components (Rpg1, Nip1, and Prt1) and the translation initiation factor Tif5, as well as an isogenic, untagged yeast strain. (A) Silver-stained SDS-PAGE separation of a TAP-Rpg1 purification. (B) MudPIT mass spectrometry analysis of the purifications from the four different TAP-tagged strains and the control strain (TAP-cntrl). The results from one of the replicate experiments are shown. The predicted molecular weights (MW) of the identified yeast proteins (rows) are shown in kDa. For each tagged strain and the control, protein abundance factors (PAFs) were calculated for the identified proteins (PAF = (the number of non-redundant spectra identifying the protein) / (MW of the protein) $x10^4$ (Powell et. al., 2004). The relative stoichiometry of each protein (in parentheses) was determined by normalizing its PAF to the PAF of the TAP-tagged protein targeted in the purification. (nd:not detected).

We routinely identified the five primary components of yeast eIF3 (Rpg1, Nip1, Prt1, Tif34, and Tif35) at greater than 75% coverage (Fig. 1B). The PAFs suggest that these proteins have equivalent stoichiometries. I also identified other translation initiation factors co-purifying in our eIF3 preparations, including the yeast orthologs of mammalian eIF5 (Tif5), eIF3j (Hcr1), eIF1 (Sui1), eIF2β (Sui3), eIF5B (Fun12), and PABC1 (Pab1) (Fig 1B). With the exception of Fun12 and Pab1, earlier studies have reported similar eIF3 interactions (Hinnebusch et. al., 2004). As expected, the PAFs values were lower for these six non-core, co-purifying translation initiation factors.

Interestingly, purifications based on different tagged targets yielded distinct subsets of co-purifying translation initiation factors, and the results were consistent in replicate purifications (Figure 2-1B). I performed reciprocal purifications targeting the previously uncharacterized interactions of Fun12 and Pab1 and detected co-purifying eIF3 components but at lower abundances (Fig. 2-1B, Table 2-1 and Table 2-2). These results are consistent with a model in which these six translation initiation factors act as accessories in eIF3 function. Additionally, I consistently observed the yeast Casein Kinase 2 complex (CK2) copurifying with the TAP-Rpg1 isolation of eIF3 (Fig. 2-1B). In yeast, CK2 is a tetramer consisting of two catalytic subunits (Cka1 and Cka2) and two regulatory subunits (Ckb1 and Ckb2) (Ackermann et. al., 2001; Pinna, 2002). However, the PAF values were relatively low, indicating that the CK2 subunits associate with eIF3 at substoichiometric levels, consistent with the transient nature of kinase-substrate interactions. The CK2 subunits were not detected in the controls or in

a large number of independent TAP/MudPIT experiments using yeast strains with different TAP-tagged proteins (Link *et al*, manuscript in preparation), suggesting a specific interaction of CK2 with eIF3. I further investigated the physical association of CK2 with eIF3 by targeting TAP-Ckb2 for protein purification. LC-MS/MS analysis of purified TAP-Ckb2 confirmed that the isolate contains all components of CK2 as well as all five core subunits of eIF3. Control purifications from an untagged strain contained neither CK2 nor eIF3 (Table 2-3).

Table 2-1

Yeast Protein	Locus	TAP-Fun12	negative control
Fun12	YAL035W	5.1(1)	nd
Tif34	YMR146C	0.43(0.084)	nd
Tif35	YDR429C	0.33(0.064)	nd
Rpg1	YBR079C	0.18(0.035)	nd
Nip1	YMR309C	0.071(0.014)	nd
Prt1	YOR361C	0.038(0.0074)	nd
Tif5	YBR041W	nd	nd

TABLE 2-1. Mass spectrometry identification of Fun12 interactions. Fun12 protein complexes were isolated from an *S. cerevisiae* strain expressing TAP-Fun12 and an isogenic, untagged yeast strain as a negative control. MudPIT mass spectrometry analyses of the purified complexes were performed in triplicate. PAF values were used to approximate protein abundances as in Fig. 2-1.

Table 2-2

Gene	Locus	TAP-Pab1	negative control
Pab1	YER165W	12(1)	nd
Nip1	YMR309C	0.036(0.0030)	nd
Rpg1	YBR079C	0.030(0.0025)	nd
Prt1	YOR361C	nd	nd
Tif34	YMR146C	nd	nd
Tif35	YDR429C	nd	nd
Tif5	YBR041W	nd	nd

Table 2-2. Mass spectrometry identification of Pab1 interactions. Pab1 was isolated from an *S. cerevisiae* strain expressing TAP-Pab1 and an isogenic, untagged yeast strain as a negative control. MudPIT mass spectrometry analyses of the purified complexes were performed in triplicate. PAF values were used to approximate protein abundances as in Fig. 2-1.

Table 2-3

Yeast Protein	Locus	TAP-Ckb2	negative control
Cka1	YIL035C	6.3(1.2)	nd
Cka2	YOR061C	5.6(1.0)	nd
Ckb2	YOR029C	5.5(1.0)	nd
Ckb1	YGL019W	3.6(0.66)	nd
Tif34	YMR146C	2.1(0.38)	nd
Rpg1	YBR079C	2.1(0.39)	nd
Tif35	YDR429C	1.9(0.34)	nd
Nip1	YMR309C	1.5(0.27)	nd
Prt1	YOR361C	1.5(0.28)	nd
Tif5	YBR041W	nd	nd

TABLE 2-3. Mass spectrometry identification of CK2 interactions. CK2 complexes were isolated from an *S. cerevisiae* strain expressing TAP-Ckb2 and an isogenic, untagged yeast strain as a negative control. MudPIT mass spectrometry analyses of the purified complexes were performed in triplicate. PAF values were used to approximate protein abundances as in Figure. 1.

Casein Kinase 2 Phosphorylates Nip1, Prt1, and Tif5 *In Vitro*

To test whether CK2 directly phosphorylates eIF3 components, I used an *in vitro* kinase assay. I purified GST-tagged Cka1 and Ckb1 as well as eight randomly selected serine/threonine yeast protein kinases with GST tags as controls. Isolation of the kinases was inferred from observation of SDS-PAGE bands with appropriate molecular sizes. To identify autophosphorylation, control reactions with no eIF3 substrate were performed for each kinase. The Cka1 catalytic subunit phosphorylated eIF3 components above background (Fig. 2-2). The TAP pull-down targeting the CK2 regulatory subunit, Ckb1, phosphorylated eIF3 to a lesser extent. The kinase activity of the Ckb1 preparation suggests that catalytic components of the CK2 complex co-purified with this regulatory subunit. The results of the Yck1 assays are ambiguous due to apparent Yck1 auto-phosphorylation. None of the other kinases had any effect, although I cannot say for certain they are active as no autophosphorylation was detected. Yet it is clear that Cka1 has a striking ability to phosphorylate eIF3.

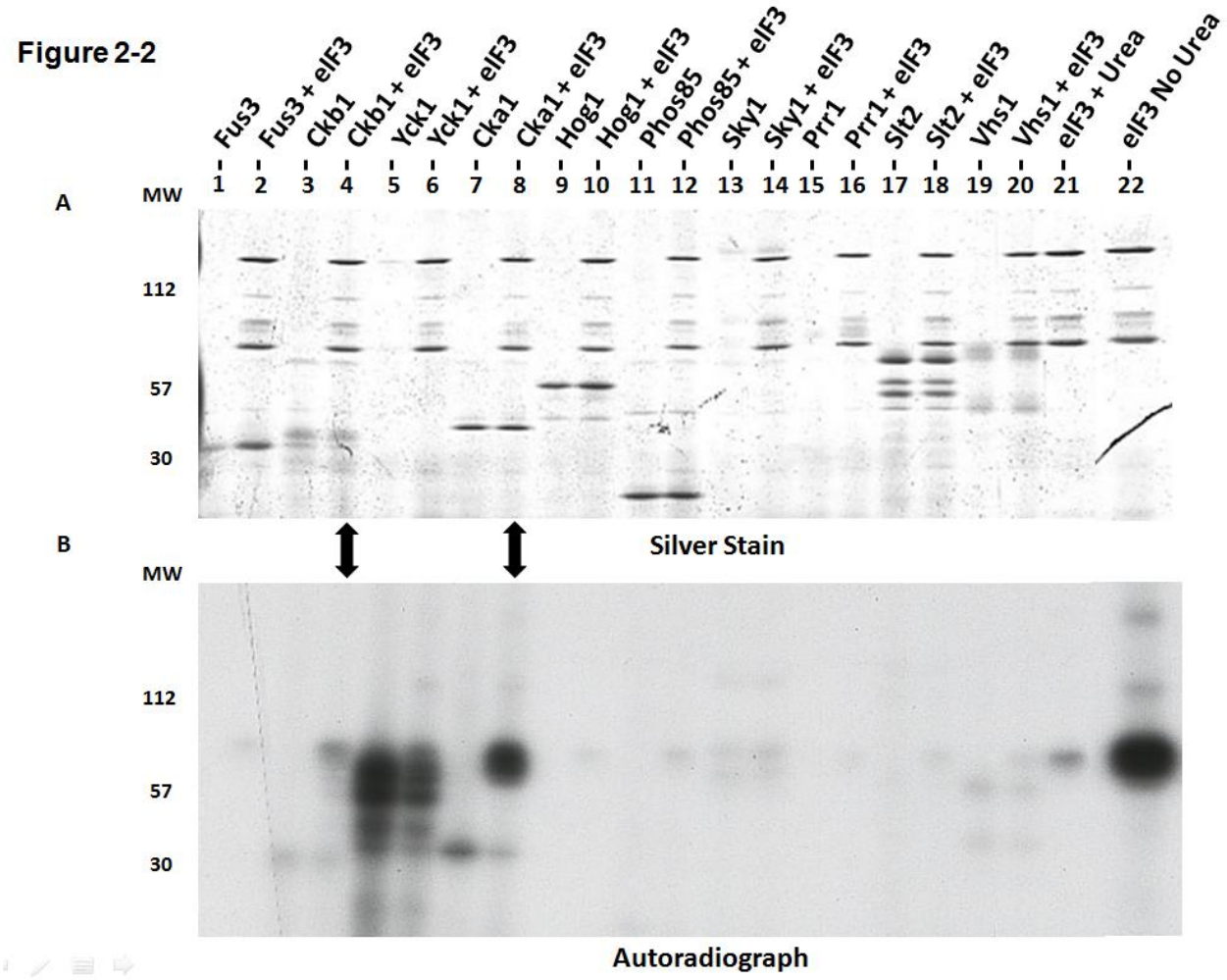

Figure 2-2. ***In vitro*** **kinase screen identifies CK2 as an eIF3 kinase.** GST-tagged Cka1, Ckb1, and eight control kinases were enriched and incubated with [γ-^{32}P]ATP plus purified eIF3 treated with urea to reduce background kinase activity. Reaction products were separated on a 10% SDS-polyacrylamide gel and subjected to autoradiography. In the far right lane, purified eIF3 without urea treatment shows significant endogenous kinase activity. Arrows highlight phosphorylation of eIF3 components above background levels by the Cka1 catalytic subunit and to a lesser extent the Ckb1 regulatory subunit.

Analysis of the eIF3-Cka1 reaction products allowed us to determine which eIF3 components are phosphorylated by Cka1. SDS-PAGE showed the major phosphorylated product is in the size range of Nip1 and Prt1 (Fig. 2-3A). A gel with a lower percentage of acrylamide allowed separation of Nip1 and Prt1 and showed that both proteins are Cka1 substrates, with Nip1 the predominant target (Fig. 2-3B). Mass spectrometry analysis of these two bands confirmed that only Nip1 and Prt1 were present but yielded no information as to the phosphorylation status of the proteins due to a failure to detect these regions of the proteins in the analysis.

Figure 2-3

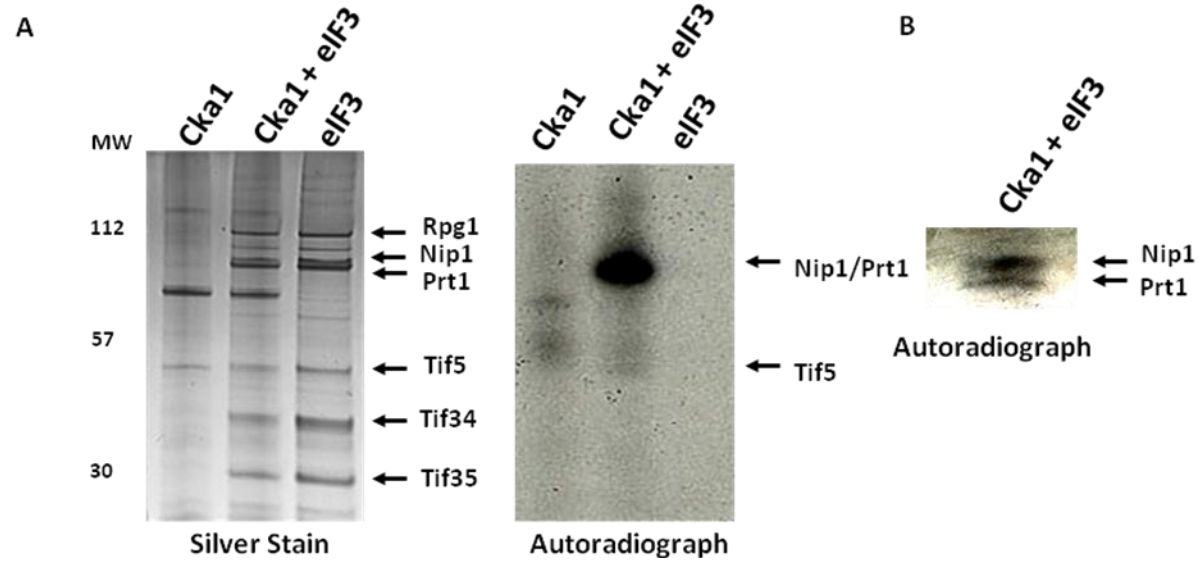

Figure 2-3. CK2 phosphorylates Nip1 and Prt1 *in vitro*. SDS-PAGE separation was used to identify eIF3 components phosphorylated in *in vitro* kinase reactions with GST-tagged Cka1. (A) Separation on a 10% gel indicates that CK2 phosphorylates Nip1 and/or Prt1. (B) Separation on a 7.5 % gel resolves the most prominent phosphorylated band in (A) into a doublet and shows both Nip1 and Prt1 are phosphorylated by Cka1. Nip1 appears to be more prominently ^{32}P-labeled compared to Prt1.

Discussion

In this study, I have used various mass spectrometry approaches to study the molecular composition of the highly conserved translation initiation factor eIF3 in *S. cerevisiae*. I used tandem affinity purification to isolate eIF3 complexes from tagged yeast strains and direct LC-MS/MS analysis of the complexes to identify core components of eIF3 as well as more loosely associated factors. To optimize our purification strategy, I affinity purified eIF3 based on three different tagged core components as well as the associated factor Tif5. The TAP-Rpg1 and TAP-Prt1 purifications resulted in the highest yield of eIF3 subunits. This finding is consistent with the previously described roles of Rpg1 and Prt1 in scaffolding and structural maintenance of the core eIF3 complex and in mediating interactions with Hcr1, eIF1, eIF5, and the eIF2 ternary complex (Asano et. al., 2000; Asano et. al., 2001; Valasek et. al., 2001).

We confirmed that the yeast eIF3 complex is composed of five conserved core components: Rpg1 (eIF3a), Nip1 (eIF3c), Prt1 (eIF3b), Tif34 (eIF3i), and Tif35 (eIF3g). I also identified other translation initiation factors co-purifying with eIF3. Similar to previous reports, I found Tif5 (eIF5), Sui1 (eIF1), Hcr1 (eIF3j), Sui3 (eIF2β) associated with eIF3 at substoichiometric levels (Hinnebusch et. al., 2004; Asano et. al., 2000; Valasek et. al., 2001). Importantly, I also identified novel interactions of eIF3 with Fun12 (eIF5B) and Pab1 (PabP). Like the other eIF3-associated factors, Fun12 and Pab1 were found at low levels and were absent from some eIF3 preparations. Fun12 has been shown to facilitate the

joining of the 40S and 60S ribosomal subunits in the terminal step of translation initiation (Pestova et. al., 2000). In addition, *Δfun12* null strains have a slow growth phenotype and altered polysome profiles suggesting a defect in translation initiation (Choi et. al., 1998). eIF3 has been shown to interact with the 40S subunit in the assembly of the 48S pre-initiation complex (Hinnebusch et. al., 2004; Asano et. al., 2001). I postulate that the interaction of eIF3 with Fun12 links the formation of the pre-initiation complex with the binding of the 60S ribosome and the termination of translation initiation. Similar to Fun12, *Δpab1* deleted strains have decreased levels of translation initiation (Sachs and Davis, 1990).

Pab1 has been shown to facilitate the joining of the 5' and 3' ends of mRNA by binding the initiation scaffold protein eIF4G (Tarun and Sachs, 1996; Cosson et. al., 2002). eIF4G along with eIF4A and eIF4E form eIF4F (Hernandez and Vazquez-Pianzola, 2005). eIF4F facilitates the interaction of the 43S pre-initiation complex with the 5' cap structure of the mRNA producing the 48S pre-initiation complex. Efficient formation of the 48S pre-initiation complex is also dependent on eIF3 (Hinnebusch et. al., 2004). Our finding that Pab1 interacts with the eIF3 complex complements the previous findings and suggests a role in this interaction in the efficient formation of the 48S pre-initiation complex. I believe that our ability to identify novel interactions of a previously well characterized complex stems from our approach combining gentle affinity

purification based on multiple eIF3 components with a sensitive and comprehensive protein identification using mass spectrometry.

We found that CK2 subunits co-purify with eIF3 and that, in a reciprocal purification of TAP-Ckb1, eIF3 components co-purify with the CK2 complex. Our data are consistent with a previously described interaction between the CK2 kinase and eIF3 (Gavin et. al., 2002). Using *in vitro* kinase assays, I found that CK2 phosphorylates both Nip1 and Prt1. Interestingly, the phosphorylated regions of Nip1 and Prt1 are predicted to stabilize both protein interactions within the eIF3 complex and interactions of eIF3 with other components of the multifactor pre-initiation complex (Hinnebusch et. al., 2004).

Casein Kinase 2 is a conserved serine/threonine protein kinase that is ubiquitous in eukaryotes. Despite numerous studies, its regulation and physiological role is still poorly understood (Glover, 1998). Yeast strains with null alleles of either one of the two catalytic subunits (*Δcka1* or *Δcka22*) are viable. However, deletion of both genes is lethal, showing that CK2 activity is essential for *S. cerevisiae* viability (Padmanabha et. al., 1990). Yeast strains with null alleles of either or both regulatory subunits (*Δckb1 or Δckb2*) are viable but are salt sensitive (Bidwai et. al., 1995). A number of CK2 substrates have been reported, leading to the hypothesis that this kinase plays an essential role in several biological processes (Pinna, 2002).

Several other components of the yeast translation initiation machinery are CK2 targets. Phosphorylation of the eIF2-α subunit of the eIF2 translation

initiation complex is required for its optimal function but is not essential for viability (Feng et. al., 1994). The yeast eIF4E cap binding protein and the 4E-BP protein Caf20/p20 are also phosphorylated *in vitro* by CK2 (Zanchin and McCarthy, 1995).

CHAPTER III

DETERMINING SITES OF PHOSPHORYLATION AND THEIR RELEVANCE IN eIF3

Abstract

The previous chapter demonstrated that eIF3 copurifies with the yeast kinase CK2. Reciprocal isolates of affinity tagged CK2 components purify all five core components of eIF3. *In vivo* experiments suggest that Nip1 is the predominant band in ^{32}P autoradiography. *In vitro* assays demonstrate that CK2 phosphorylates both Nip1 and Prt1 of eIF3. The next step was to use tandem mass spectrometry as well as immobilized metal affinity chromatography (IMAC) chromatography to enrich for and identify specific residues that are phosphorylated *in vivo* in *S. cerevisiae*. Using this approach I was able to identify three sites of phosphorylation (S98, S99, and S103) on Nip1. I also found that Prt1 is phosphorylated at S61 and T746. Both the sites on Nip1 and Prt1 are predicted to be consensus sites targeted by CK2. Additionally, the Tif5 site T191 was identified as a phosphorylated residue. However, this site is not predicted to be targeted by CK2. This study targeted Nip1 with its triply phosphorylated motif for further investigation. Using *in vitro* kinase assays, I

showed that a synthetic Nip1 peptide containing S98, S99, and S103 competitively inhibits the phosphorylation of Nip1 by CK2.

I hypothesized that the three sites of phosphorylation play a role in regulating the function of Nip1 and as a result, have implications in the activity of the eIF3 complex. Further understanding the role that these modifications have on the eIF3 complex has implications into how its role is regulated at the level of posttranslational modifications. To investigate this, I compared biochemical assays of a yeast strain with the three serines mutated to alanines with a strain harboring no mutations in this region. Drug, temperature, nutrient starvation, and salt sensitivity were evaluated for the strains using plate assays and polysome profiling. Global protein synthesis was monitored via ^{35}S-methionine incorporation. Overall, the only measureable consequence detected with replacement of the three Nip1 serines with alanines was a slow growth phenotype.

Introduction

Protein kinases are key regulators of cell function and are believed to affect translation efficiency directly (Sonenberg et. al., 2000; Klann and Dever, 2004). By phosphorylating a protein, kinases can alter the substrate's activity, interactions, and stability. The functions of several eIF complexes are regulated by phosphorylation. The best characterized of these phosphorylation events involve regulation of eIF2 and eIF4E (Gray et. al., 1998). eIF2 is bound to GDP in an inactive state at the end of each round of translation initiation. To

reconstitute a functional ternary complex for a new round of translation initiation, eIF2B catalyzes the exchange of GDP for GTP (Unbehaun et. al., 2004). Phosphorylation of the eIF2 subunit eIF2α effectively blocks eIF2B-mediated GDP-GTP exchange, thus inhibiting protein synthesis (Sudhakar et. al., 2000). Phosphorylation also regulates association of eIF4E with the eIF4F mRNA-cap binding complex. This interaction is required for cap-dependent mRNA translation initiation and is inhibited by the eIF4E-binding protein (4E-BP) (Hernandez and Vazquez-Pianzola, 2005). Phosphorylation of 4E-BP attenuates this inhibition (Waskiewicz et. al., 1999). In its hypophosphorylated state, 4E-BP binds to eIF4E and prevents its association with eIF4F (Gingras et. al., 1999). In its hyperphosphoryated state, 4E-BP binds poorly to eIF4E. 4E-BP phosphorylation is stimulated by many different external stimuli including growth factors, hormones, and mitogens (Gingras et. al., 1999). Finally, eIF4 is also phosphorylated. Phosphorylation of S209 is stimulated by different mitogen-activated protein kinase pathways and correlates with increased translation rates (Pyronnet et. al., 1999; Waskiewicz et. al., 1999; Scheper et. al., 2001).

Casein Kinase 2 (CK2) is a selective serine/threonine protein kinase composed of 4 subunits capable of phosphorylating a broad range of substrates including transcription factors and RNA polymerases (Ahmed and Thornalley, 2003). In yeast, CK2 has been implicated in cell growth and proliferation (Ackerman et. al., 2001). Two subunits alpha one and alpha two contain the catalytic domains of the complex. The other two beta subunits are regulatory domains that undergo transphosphorylation (Bidwai et. al., 1994). The subunits

share > 90% homology. Deletion of a single alpha or beta domain allows the cells to remain viable. However, deletion of both of either the alpha or beta proteins causes lethality. CK2 is constitutively expressed at modest levels and is predominantly localized to the nucleus (Poole et. al., 2005). It is predicted to phosphorylate hundreds of proteins that reside in either the nucleus or cytoplasm (Lee et. al., 2004).

We have used mass spectrometry techniques to identify the components of eIF3 and specific residues that are phosphorylated *in vivo*. Mass spectrometry has become the method of choice for identifying the composition of a protein complex (Aebersold and Mann, 2003). However, although protein identification by mass spectrometry has become routine, protein phosphorylation analysis remains a challenging problem. Low phosphorylation stoichiometry, heterogeneous phosphorylation sites, and low protein abundance contribute to the difficulty of phosphoprotein analysis (Farley and Link, 2009). In addition, phosphopeptides are generally difficult to analyze by mass spectrometry for a number of reasons (Mann et. al., 2002). Reduced ionization efficiency in positive ionization mode and suppression by nonphosphorylated peptides exacerbate the problems. To improve the efficiency of phosphopeptide analysis, various strategies have been developed to enrich for phosphopeptides including strong cation exchange chromatography (SCX), immunoaffinity capture using antiphosphotyrosine antibodies, and immobilized metal affinity chromatography (IMAC) (Beausoleil et. al., 2004; Rush et. al., 2005; Andersson and Porath, 1986). IMAC was initially plagued by the nonspecific retention of peptides rich in

acidic amino acids, but improvements have increased both the specificity and sensitivity of IMAC (Ficarro, 2002; Ficarro, 2005; Moser and White, 2006). The direct coupling of IMAC with high sensitivity reversed-phase liquid chromatography and tandem mass spectrometry has enabled us to identify phosphopeptides starting with small amounts of material.

Materials and Methods

Plasmids

Plasmid pNip1entry (ScCD00008839) containing the wild-type Nip1 gene in a Gateway entry vector was obtained from the Harvard Institute of Proteomics (Boston, MA) and sequenced verified. It was recombined with the destination clone pAG415GPD-ccdB-TAP from Addgene (Cambridge, MA) as previously described (Alberti et. al., 2007) to generate pNip1a. The identified sites of phosphorylation, S98, S99 and S101, were converted to alanines by site directed mutagenesis (Ishii et. al., 1998) using the primers nip1mutfwd (GCTCTAACTATGATGCCGCTGATGAAGAAGCCGATGAAGAAG) and nip1mutrev (CTTCTTCATCGGCTTCTTCATCAGCGGCATCATAGTTAGAGC) to generate pNip1b. The endogenous stop codon was removed from both pNip1a and pNip1b with the primers nip1stopfwd (CCATCAAATCGTCGTGCGACCCAGC) and nip1stoprev (GCTGGGTCGCACGACGATTTGATGG) to generate pNip1wtTAP and pNip1mutTAP. All clones were sequence verified. pNip1comp, expressing Nip1

with a URA3 selectable marker (Valasek et. al., 2004), was obtained from Dr. Alan Hinnebusch's laboratory.

Direct Mapping of Phosphorylated Sites on eIF3 Components with Tandem Mass Spectrometry

The eIF3 complex was purified from whole-cell lysates prepared from 4 L overnight cultures of the TAP-Rpg1 strain (Powell et. al., 2004; Link et. al., 2005). Purified complexes were digested directly in solution with sequencing grade trypsin (Promega, Madison, WI) or chymotrypsin (Roche Diagnostics Corp., Indianapolis, IN) (Sanders et. al., 2002) and analyzed by MudPIT using an LTQ linear ion trap mass spectrometer (Thermo Electron, Inc).

Mapping eIF3 Phosphopeptides using IMAC Enrichment and Tandem Mass Spectrometry.

The *S. cerevisiae* strain expressing a TAP-Rpg1 was grown overnight ($O.D._{600}$ 2-4) in 16 L of YPD medium. eIF3 complexes were TAP-isolated from whole cell lysates (Link et. al., 2005). The pH of the eluted eIF3 mixture was adjusted to 8.0 using 1 M Tris pH 8.0. Cysteine residues were reduced with DTT and alkylated with iodoacetamide. The proteins were digested with 20 µg of sequencing grade trypsin (Sanders et. al., 2002) (Promega, Madison, WI). The tryptic peptide mixture was divided into 1 mL aliquots and lyophilized. To methyl esterify the peptides, a pre-mix of 1 mL anhydrous methanol and 50 µL thionyl chloride (Sigma-Aldrich, St. Louis, MO) was added to the dried peptides. The

mixture was sonicated for 15 min at room temperature and incubated at room temperature for 2 h. Esterified peptides were lyophilized to dryness.

An IMAC column was constructed using a fritted 20 cm long piece of 200 x 360 μm fused silica capillary (FSC). The column was packed with POROS MC 20 beads (Applied Biosystems, Foster City, CA) to a length of 15 cm. The column was rinsed with 100 mM EDTA (Sigma-Aldrich, St. Louis, MO), pH 8.5 and then with deionized water. The column was charged with 100 mM Iron(III) chloride solution (Sigma-Aldrich, St. Louis, MO). Finally, the IMAC column was rinsed with 0.1% acetic acid.

The dried, esterified peptides were resuspended in 180 μL of 33% methanol, 33% acetonitrile, and 0.034% acetic acid and loaded onto the IMAC column. Following loading, the column was rinsed with a solution of 25% acetonitrile, 100 mM NaCl, and 1% acetic acid.

A reversed-phase capture column was constructed from 20 cm of 100 x 360 μm FSC fritted at one end using an inline MicroFilter Assembly (Upchurch Scientific, Inc, Oak Harbor, WA). The RP-capture column was packed with POROS 10 R2 (Applied Biosystems, Foster City, CA) to a length of 10 cm. Using a 0.012 X 0.060 inch piece of Teflon tubing (Zeus, Orangeburg, SC), the RP-capture column was butt-jointed to the IMAC column. Phosphopeptides were eluted from the IMAC column onto the RP-capture column with 250 mM sodium phosphate, pH 8.0 solution.

The RP-capture column was rinsed overnight with 5% acetonitrile and 0.1% formic acid and attached to an analytical RP chromatography column (100 x 365 μm FSC with an integrated laser-pulled emitter tip packed with 10 cm of Synergi 4 μm RP80A (Phenomenex) via the inline MicroFilter Assembly for LC-ESI-MS/MS analysis. Peptides were eluted using the following linear gradient: 0 min: 0% B, 120 min: 40% B, 140 min: 60% B, 160 min: 100% B at a flow rate of 400 nL/min (mobile phase A: 5% acetonitrile, 0.1% formic acid and mobile phase B: 80% acetonitrile, 0.1% formic acid).

Spectra were acquired with a LTQ linear ion trap mass spectrometer (Thermo Electron, Inc). During LC-MS/MS analysis, the mass spectrometer performed automated data-dependent acquisition with a full MS scan followed by three MS/MS scans on the most intense ions while operating under dynamic exclusion.

Mass Spectrometry Data Analysis

Data analysis of spectra generated by the mass spectrometer was performed as described in Chapter 2. To validate candidate phosphopeptides, tandem mass spectra were manually evaluated to identify evidence of neutral loss of phosphoric acid caused by fragmentation of the precursor ion (98 (z=+1), 49 (z=+2), or 32.7 (z=+3) *m/z* units relative to the precursor). For all IMAC mass spectrometry data, the acquired mass spectrometry data were searched against the yeast ORF database using the Sequest algorithm assuming static modifications of +14 on D, E, and the C-termini, static modification of +57 on C,

and variable modifications of +80 on S, T, and Y (Yates et. al., 1995). Our criteria in identifying phosphorylations were: 1) a series of at least 3 y or b ions with an appropriate +80 Dalton shift, and 2) ions indicating a neutral loss of phosphoric acid from the precursor ion.

Scansite Predictions

The Scansite computational tool is accessible via the web-page (http://scansite.mit.edu). The accession number for each individual protein of interest is entered into the appropriate field and the yeast database selected. The casein kinase 2 motif is selected (SXXE/D) along with the stringency level (high) and the scan is submitted. Scansite generates scores based upon how well the submitted sequence matches the predicted motif. A high stringency level reflects a Scansite score that falls within the top 0.2% of scores when the motif matrix is applied to a reference dataset from SWISS-PROT. Medium and low stringencies reflect Scansite scores of 1% and 5% respectively. The search is then subsequently repeated at the medium and low stringency levels.

Inhibition of *In Vitro* Phosphorylation

A peptide inhibitor containing Nip1 phosphorylation sites (H2N-SSNYDSSDEEDSDDDGK-OH) was synthesized to mimic the tryptic peptide of Nip1 identified by mass spectrometry (New England Peptides Gardner, MA). A control peptide (H_2N-ISQAVAHAHAEINEAGR-OH) that contains an identical number of amino acids but lacks CK2 consensus sequence sites for

phosphorylation was synthesized (New England Peptides). The peptides were suspended at 1 mg/mL in 100 mM Tris, pH 8.0 to a concentration of 1 mg/mL. The CK2 inhibitor (E)-3-(2,3,4,5-Tetrabromophenyl)acrylic acid (TBCA) and the CK1 inhibitor 3-[(2,4,6-Trimethoxyphenyl)methylidenyl]-indolin-2-one (IC261) were obtained from Calbiochem (Gibbstown, NJ) and resuspended to 1 mg/mL in DMSO (Pagano et. al., 2007; Knippschild et. al., 1997). The peptides and kinase inhibitors were added to kinase reactions described above to a final concentration of 33 μg/mL.

Polysome Profile Analysis

Overnight cultures of the appropriate yeast strains were grown overnight from single colony inoculations of 50 mL of YPD culture to an OD_{600}=0.5-1. Cyclohexamide is added to a concentration of 50 μg/mL and the resulting mixture chilled on ice. Cells were centrifuged for 10 min at 3000 g and washed once with breaking buffer (10 mM Tris-HCl, pH 7.5, 100 mM NaCl, 30 mM $MgCl_2$, 50 μg/mL cyclohexamide, 200 μg/mL heparin). Cells were lysed in 200 μL of breaking buffer in a bead beater with 0.5 mm glass beads for three cycles of one min beating followed by one min on ice. Lysates were centrifuged for 2 min at 13,000 g and the cleared supernatant loaded onto a 12 mL 7-47% sucrose gradient. Gradient solutions were prepared in gradient buffer (50 mM Tris-acetate, pH 7.0, 50 mM NH_4Cl, 12 mM $MgCl_2$). Lysates were separated within the gradients by spinning for 18 hr at 20,000 rpm in a Sorvall SW-41 rotor. Polysome profiles

were collected and monitored at an absorbance of 254 nm using an Agilent 1100 series microfraction collector and flow cell.

Halo Growth Assay

Plates for this assay were prepared with YPD plus 1% agar. 50 μL of an overnight culture of BY4741 yeast was added to the surface of the plate and spread evenly with a flame sterilized applicator. Four sterile discs were added evenly spaced onto the surface of the plate containing the yeast culture. Casein kinase 2 inhibitors, casein kinase II inhibitor 1 (TBB), casein kinase I inhibitor (D4476), casein kinase II inhibitor III (TBCA), casein kinase II inhibitor (DMAT), 3-[(2,4,6-Trimethoxyphenyl)methylidenyl]-indolin-2-one (IC261), 5,6-Dichloro-1-b-D-ribofuranosylbenzimidazole (DRB) (all EMD Chemicals), were added to a concentration up to 10X their inhibitory constant. The kinase inhibitors were either obtained in solution (10 mM DMSO) or dissolved to 10 mM in DMSO and tested by spotting onto sterile discs on a lawn of BY4741 yeast cells. As a negative control, DMSO was spotted onto each lawn. Inhibition of growth should be evident as a halo of nongrowth around the sterile paper disc spotted with the kinase inhibitor.

^{35}S-Met Incorporation

Overnight cultures grown in YPD were diluted 1:10 into 1 mL of SC-Met to an OD_{600} of approximately 0.5 in triplicate in a 96-well 2 mL culture plate and grown for 3 hr at 30°C. Cells were counted and normalized to each other. Each

sample in triplicate was labeled with 10 μCi/mL ^{35}S-methionine for 15 min at 30°C. Labeling was stopped by the addition of 1/10 volume of 100% TCA to each culture and heating the entire 96-well plate at 100°C for 30 min. TCA precipitates were collected on Whatman GPC filters, washed sequentially with 2 mL of each 10% TCA and 95% ethanol. The filter papers were then scintillation counted in 5 mL of Universol (ICN). Experiments were performed in triplicate to measure the standard deviation.

Quantifying the Doubling time of Wild-type and Mutant of Nip1

The growth rate of Δ*nip1* deletion mutants carrying either pNip1a (NIP1^{+}), pNip1b (nip1-S98,99,101A) or pNIP1b plus pNip1comp (NIP1^{+}) was measured. Single colonies from each strain were inoculated into YPD and grown overnight at 30°C. Cell density was calculated using a Countess automated cell counter from Invitrogen (Carlsbad, CA). 10,000 cells of each strain were transferred to fresh 6 mL cultures of YPD at 30°C. Aliquots from each strain were collected periodically, and cell density was calculated in triplicate until the cultures reached stationary phase. The triplicate density measurements were averaged. The doubling time (t_{dub}) for each strain was determined from the logarithmic growth phase of the cells using the following formula:

$$t_{dub} = \ln 2/((\ln D_2/D_1)/\Delta t_{min})$$

Where D is the cell density and Δt_{min} is the change in time in min from D_1 to D_2. The experiment was repeated in triplicate and the resulting doubling times were

averaged for each strain. A Student's *t*-test (95% confidence interval) was performed on the data to determine its statistical significance.

Results

Mass spectrometry Identification of *In Vivo* Prt1 and Tif5 Phosphorylation Sites

Mass spectrometry techniques can be used to pinpoint exact sites of protein modification, including phosphorylation. Our initial approach used MudPIT to identify eIF3 phosphopeptides directly from complexes purified from the TAP-Rpg1 strain. This direct approach avoided sample loss associated with strategies to enrich for phosphopeptides. TAP-isolated eIF3 samples were digested separately with either trypsin or chymotrypsin and analyzed using MudPIT. I used two different proteolytic enzymes to maximize peptide coverage and to facilitate identification of candidate phosphorylation sites on multiple overlapping peptides (MacCoss et. al., 2002).

Phosphorylations present several hallmarks in mass spectrometry analysis. First, the mass of a phosphorylated residue is increased by 80 Da. Second, when peptides containing phosphorylated serine or threonine residues are fragmented by resonance excitation in an ion trap, they commonly undergo a gas-phase ß-elimination reaction, resulting in the neutral loss of phosphoric acid ($-H_3PO_4$ or 98 Da) (Mann et. al., 2002). Depending on the charge of the precursor ion, neutral loss of phosphoric acid appears as a decrease of 98 (z=+1), 49 (z=+2), or 32.7 (z=+3) m/z units from the precursor. Finally, because

a phosphorylated residue increases the net negativity of the peptide in solution, it is expected to have a shorter retention time during SCX chromatography compared to the unmodified peptide (Beausoleil et. al., 2004). Our criteria in identifying phosphorylations were: 1) a series of at least 3 y or b ions with an appropriate +80 Dalton shift for the addition of a phosphate group, and 2) ions indicating a neutral loss of 98 Da from the precursor ion.

To identify candidate phosphorylation sites I used the Sequest algorithm to search for additions of 80 Da at serine, threonine, and tyrosine residues (Yates et. al., 1995). I anticipated that the *in vivo* phosphorylation would be incomplete (< 50%), and therefore I expected to identify the corresponding unmodified peptide as well. Once candidate sites were identified, I manually inspected the data for evidence of neutral loss events indicating phosphorylation. In this way, I identified two phosphorylation sites in Prt1 (Figure 3-1 and 3-2). Phosphorylation of a high stringency CK2 consensus site at S61 (PVDDIDF**pS**DLEEQYK) was identified in two independent trypsin and chymotrypsin experiments (http://scansite.mit.edu). Phosphorylation of a low stringency CK2 consensus site at T746 (CK2 consensus sequence: DASSDDFT**pT**IEEIVEE) was identified following trypsin digestion, but not using chymotrypsin (Figure 3-3). The corresponding unmodified versions of these peptides were also identified. As predicted, analysis of the SCX fractions in the MudPIT runs showed the phosphorylated peptides eluted first followed by the unmodified peptides. Additionally, a single Tif5 phosphopeptide was detected that contained a phosphorylated T191 (SQNAPSDGTGSS**pT**PQHHDEDEDELSR) (Figure 3-4).

However, the site does not fit the CK2 consensus sequence. To our surprise, I did not detect phosphopeptides from Nip1.

Figure 3-1

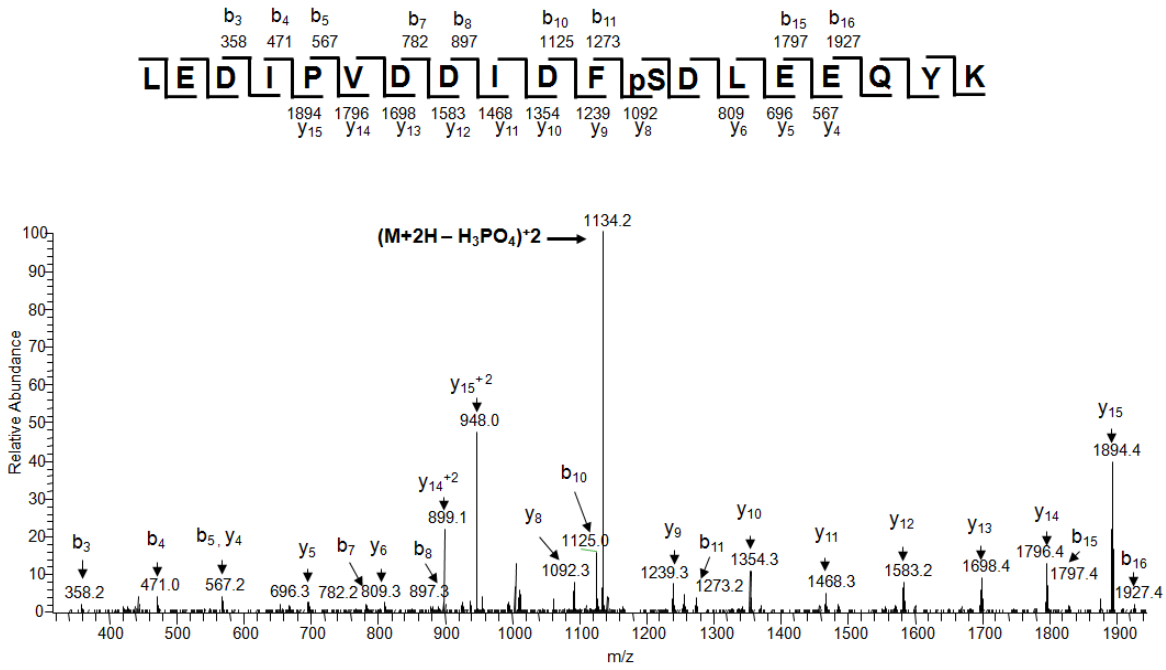

Figure 3-1. MS/MS spectra from eIF3 showing *in vivo* phosphorylation of Prt1 at S61. An MS/MS spectrum generated from trypsin-digested eIF3 showing *in vivo* phosphorylation of a Prt1 peptide at S61. The spectrum significantly matched the trypsin-generated peptide of Prt1 (Sequest Xcorr = 5.5). The spectrum shows the addition of 80 Da in the *m/z* values for the $y_{8\text{-}15}$ and $b_{15\text{-}16}$ ions. The *m/z* value of the most prominent ion corresponds to the neutral loss of phosphoric acid (+2) from the precursor ion of 1184.18 (+2).

Figure 3-2

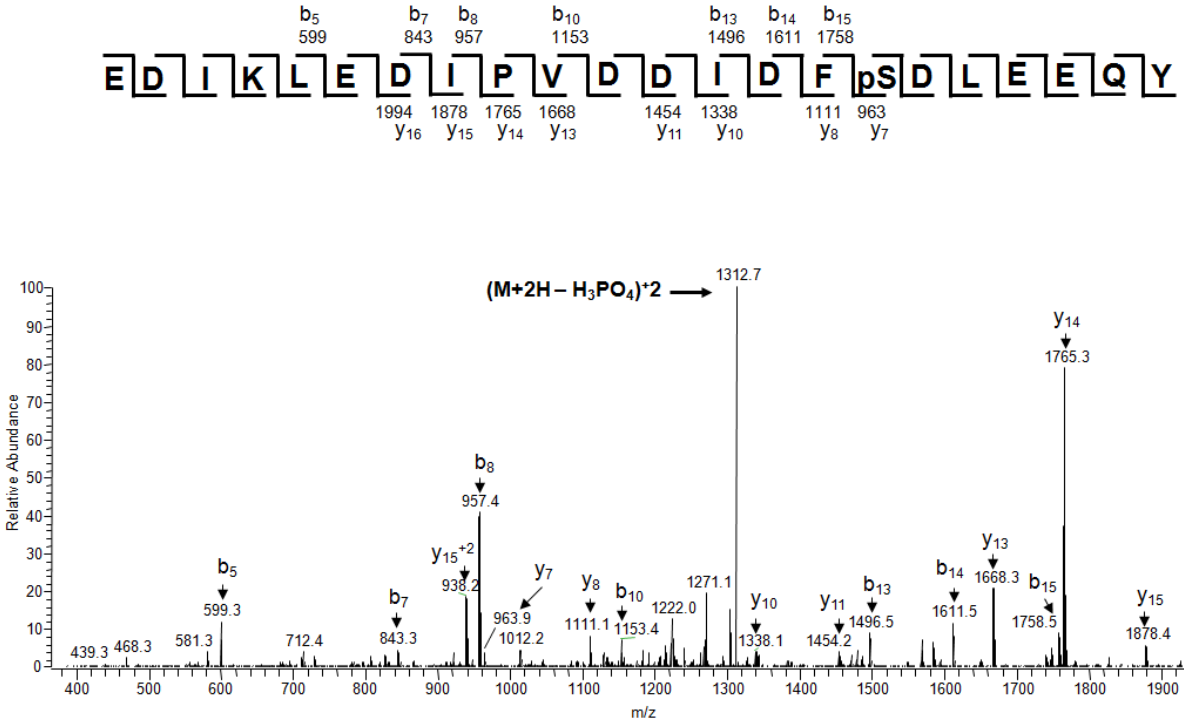

Figure 3-2. MS/MS spectra from eIF3 showing *in vivo* phosphorylation of Prt1 at S61. An MS/MS spectrum generated from chymotrypsin-digested eIF3 showing *in vivo* phosphorylation of a Prt1 peptide at S61. The spectrum significantly matched the chymotrypsin-generated peptide of Prt1 (Sequest Xcorr = 4.0). The spectrum shows the addition of 80 Da in the *m/z* values for the $y_{7\text{-}16}$ ions. The *m/z* value of the most prominent ion corresponds to the neutral loss of phosphoric acid (+2) from the precursor ion of 1362.8 (+2).

Figure 3-3

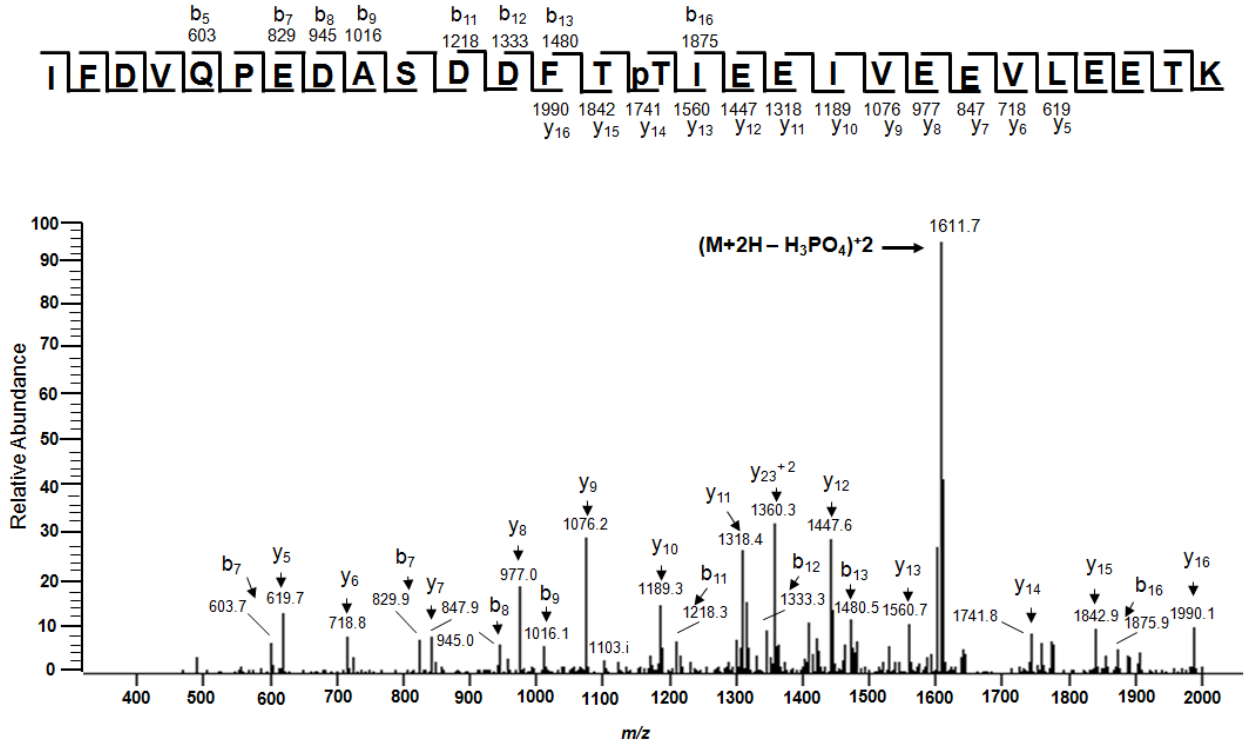

Figure 3-3. MS/MS spectra from eIF3 showing *in vivo* phosphorylation of Prt1 at T746. An MS/MS spectrum generated from trypsin-digested eIF3 showing *in vivo* phosphorylation of a Prt1 peptide at T746. The spectrum significantly matched the trypsin-generated peptide of Prt1 (Sequest Xcorr = 3.5). The spectrum shows the addition of 80 Da in the *m/z* values for the $y_{14\text{-}16}$ and b_{16} ions. The *m/z* value of the most prominent ion corresponds to the neutral loss of phosphoric acid (+2) from the precursor ion of 1661.1 (+2).

Figure 3-4

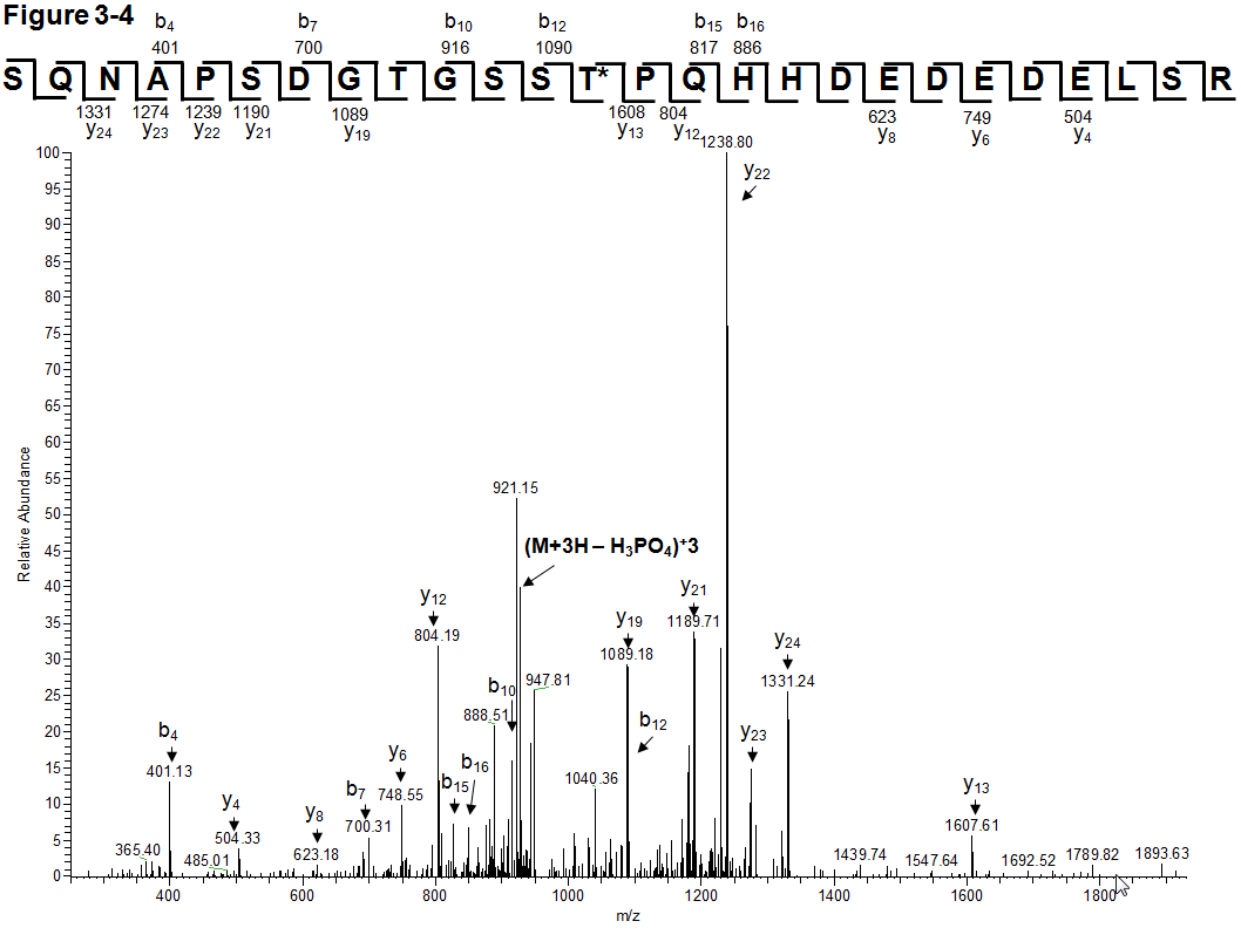

Figure 3-4. MS/MS spectra from eIF3 showing *in vivo* phosphorylation of Tif5 at T191. An MS/MS spectrum generated from trypsin-digested eIF3 showing *in vivo* phosphorylation of a Tif5 peptide at T191. The spectrum significantly matched the trypsin-generated peptide of Tif5 (Sequest Xcorr = 4.2). The spectrum shows the addition of 80 Da in the *m/z* values for the $y_{19\text{-}24}$ and $b_{15\text{-}16}$ ions. The *m/z* value of the peak at 927.2 corresponds to the neutral loss of phosphoric acid (+3) from the precursor ion of 959.8 (+3).

Our results using metabolic labeling (Figure 2-3) and the mass spectrometry illustrate the need for a multifaceted approach to comprehensively identify phosphorylations. ^{32}P-metabolic labeling revealed that Nip1 is phosphorylated. Mass spectrometry analysis of eIF3 complexes identified specific sites of phosphorylation in Prt1 and Tif5, but not Nip1.

Mass spectrometry Identification of *In Vivo* Phosphorylation of Nip1 at S98, S99, and S103 using IMAC phosphopeptide enrichment

In considering our failure to identify Nip1 phosphopeptides in our direct mass spectrometry analysis, I speculated that either Nip1 phosphopeptides were not retained in either the 2-D LC's SCX or RP chromatography steps or that the phosphopeptide ion signals were being repressed by co-eluting nonphosphorylated peptides. Therefore, I enriched for phosphorylated peptides from digested eIF3 complexes using an optimized immobilized metal affinity chromatography (IMAC) protocol (Moser and White, 2006). Purified eIF3 complexes were digested with trypsin, and the peptides were converted to methyl esters. Phosphorylated peptides were enriched by Fe(III)-charged IMAC prior to LC-MS/MS analysis. Using this approach and the criteria described earlier for validating the MS/MS spectra, I identified multiple Nip1 peptides that were phosphorylated at S98, S99, and S103 (Fig. 3-5). All three sites are predicted to be high stringency substrates for CK2 (CK2 consensus sequence: LKSSNYD**pSpS**DEE**pS**DEEDGKK) (Obenauer et. al., 2003). The stringency is defined by the Scansite algorithm and reflects a motif match of the target protein with the casein kinase 2 motif of SXXD/E that falls within the top 0.2% of scores

when the motif matrix is applied to a reference dataset from SWISS-PROT using Scansite. S99 was phosphorylated in all the Nip1 phosphopeptides that I identified, suggesting constitutive phosphorylation, while the phosphorylation of S98 and S103 was variable (Table 3-1). The corresponding unmodified peptides were not identified in our LC-MS/MS analysis of unenriched samples. Thus the IMAC enrichment enabled us to analyze these particular peptides. However, the IMAC approach did not allow us to detect the singly modified peptides previously identified in this study for Prt1 and Tif5. This is a commonly cited limitation of the IMAC protocol in that it preferentially binds multiply phosphorylated peptides (Bodenmiller et. al., 2007).

Figure 3-5

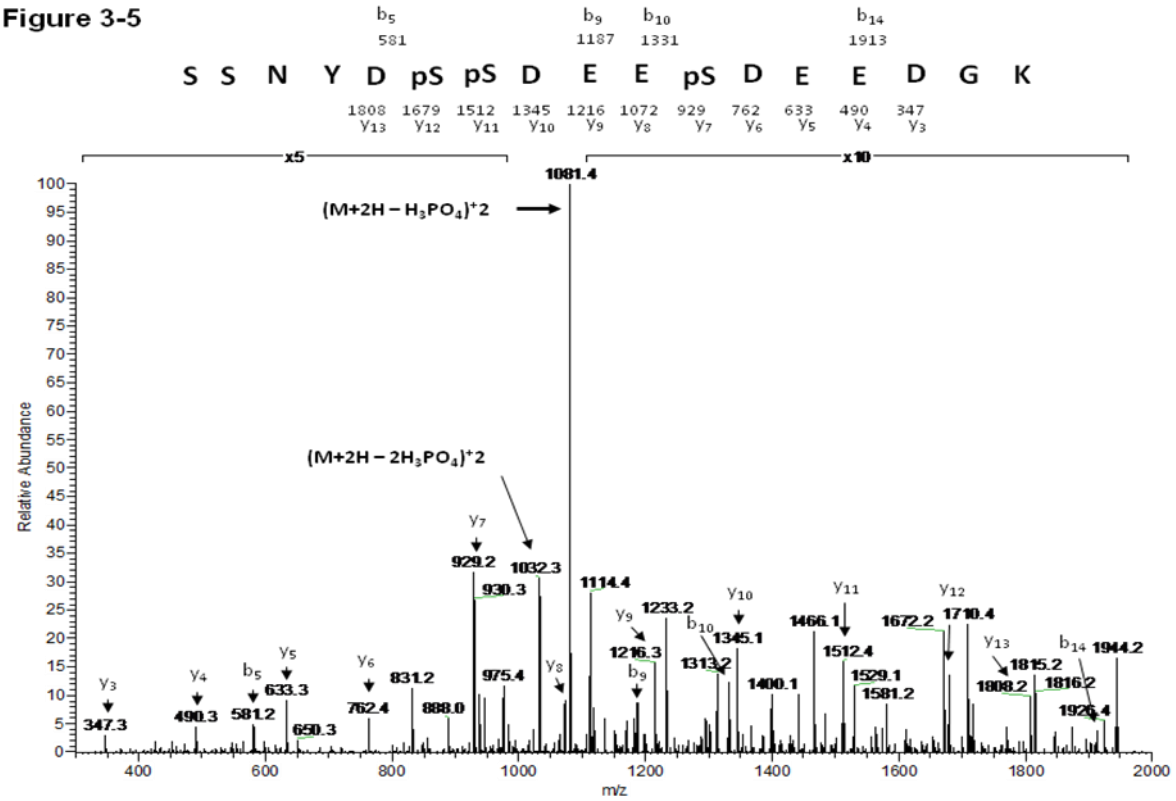

Figure 3-5. Nip1 is phosphorylated at S98, S99, and S103. An MS/MS spectrum generated after IMAC-enrichment of phosphopeptides from trypsin-digested eIF3 showing *in vivo* phosphorylation of a Nip1 peptide at S98, S99, and S103. The spectrum significantly matched the trypsin-generated peptide of Nip1 (Sequest Xcorr = 3.1). The spectrum shows the addition of 80 Da at S98, S99, and S103. The *m/z* values of the most prominent ions in the MS/MS spectrum correspond to the neutral loss of one and two phosphoric acids from the precursor ion of 1131.6 (+2).

Table 3-1

Parent *m/z*	*m/z* of MS/MS base peak	Neutral loss	Z	Cn	Peptide sequence
1131.6	1081.4	50.2	+2	3.1	K.SSNYD**p**S**p**SDEE**p**SDEEDGK.K
796.8	764.1	32.7	+3	2.6	K.SSNYD**p**S**p**SDEE**p**SDEEDGKK.V
1090.5	1040.7	49.1	+2	2.8	K.SSNYD**p**S**p**SDEESDEEDGK.K
1155.1	1105.6	49.3	+2	2.2	K.SSNYD**p**S**p**SDEESDEEDGKK.V
770.1	737.0	33.1	+3	2.3	K.SSNYD**p**S**p**SDEESDEEDGKK.V
1090.3	1041.5	48.8	+2	2.3	K.SSNYDS**p**SDEE**p**SDEEDGK.K
1155.2	1105.1	50.1	+2	2.7	K.SSNYDS**p**SDEE**p**SDEEDGKK.V

TABLE 3-1. Summary of Nip1 peptides identified by LC-MS/MS after IMAC-enrichment of phosphopeptides from trypsin-digested endogenous eIF3. The table shows the precursor ion and the *m/z* of the most intense fragment ion (base peak) in the corresponding MS/MS spectrum. The observed neutral loss, predicted charge state of the precursor ion (Z), and the Sequest cross-correlation value (Cn) to the phosphopeptide sequences are shown. The peptide sequences show the predicted upstream and downstream amino acids flanking the peptides.

Phosphorylation of Nip1 by CK2

To test whether CK2 targets Nip1 specifically at S98, S99, and S103, the sites identified by mass spectrometry, a synthetic peptide with a sequence identical to the tryptic fragment (H2N-SSNYDSSDEEDSDDDGK-OH) was generated and added to the *in vitro* kinase assays. Addition of the competitor peptide reduced phosphorylation of Nip1 (Fig. 3-6, compare lanes 1 and 2), indicating that these specific sites identified on Nip1 are phosphorylated by CK2 *in vitro*. The residual phosphorylation of Nip1 in the lane with the peptide mimic may result from either incomplete competition or CK2 phosphorylation of Nip1 at other site(s). The addition of a control peptide of unrelated sequence and identical length (H2N-ISQAVAHAHAEINEAGR-OH) had no effect on Nip1 phosphorylation (Fig 3-6, lane 3).

Figure 3-6

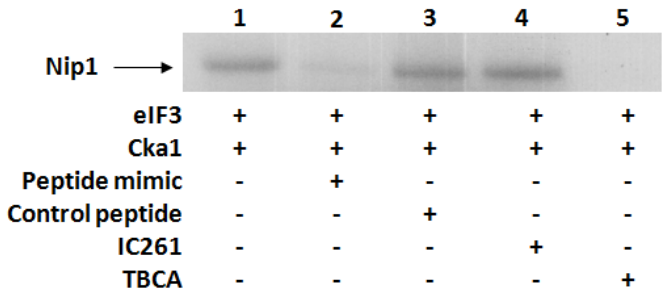

Figure 3-6. Synthetic Nip1 peptide inhibits the *in vitro* phosphorylation of Nip1. A peptide was synthesized that mimics the unmodified tryptic peptide of Nip1 identified as phosphorylated by mass spectrometry. Separation on a 4-12% gradient gel for an extended time allows for better resolution of the Nip1-Prt1 region of the gel. The ability of this peptide mimic to inhibit *in vitro* phosphorylation is shown (lane 2). A control peptide added to the kinase assay indicates that this inhibition is specific to the Nip1 peptide (lane 3). Addition of a CK2 inhibitor, TBCA, abolishes the *in vitro* phosphorylation of Nip1 (lane 5). An unrelated kinase inhibitor, IC261, does not affect the *in vitro* phosphorylation of Nip1 (lane 4).

Phosphorylation of Nip1 at Additional Sites

The incomplete inhibition of *in vitro* Nip1 phosphorylation by the peptide containing S98, S99, and S103 suggested that there may be additional phosphorylation sites on Nip1. To address this possibility, I examined *in vivo* phosphorylation of a mutant version of Nip1 lacking these three CK2 sites. Using a TAP-tagged Nip1 plasmid, I replaced S98, S99, and S103 with alanines. Strains with the wild-type and *nip1S98,99,101A* mutant plasmids in a Δ*nip1* null background were metabolically labeled with ^{32}P-orthophosphate. Following TAP purification of Nip1, autoradiography showed a reduction in the level of phosphorylation of *nip1S98,99,101A* mutant protein (Fig. 3-7). The signal for the mutant strain represents a 41% reduction compared to the wild-type as determined by densitometry (Fig. 3-6), consistent with the phosphorylation of other Nip1 sites.

Figure 3-7

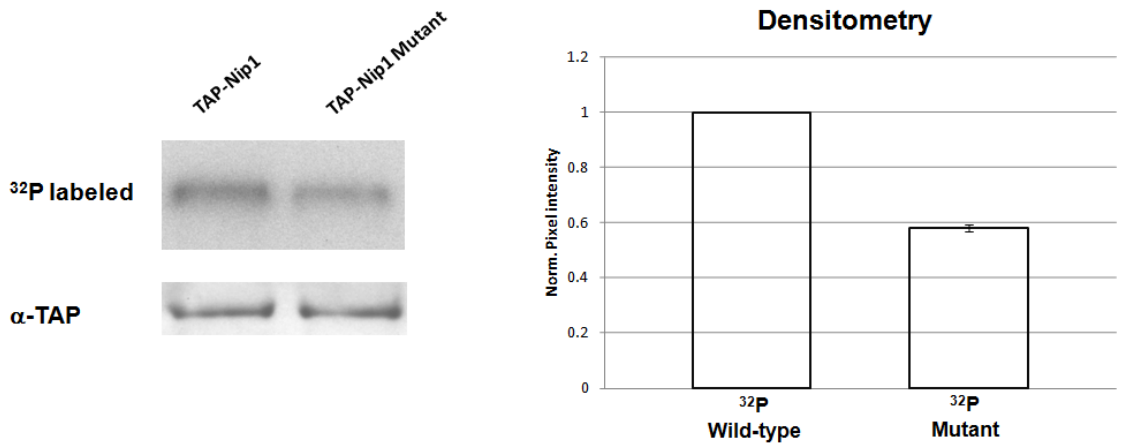

Figure 3-7. Mutation of S98, S99 and S103 in Nip1 reduces *in vivo* phosphorylation. Δ*nip1* null mutants containing plasmids expressing either wild-type Nip1 or a Nip1 mutant protein in which S98, S99 and S103 were replaced by alanines were examined. SDS-PAGE separation of TAP-Nip1 following *in vivo* ^{32}P metabolic labeling. The S98,S99, S103A mutation results in a 41% reduction of the mutant signal relative to wild-type based on densitometry using values normalized for the α-TAP loading control and measured in triplicate. The error bar represents deviation among the densitometry measurements in triplicate of the mutant sample normalized relative to the wild-type control. Error bars are absent in the wild-type since the value is normalized to itself. As a control, western blotting with an α-TAP antibody shows equivalent amounts of TAP-Nip1 in each lane.

The Biological Significance of the Nip1 Phosphorylation at S98, S99, and S103

To test the functional importance of the S98, S99, and S103 phosphorylation sites, I closely examined a *nip1S98,99,101A* mutant strain. I compared yeast strains with either wild-type Nip1 or *nip1S98,99,101A* expressed from low-copy-number plasmids in a *Δnip1* null background. The most striking difference observed between the mutant and wild-type strains was a marked increase in doubling time for the *nip1S98,99,101A* mutant (Fig. 3-8). The wild-type strain doubled every 111 ± 12 min, within the normal range for *S. cerevisiae.* However, the *nip1S98,99,101A* mutant strain doubled every 148 min ± 10 min, a 33% increase (p-value = 0.00687). Complementing the mutant strain with a wild-type Nip1 plasmid results in a restoration of the doubling time to normal levels (112 min ±8 min).

Figure 3-8

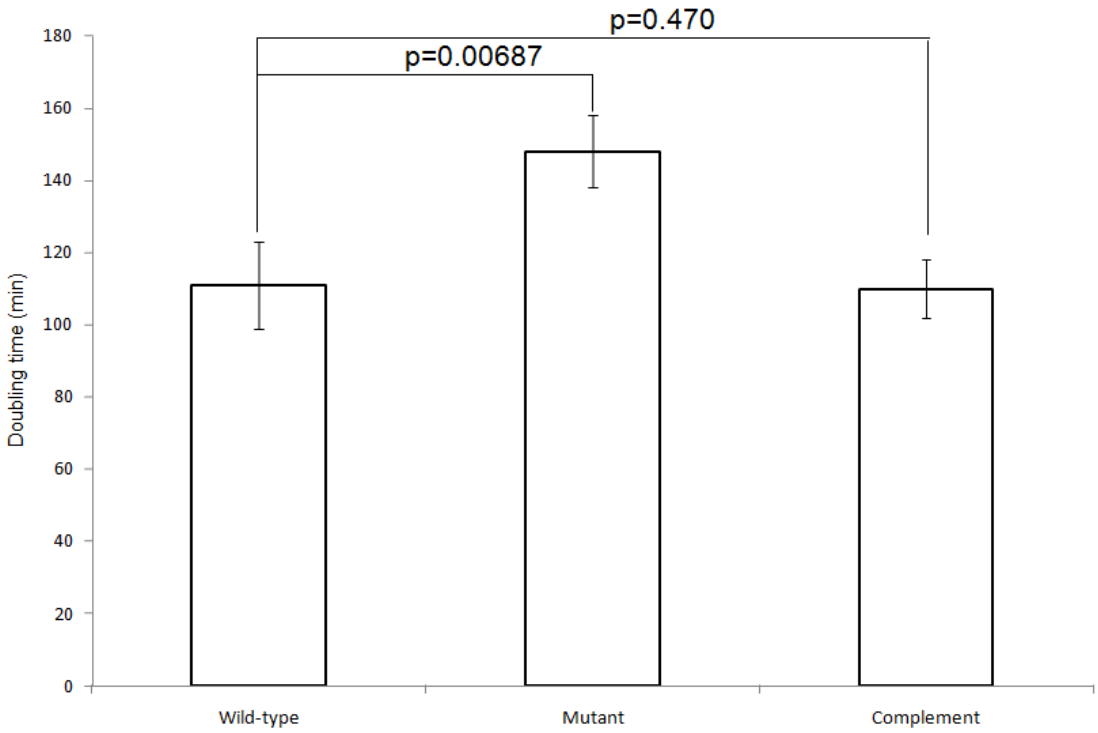

Figure 3-8. Mutation of S98, S99 and S103 in Nip1 increases the doubling time of yeast. Doubling time for each strain (wild-type Nip1 and a *nip1S98,99,101A* mutant) was determined from the logarithmic growth phase of the cells in triplicate (n=3). Comparison of doubling times reveals that the strains harboring the mutation have a doubling time increased by 33%. A one-tailed t-test reveals a p-value between the wild-type and mutant doubling times of 0.00687. This defect is rescued with a wild-type copy of Nip1 in the mutant strain. The error bars represent the standard deviation of the measurements of doubling times performed in triplicate.

To further investigate the biological significance of the identified phosphorylation events, I investigated the polysome profiles of the mutant and wild-type strains. Polysome profile defects can indicate problems in a multitude of cellular process including ribosome biogenesis, translation initiation, and translational processes. Mutant and wild-type strains were tested under a variety of conditions including temperature selection, salt stress, and drug exposure. Figure 3-9 shows a representative set of polysome profiles comparing wild-type and mutant strains of *nip1*. The representative profiles reflect what was consistently observed for the conditions tested. There were no discernable differences between the two strains. If a defect were present for the mutant strain, the peak intensities shown in the profiles would be different between the strains. For example, an increase in the populations of the 40S and 60S peaks with a simultaneous decrease in the 80S peak intensity would be indicative in an observed defect in translation initiation. However, this was not the case.

The rate at which the mutants globally synthesize proteins was measured via ^{35}S-methionine experiments. Decreased ^{35}S incorporation reflects a global decrease in protein synthesis. However, this set of experiments showed no difference between the incorporation rates of ^{35}S between the wild-type and mutant strains, thereby indicating no measurable defect in overall rates of protein synthesis (Figure 3-10). Given that the growth rate quantification experiment yielded a measurable difference between the doubling times of the mutant and wild-type strains, I further investigated the growth rate of the strains under stressed conditions. These stressed conditions included high salt, drugs that

selectively inhibit steps in translation (hygromycin, rapamycin, paromycin), nutrient starvation (-uracil, -leucine), and temperature shock (25°C and 37°C). Under the conditions tested, no additional defect in the growth rates of the strains was observed (Figure 3-11). As an addition, growth in the presence of the drug sulfometuron methyl (SM) was tested. SM induces amino acid starvation by selectively inhibiting translation initiation. If the mutant *nip1* has defects in translation initiation, I postulated that strains exposed to the drug and harboring the mutation, would be hypersensitive to its presence and show diminished growth rates compared to wild-type strains. Unfortunately, these experiments showed no discernable growth rate differences between the strains (Figure 3-12). This experiment was repeated at 25°C, 30°C, and 37°C with similar results. *Δgcn2* strains were chosen as a positive control since they have a known hypersensitivity to SM.

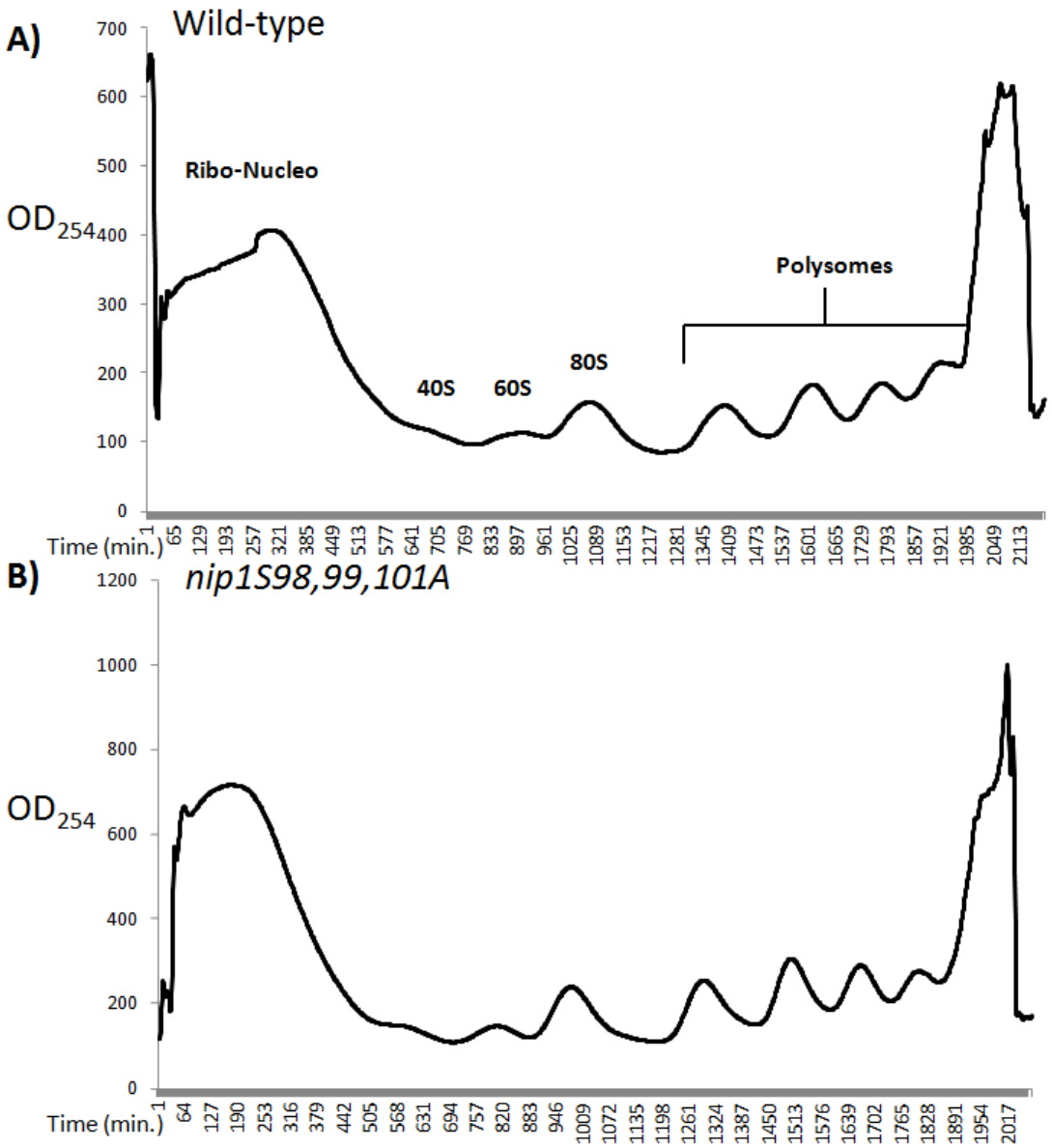

Figure 3-9. Polysome profiles of wild-type and mutant strains at 30℃. A) Wild-type yeast polysome profile with the corresponding peaks labeled as to the proteins the predominantly compose them. B) A *nip1S98,99,101A* mutant yeast lacking the identified phosphorylation sites on Nip1 were analyzed in this polysome profile.

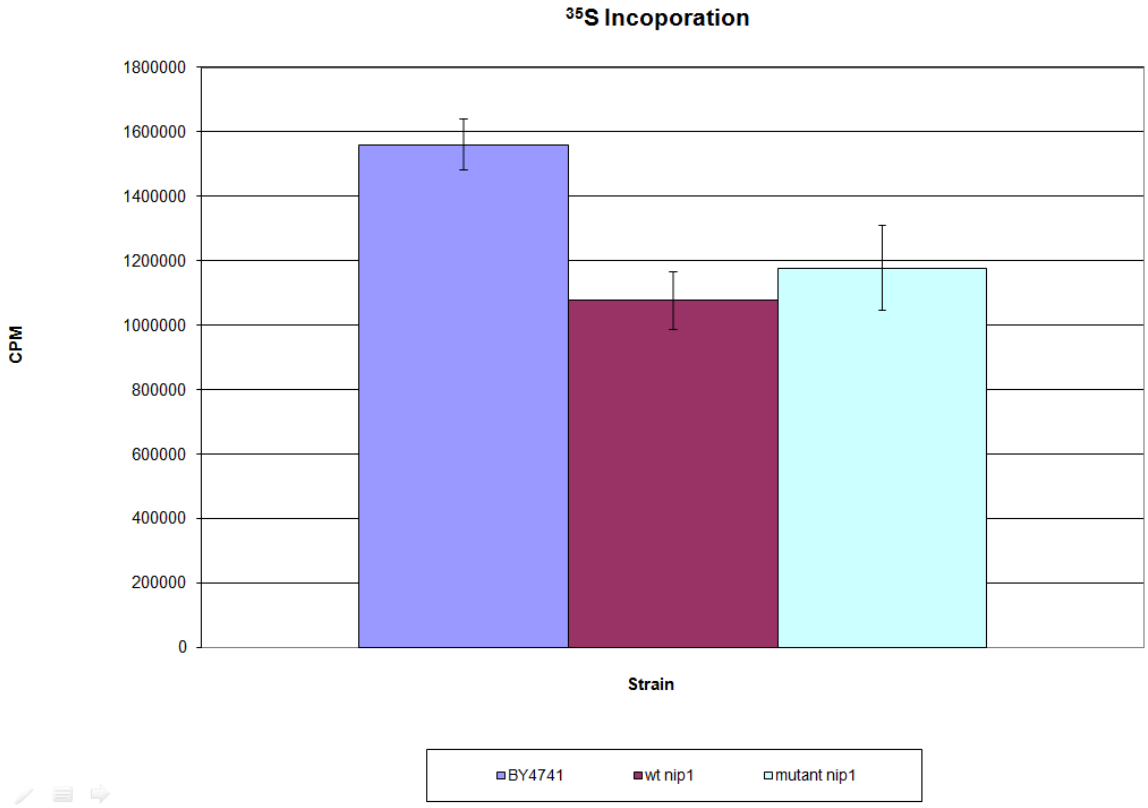

Figure 3-10. ^{35}S-methionine incorporation. The global rates of protein synthesis were compared for the mutant and wild-type Nip1 strains. A control strain of BY4741 yeast cells containing Nip1 on its chromosomal locus was used as a control. No difference was observed for the rates of ^{35}S-met incorporation between the strains containing either wild-type or a *nip1S98,99,101A* mutant allele on a plasmid.

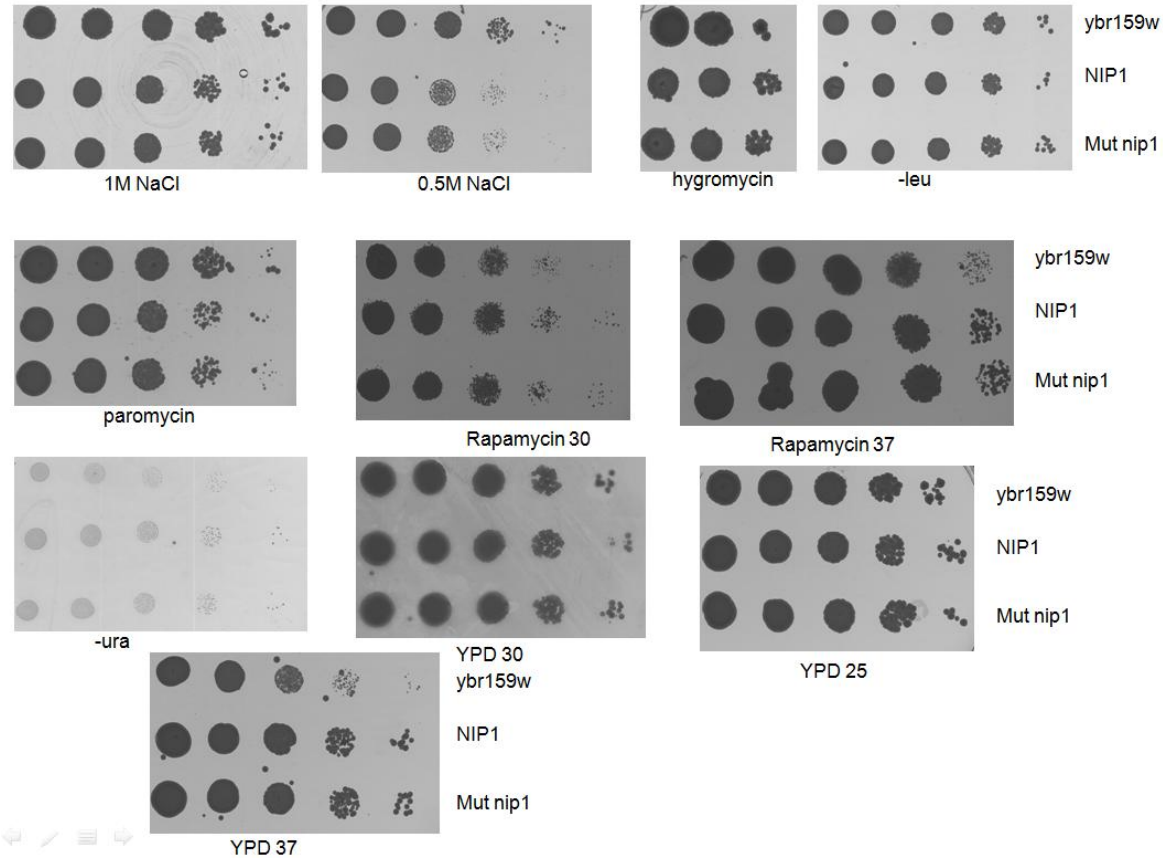

Figure 3-11. Plate growth assay comparison between a *nip1S98,99,101A* mutant and wild-type Nip1 strains. Strains harboring the alanines mutations were compared with strains containing wild-type copies of Nip1 for their ability to grow on a variety of media. None of the conditions produced a difference between the two strains. The YBR159W strain was chosen as a positive control.

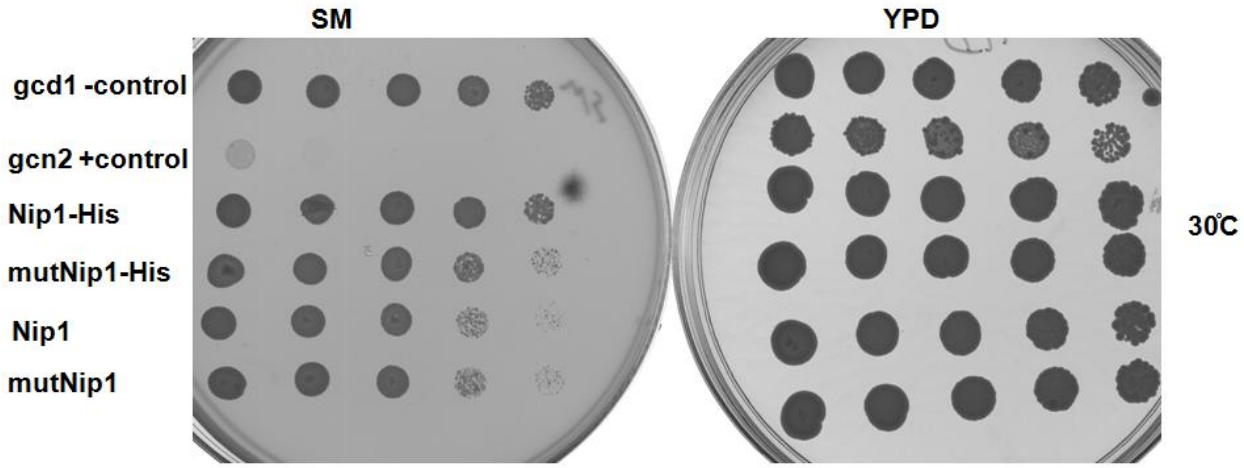

Figure 3-12. SM growth assay. The drug sulfometuron methyl was used to evaluate defects in translation initiation for the mutant *nip1S98,99,101A* strain. However, the mutant *nip1* strains showed no hypersensitivity to the drug as is seen with the positive control *Δgcn2* null strain.

Discussion

To identify specific sites of phosphorylation, I analyzed TAP-isolated eIF3 complexes directly by LC/MS/MS. In this way, I identified two phosphorylation sites in Prt1 (S61 and T746) and one in Tif5 (T191). To our surprise, I were unable to identify any phosphorylation sites in Nip1 using this method. I enriched for eIF3 phosphopeptides using IMAC and then analyzed the peptides using LC/MS/MS. This approach enabled us to identify three phosphorylation sites in Nip1 (S98, S99, and S103). Using the Scansite algorithm (http://scansite.mit.edu), Nip1 is predicted to contain 5 sites that are high stringency CK2 targets. Of these five, S98, S99, and S103 were identified in this study. There was no evidence found to support the remaining two sites S56 and S62. However, our mass spectrometry data showed evidence of additional phosphorylations. In a number of tandem spectra, the most intense fragment ion was due to a neutral loss of 98, 49, or 32.6 Da, indicating phosphorylation. However, insufficient fragmentation prevented us from confidently identifying the sequences. Additionally, Rpg1 is the only other member of the eIF3 complex predicted to contain a high stringency CK2 site at T513. No evidence was found to support this and the lack of a signal in the Rpg1 region of the autoradiography (Fig. 2, lane C) supports the conclusion that this particular potential CK2 site is not targeted for phosphorylation.

To comprehensively identify the eIF3 phosphorylation sites, complete sequence coverage of proteins by mass spectrometry will be required. However, current mass spectrometry protocols seldom achieve complete coverage. A

fraction of the proteolytic peptide fragments are either too small or too large to be confidently analyzed by mass spectrometry. In addition, the physiochemical properties of phosphopeptides compound the problems of obtaining comprehensive coverage. Because of the negative charge on phosphate groups, the ionization efficiency of phosphopeptides in positive ion mode is reduced. Furthermore, because a phosphopeptide is typically at a lower abundance relative to the equivalent nonphosphorylated peptide, the more prevalent mass spectrometry signal of nonphosphorylated peptide can suppress the signal of the phosphopeptides (Chang, 2006; Bodnar et. al., 2003; Zhen et. al., 2004; Mirgorodskaya et. al., 2005).

We have found that casein kinase 2 (CK2) plays an important role in phosphorylating eIF3 components. Most of the phosphorylation sites I have identified fit the CK2 consensus sequence with high stringency: S98, S99, and S103 on Nip1 and S61 on Prt1. T746 on Prt1 fits the consensus with low stringency, while T191 on Tif5 does not match.

To further our understanding of how phosphorylation might regulate translation initiation, I used mutational analysis to investigate the functional importance of the phosphorylated CK2 consensus sites in Nip1. Mutation of S98, S99 and S103 causes a 33% increase in the doubling times for the mutant strain. This observation suggests that the phosphorylation events occurring in the region of these sites S98, S99 and S103 are necessary for normal cell growth or division. In the absence of these three sites, *in vivo* phosphorylation of Nip1 was

reduced by only 41%. This observation is consistent with our mass spectrometry analysis in which I was tantalized by several spectra that showed hallmarks of phosphorylation but did not contain enough fragment ions to provide sequence information. Therefore, I believe there are additional phosphorylation sites in the eIF3 complex yet to be identified. It is interesting that while the mutant strains show an increase in their doubling times, their ^{35}S incorporation and polysome profiles appear normal. A defect could still exist in translation initiation, but it is possible that the available techniques are not sensitive enough to detect it. Translation is also a complicated process and involved in many aspects of cell functioning. It could be that the phosphorylations of Nip1 are a triggering event in cell cycle progression but not necessary for efficient translation initiation. Additional genetic and biochemical experiments will be required to dissect the functional and mechanistic consequences of these phosphorylation events.

Collectively, our results provide a comprehensive characterization of the phosphorylation of eIF3 and its targeting by CK2. Experiments designed to more precisely determine the consequence of the phosphorylation evens observed for Nip1 yielded little proof as to its role. However, this region is proposed to be involved with stabilizing interactions between Nip1 and Prt1 to form the active eIF3 complex. It could be speculated that losing the phosphorylation events will greatly increase the hydrophobicity in the region of Nip1. A loss of strong polar interactions between Prt1 and Nip1 could reduce the stability of the eIF3 complex. The net result would be a smaller pool of eIF3 available to perform its native biological functions. This could account for the marked increase in the

doubling times observed for strains lacking the three serine sites on Nip1. Chapter five will further discuss how future experiments could address this concept. Overall, this work can serve as a blueprint for the discovery of kinases that phosphorylate components of other protein complexes *in vivo*. In addition, this approach can be employed in the discovery of enzymes responsible for other types of post-translational modification including ubiquitination, acetylation, and methylation.

CHAPTER IV

THE UTILITY OF USING iTRAQ WITH PQD

Abstract

The use of iTRAQ reagents to quantify either the relative or absolute amounts of proteins in biological samples has become a widespread technique in quantitative proteomics. The method provides a robust method to simultaneously identify proteins in complex mixture while yielding precise quantification data. However, ion trap mass spectrometers are typically not useful for iTRAQ analysis because the reporter ions generated from the fragmentation of the iTRAQ tags are lost along with the lower 1/3 of the MS/MS data. This is a result of using the ion trap to trigger collision induced dissociation (CID). Other types of mass analyzers including time of flight (TOF) instruments such as a quadrupole-TOF (Q-TOF) and TOF-TOFs contain a dedicated collision cell to perform CID. The Orbitrap mass analyzer, in combination with the higher energy collision dissociation cell (HCD), is also able to retain the lower mass ions. To expand the use of iTRAQ reagents to ion trap mass spectrometers, the ion trap's manufacturer introduced the use of pulsed-q dissociation (PQD) for retention of the lower 1/3 of the MS/MS data. Using the 4-plex iTRAQ system, I evaluated the utility of using PQD to generate both peptide sequencing

information and iTRAQ reporter ions for quantitation. When compared with CID, PQD produces more reliable detection of iTRAQ reporter ions. However, when using PQD, fewer peptides are identified in biological samples due to the less efficient nature of PQD fragmentation.

Introduction

Mass spectrometry-based proteomic analyses rely on the fragmentation of peptides in the gas phase to fragment ions. The resulting fragmentation ions are then used to determine the sequence of the peptide, and from this, the associated protein can be identified. The primary method for peptide fragmentation is collision induced dissociation (CID) (Swaney et al., 2008). The LTQ, Orbitrap, q-TOF, and MALDI-TOF/ TOF instruments are all capable of performing CID fragmentation of peptides. CID is best utilized for small and unmodified peptide cations (Dongre et al., 1996; Good et al., 2007; Huang et al., 2005). For the ion trap, resonance excitation of the peptide is achieved through intermolecular collisions with the peptide and an inert gas. The collision energy transferred to peptides in CID results in the vibrational excitation of the peptide and is distributed among the covalent bonds of the peptide chain. When the internal energy transferred to the peptide in CID exceeds the activation barrier for bond cleavage, the peptide can fragment. These fragments can be detected by the mass spectrometer if they occur within the timescale of the instrument. Fragments produced are dependent on the size, sequence, and charge state of the peptide as well as the amount of collision energy supplied. For CID, the

fragmentation typically occurs at the amide bonds of the peptide backbone due to the low activation barrier that exists at these locations. This generates the characteristic b- and y-product ions seen in CID spectra (Swaney et al., 2008).

The model that is typically used to describe how peptides fragment in CID is the “mobile proton theory” (Wysocki et. al., 2000). The mobile proton theory arises from the observation that fragmentation of most protonated peptides requires the involvement of a proton at the cleavage site. If an amino acid side-chain holds a proton, energy will be required to move the proton from the basic side-chain to the peptide backbone to induce dissociation. Common proteomic approaches involve the use of trypsin as the proteolytic enzyme, and therefore, peptides produced as such contain at least two basic residues. The addition of energy supplied by the tandem mass spectrometer alters the initial population of protonated forms in favor of those with energies higher than that of the most stable structure (Wysocki et. al., 2000). Protonation of backbone sites induces charge-directed cleavage of the backbone to generate b- and y-type sequence ions in CID. Since basic residues are more electronically rich, they more tightly sequester protons. This tendency for more basic residues to sequester protons increases the charge-directed cleavage at these residues in the peptide backbone. A prominent example of this is observed for peptides containing an internal proline residue. Cleavage of a peptide at the C-terminal side of a proline is energetically unfavorable and results in an intense b-type ion housing the protonated proline residue (Schlosser and Lehmann, 2000). This diagnostic trait can be useful in *de novo* sequencing of experimental spectra.

Although CID is effective in generating ion series suitable for peptide sequencing, some caveats exist that diminish its ability to fragment particular peptides. Internal basic residues and proline amino acids can prevent the random protonation of the peptide backbone in accordance with the mobile proton theory. These residues direct amide bond dissociation to specific sites and can inhibit the fragmentation of the peptide resulting in an insufficiently diverse set of sequencing ions (Schlosser and Lehmann, 2000; Mikesh et al., 2006). The common use of trypsin as a protease alleviates some of these concerns by generating peptides with a basic residue at the C-terminus. Labile PTMs such as phosphorylation and glycosylation also present alternative low-energy fragmentation pathways. In these cases, the aforementioned neutral loss events can occur, generating spectra with insufficient sequencing ion coverage. Some PTMs can also inhibit the random protonation of the peptide backbone and subsequently inhibit fragmentation via CID (Tsaprailis et al., 1999).

To overcome some of the limitations of true CID, Thermo Scientific introduced a variation of CID termed pulsed-q collision induced dissociation (PQD). PQD occurs under controlled resonance excitation amplitude and main RF amplitude. The first step of PQD places the precursor ion at an elevated Q value of 0.6-0.8 and pulses the ion with a high amplitude resonance excitation pulse. This pulse kinetically excites the precursor ion. The ions are then held at the elevated Q value for approximately 100 μs to convert the kinetic energy of the precursor ion into internal energy through collisions. This short time frame prevents significant bond dissociation. The final event of PQD pulses the

precursor ion's Q value to a lower state by a rapid drop of the RF amplitude. Following this rapid drop, precursor ions undergo fragmentation to produce spectral information. The process of activating at both high Q values generates sequencing fragments while the activation at the low Q values traps low m/z fragments. Therefore PQD retains the lower 1/3 of the spectra typically lost in normal CID (Bantscheff et al., 2008).

An alternative fragmentation method termed electron-capture dissociation (ECD) has the ability to overcome some of the limitations posed by CID. In ECD, protonated peptides are held in the Penning trap of an FT-ICR and exposed to a beam of electrons at thermal or near-thermal energies. The capture of the thermal electron by the protonated peptide results in backbone fragmentation without intramolecular vibrational energy redistribution (Udeshi et al., 2007). ECD fragmentation generally produces c- and z-ions series as opposed to the b- and y-ions generated in CID. ECD is a size and sequence independent process and can be used to fragment intact proteins. However, for ECD to be efficient, the sample must be in a dense population of the thermal electrons. This situation is technically difficult to achieve on instruments using electrostatic radiofrequency fields to isolate ions but is easier in FT-ICRs that use static magnetic fields. In addition, ECD spectra suitable for sequencing require the averaging of a large number of scans on a time scale of minutes. This necessitates the introduction of large amounts of analyte into the instrument and precludes the detection of peptides or proteins in a complex sample mixture (Udeshi et al., 2007).

The use of a similar fragmentation method called electron transfer dissociation (ETD) overcomes the limitations generated by ECD. ETD uses ionized radical anions of polyaromatic hydrocarbons to react with multiply protonated peptides in the gas phase. These radical anions are added and stored in the linear quadrupole ion trap of the mass spectrometer along with the peptides ions. The radical anions transfer an electron to the ionized peptides and the resulting charge reduced peptide fragments in a mechanism believed to be analogous to ECD, generating characteristic c- and z-sequencing ions (Syka et al., 2004). The fragmentation patterns generated with ECD and ETD are independent of peptide length, amino acid composition, and the presence of PTMs (Udeshiet al., 2007). This fragmentation process is highly efficient and occurs on a millisecond time scale. Therefore, ETD is sensitive down to femtomole amounts of sample and occurs on a time scale corresponding to current chromatographic separation techniques (Syka et al., 2004). The main benefit of this fragmentation technique is its ability to preserve labile PTMs while still allowing sufficient amide bond cleavage to generate spectra from which sequencing information can be obtained. However, this method suffers from a decrease in fragment ion production as the precursor ion charge decreases (Swaney et al., 2007).

A recent study has utilized a hybrid approach of ETD and CID (ETcaD) to target the nondissociative electron transfer product ions of ETD with CID. This method resulted in median sequence coverage of 88.9% for ETcaD as opposed to 62.5% for ETD and 77.4% for CID alone (Swaney et al., 2007). Other studies

have utilized ETD to identify PTMs, namely phosphorylation. One group used CID based fragmentation to detect over 1000 phosphopeptides but was only able to define 383 sites of phosphorylation, largely due to the neutral loss events on the modified peptides (Udeshi et al., 2007). Using an LTQ modified with ETD, 1252 sites of phosphorylation on 629 proteins of a complex mixture were identified (Udeshi et al., 2007). A separate analysis of the overlap between phosphopeptides identified with ETD and CID found that only 17.9% of the sites identified were shared among the two datasets generated (Swaney et al., 2008). This suggests that the best approach to fragmenting and identifying sites of PTMs may be a combination of CID and ETD.

Another variant of CID has been introduced in hybrid Orbitrap mass spectrometers taking advantage of the presence of a C-trap in their design. This method of fragmentation known as higher energy collision dissociation cell (HCD) allows for the retention of the low m/z region on the spectra where reporter ions are often encountered (Olsen et. al., 2007). HCD is performed by injecting peptide ions from the ion trap into a collision cell at the far side of the C-trap. Fragment ions are transferred back to the C-trap for activation and subsequent dissociation and passed to the Orbitrap mass analyzer via a supplementary hexapole (Olsen et. al., 2007). Analysis in the Orbitrap results in high resolution and high mass accuracy data. HCD fragmentation is similar to fragmentation in a Q-TOF and overcomes the problems of low mass cutoff seen in ion trap fragmentation (Nagaraj et. al., 2010). However, since fragmentation ions in HCD are detected in the Orbitrap as opposed to the ion trap in CID or PQD, the

technique is limited by the lower duty cycle of the instrument (Kocker, 2009). In addition, HCD has been correlated with a decrease in sensitivity due to a lack of backbone fragments useful for peptide identification (Dayon et. al., 2009). It is important to note that at the time this study was investigated, we were not equipped with an instrument capable of performing HCD. Recent group have proven the utility of combining CID with HCD activation modes in an LTQ-Orbitrap mass spectrometer for the precise identification of peptides without compromising peptide identifications with the linear ion trap analyzer. To accomplish this, both HCD and lower energy CID were acquired for each selected precursor ion. CID generated spectra were used for peptide ion identification and HCD spectra were used for quantification (Dayon et. al., 2010).

Summary

To investigate the utility of using PQD for protein quantitation with the iTRAQ system I used affinity purified protein samples and a LTQ linear ion trap mass spectrometer not equipped with a HCD cell. The ability to identify peptides at varied pulsed-Q levels was evaluated and compared to a set of proteins identified at varied percent CID levels. After determining what PQD percentage resulted in reliable peptide identifications, iTRAQ labeling was performed on a set of peptide standards. I then evaluated at what percent PQD level iTRAQ reporter ions could be detected and compared this to reporter ion detection obtained using CID.

Materials and Methods

Protein extracts

TAP-Rpg1 strains were grown, purified, trypsin digested, and desalted as previously described from 4L of culture (Powell et. al., 2004; Link et. al., 2005). Desalted sample was vacuum centrifuged to dryness for use in iTRAQ experiments. 50 μg of material was loaded onto the reverse phase column for MS/MS analysis. The 6 protein standard mixture utilized for reporter ion detection is supplied with the iTRAQ kit. This mixture consisted of bovine serum albumin, β-galactosidase, α-lactalbumin, β-lactoglobulin, lysozyme, and apotransferrin.

iTRAQ labeling

iTRAQ labeling reagents used were obtained from the iTRAQ 2-Plex methods development kit (Applied Biosystems). Dry samples were reconstituted in 30 μL of dissolution buffer (supplied with the kit), vortexed for 30 s at room temperature and centrifuged briefly. iTRAQ reagents were brought to room temperature from -20°C. Seventy μL of ethanol was added to each iTRAQ reagent vial (114 and 117 reporter tags). Each vial was vortexed for 1 min then briefly centrifuged. The contents of each iTRAQ reagent vial were added to 50% of the supplied 6 protein mixture (129 μg) standard in a 1:1 ratio. Each vial was vortexed, briefly centrifuged, and incubated at room temperature for 1 h. Samples were combined and desalted as previously described to remove iTRAQ

reagents and vacuum centrifuged to dryness (Powell et. al., 2004; Link et. al., 2005). Dry samples were reconstituted in 40 μL 0.1% formic acid.

Mass spectrometry

Experiments were performed on a Thermo LTQ mass spectrometer coupled to an Eksigent NanoLC system (Thermo Electron, Inc) (Link et. al., 1999; Sanders et. al., 2002; Powell et. al., 2004). Data acquisition of samples was performed as previously described with the exception that either 3 CID or 3 PQD scans were performed following the initial full MS scan. Normalized collision energies were varied for both PQD and CID in individual experiments from 20% to 45% at 5% step intervals.

Mass spectrometry data analysis

Spectral information in the low mass range for the reporter ions of iTRAQ was visualized with the Thermo's supplied Xcalibur software. To process and analyze the mass spectrometry data, the program *extractms2* was used to generate an ASCII peak list and identify +1 or multiply charged precursor ions from native *.RAW mass spectrometry data files (Jimmy Eng and John R. Yates III, unpublished). Tandem spectra were searched with no protease specificity using SEQUEST-PVM (Sadygov et. al., 2002) against the SGD yeast_orfs database containing 6,000 entries with a static modification of +57 on C (addition of a carbamidomethyl group). In addition, the isobaric tags used in iTRAQ add +145 to the N-terminus and lysine residues. For multiply charged precursor ions

($z \geq +2$), an independent search was performed on both the +2 and +3 mass of the parent ion. Data were processed and organized using the BIGCAT software analysis suite (McAfee et al., 2006). A weighted scoring matrix was used to select the most likely charge state of multiply charged precursor ions (Link et al., 1999; McAfee et al., 2006). From the database search, tryptic peptide sequences with SEQUEST cross-correlation scores (Cn) $\geq$ 1.5 for +1 ions, $\geq$ 2 for +2 ions, and $\geq$ 2 for +3 ions were considered significant and used to create a list of identified proteins.

Results

Experiment Workflow

To establish the utility of using PQD to identify and quantify proteins in complex mixtures, I first had to determine if sufficient fragmentation information could be interpreted from MS/MS spectra generated using PQD. To this end, I performed PQD based fragmentation experiments using affinity purified eIF3 samples. The results of the experiments with varied PQD were compared to results of fragmentation and identifications obtained using CID. I was able to establish a defined percent PQD level to reliably generated MS/MS spectra that would lead to peptide identifications. With these parameters established, I extended this approach to evaluate its utility for quantitating proteins using the iTRAQ system coupled to PQD in the mass spectrometer. For the latter set of experiments, a six protein standard mixture was labeled with the iTRAQ reagents at defined ratios and analyzed with both PQD and CID. The results of this set of

experiments yielded operating parameters for the mass spectrometer for detection of iTRAQ reporter ions operating in PQD mode.

PQD vs. CID for peptide identification

The default instrument parameter for normalized collision dissociation energy in the linear trap is 35%. In an attempt to find a comparable PQD normalized collision dissociation energy, this value was varied within the LTQ instrument settings. First, a sample of TAP purified and digested eIF3 protein complex was analyzed by 35% normalized collision dissociation energy in CID. The resulting Sequest search returned 150 protein identifications within the previously described data filtering parameters. Results for the PQD normalized collision dissociation energy varied from 20-45% are shown in Table 4-1. A comparison of 35% normalized collision energy for a peptide generated in both CID and PQD appear similar in their fragmentation patterns although the PQD spectrum contains more noise (Figure 4-1).

%PQD	Proteins Identified	Peptides Identified
20	13	41
25	100	348
30	87	300
35	108	313
40	94	232
45	57	125

Table 4-1. Proteins identified for varied PQD normalized collision dissociation energies.

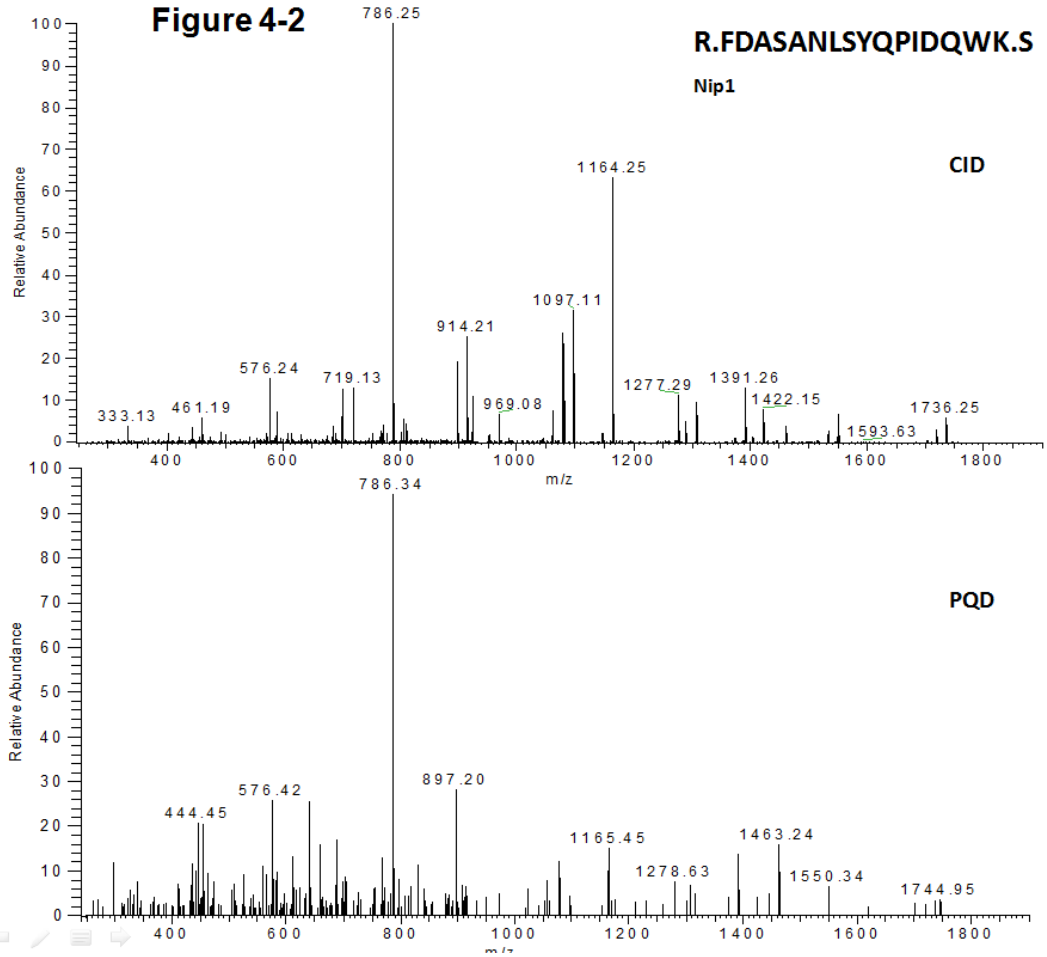

Figure 4-1. CID vs. PQD spectra for a Nip1 peptide. Both spectra were generated using 35% normalized collision energy. The top spectra was generated using CID, while the bottom was generated using PQD. Both spectra were matched by Sequest to the Nip1 peptide FDASANLSYQPIDQWK.

PQD iTRAQ reporter ion detection

The six protein standard supplied with the iTRAQ kit was used to evaluate the ability of PQD to reliably detect iTRAQ reporter ions in the low m/z range (114-117). The previous set of experiments established that a normalized collision energy of between 25-35% provided the most protein identifications per complex protein mixture. Next we tested PQD's ability to detect the 114 and 117 m/z reporter ions of iTRAQ in normalized collision energies of between 15-35%. At a normalized collision energy of 15%, we were unable to match any spectra to peptides in the 6 protein standard iTRAQ mix. Manual inspection of the spectra reveals that very little sequencing ion information is obtained at the low percentage normalized collision energies (Figure 4-3 A). This same case holds true for a 20% normalized collision energy, although a few spectra did match to peptides in the mixture (Figure 4-3 B). Upon increasing the normalized collision energy to 25%, we observed a marked increase in spectra matching peptides in the mixture. This trend peaked at 30% normalized collision energy and trailed off at 35% (Table 4-2). Investigating the reporter ion m/z range reveals that at 30% normalized collision energy, 100% of the spectra that corresponded to peptide hits in Sequest also contained peaks at either of 114 m/z or 117 m/z or both. However, when comparing relative reporter ion intensities for normalized collision energies ranging from 25-35% for a single peptide, we observe inconsistent patterns (Figure 4-2).

PQD	#Spectra	#Peptides	%Reporter
15	0	0	0%
20	10	7	0%
25	106	53	48%
30	622	126	100%
35	575	117	90%

Table 4-2. Various percent collision energies in PQD and the effect this has on peptide identification and reporter ion detection. The PQD collision energies were varied between 15 to 35%. At 30%, the most peptides were identified as well as peaking in the percent of the spectra that contained reporter ions.

Figure 4-4

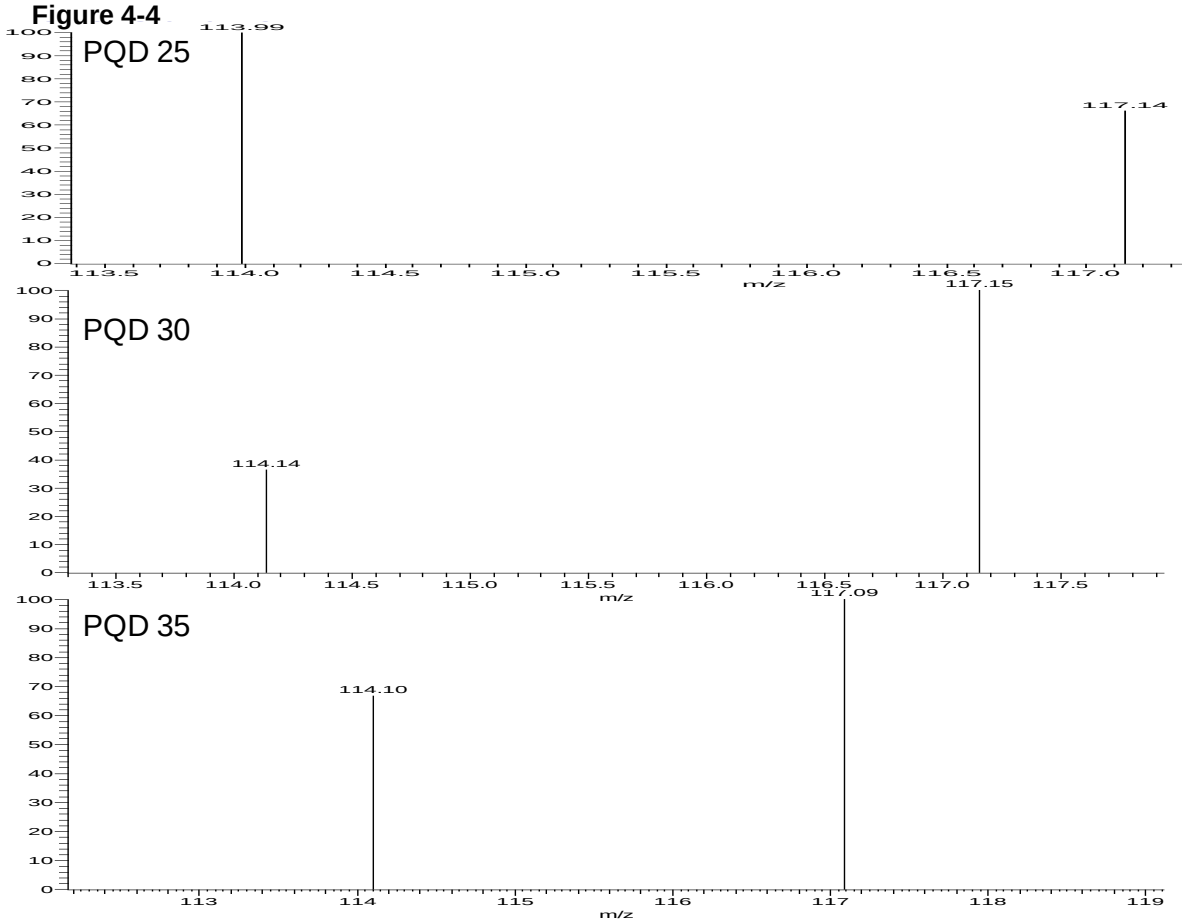

Figure 4-2. The reporter ion series for the standard peptide YNGVFQECCQAEDK. The normalized percent collision energy was varied for each spectrum from 25-35%. The expected ratio of peak intensities is expected to be 1:1. However, the ratios deviate from the expected in an unpredictable manner.

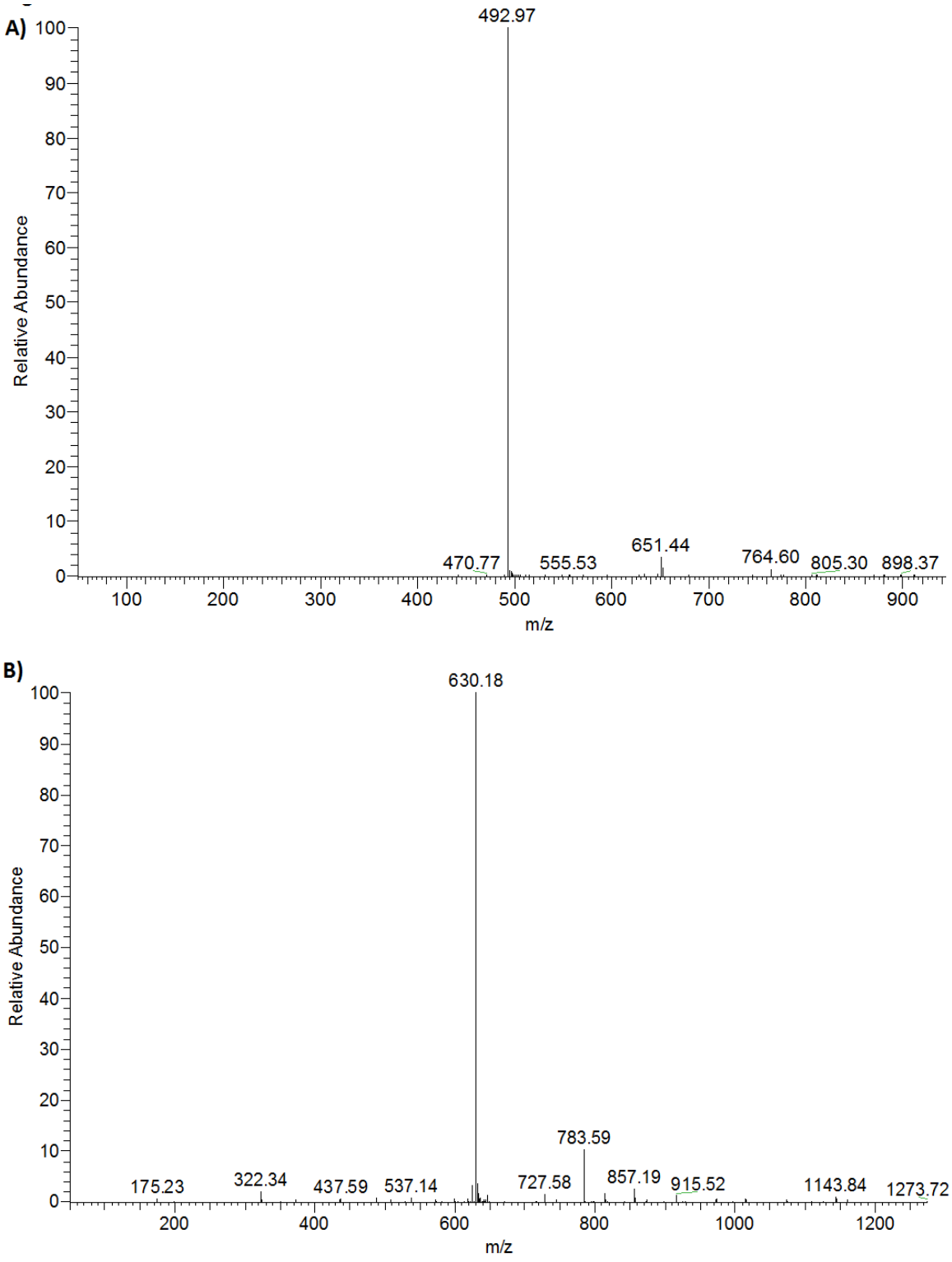

Figure 4-3. Spectra of standard mix generated using PQD at 15% (A) and 20% (B). The resulting spectra contain very little sequencing ion information at the low PQD energies.

Discussion

We determined that a PQD normalized percent collision energy of between 25-35% will yield the best fragmentation data for use in identifying proteins in a complex biological mixture (Table 4-1). However, PQD fails to provide as many peptide identifications when spectra are searched as does typical CID. This may be due to the time delay imparted by the pulse in PQD whereby the precursor ion can lose kinetic energy via routes other than collision energy as the Q is pulsed. This loss of energy would lead to reduced amide bond fragmentation and fewer ions in the spectra for sequencing information. This may be of concern for investigators who are looking to maximize proteome coverage in an iTRAQ experiment. The presence of fewer peptides matching to spectra also leads to a loss of reporter ion data and thereby quantification information.

A study by Bantscheff and coworkers found that PQD suffered from poor peptide fragmentation efficiency (Bantscheff et. al., 2008). PQD spectra that were observed were dominated by the unfragmented precursor ion indicating poor fragmentation efficiency and a resulting limited iTRAQ reporter ion intensity (Bantscheff et. al., 2008). This group spent considerable time and effort in optimizing the parameters to obtain the most efficient fragmentation possible. They found that careful optimization of activation Q, delay time, ion isolation width, number of microscans, and the number of trapped ions, fragment ion intensities can be generated that enable the accurate quantification at the 100 amol level (Bantscheff et. al., 2008). Bantscheff and coworkers also possessed

a mass spectrometer capable of HCD, unlike the one available for this study. Interestingly, they found that PQD outperformed HCD in terms of the lower limit of quantification with a 10X greater sensitivity. However, HCD spectra generated more reliable sequencing information (Bantscheff et. al., 2008).

With the normalized percent collision energy for PQD established at approximately 30%, we next wanted to determine at which percentages would give us the most reliable detection of the reporter ions. By varying the normalized collision energy percentages between 15 and 35%, we found that 30% normalized collision energy afforded the most reporter ion information for the number of spectra generated. Under these conditions, 100% of the spectra generated by the normalized collision energy values contained a reporter ion at 114 and/or 117 m/z. Although a normalized collision energy of 30% resulted in fewer overall peptide identifications and a good starting value for investigating the applicability of this technique to using iTRAQ to quantitate complex protein mixtures. However, the inconsistent relative reporter ion intensities do raise some concern as to the widespread applicability of this technique (Figure 4-2).

Griffen and coworkers found that an optimized collision energy between 5-30% results in the greatest number of reporter ions using the iTRAQ system (Griffin, 2007). Interestingly, they also determined that this value is instrument-dependent and may change with routine maintenance of an individual instrument (Griffin, 2007). An approach they explored to improve the detection of iTRAQ reporter ions was to increase microscan acquisition and repeat spectral counts to

improve the quantification data. However, this results in an increased duty cycle time for the instrument at the cost of identifying fewer peptides. Overall, this group found that in order to effectively use PQD and iTRAQ, they had to develop software to calculate abundance ratios of reporter ions by summing intensities across spectra matching to each protein (Griffin, 2007).

We attempted to extend the iTRAQ approach to analyzing complex protein mixtures using the iTRAQ system. Affinity purified eIF3 was labeled with the 114 and 117 reporter groups and mixed in a 1:2 ratio. However, among peptides from the same protein, we detected widely varying ratios of reporter ions. Some groups have found mild success using PQD and iTRAQ, namely Zhang and colleagues who used this approach to profile serum proteins (Zhang et. al., 2008). They were able to use SDS-PAGE to reduce overly abundant proteins in the mixture and quantify the relative abundance of 64 proteins from a total of 84 identifications (Zhang et. al., 2008). Making useful sense of the iTRAQ data necessitates new bioinformatics tools for calculating relative abundances by averaging reporter ion intensities across multiple peptides for a single protein to get confident data. Griffen and coworkers found similar results and developed specialized software to calculate relative abundances based on this observation. Since this was beyond the scope of what we wanted to accomplish in the lab, we abandoned this study here. Several groups have published on the utility of using PQD with iTRAQ labeling with limited success (Kocher et. al., 2009; Yang and Wu, 2009; Bantscheff et. al., 2008). Overall, this approach has not found widespread applicability in the field of proteomics.

CHAPTER V

SUMMARY AND CONCLUSIONS

The main focus of this dissertation was a comprehensive investigation into the interactions and phosphorylations of the eukaryotic translation initiation factor eIF3. The central hypothesis of my thesis is that there are unexpected and unidentified eIF3 protein-protein interactions and protein phosphorylations that regulate its function and activity in the essential process of translation initiation. The summary and conclusions section is divided into three parts. The first part deals with characterizing the proteins that interact with the eIF3 complex and identifying novel interacting partners. The second part deals with identifying phosphoproteins within the eIF3 complex and localizing these observed events to specific amino acid residues within the core components of eIF3. Each of the first two parts will address the biological significance of the findings as well as suggest further routes of investigation that may provide additional information as to eIF3's essential role in protein translation. The third and final section will address the utility of using pulsed Q-dissociation for the reliable detection of iTRAQ labeled peptides for quantitative proteomics.

Part 1: The eIF3 Interactome

eIF3 is crucial for the assembly and function of the 48S preinitiation complex. Previous studies have shown that eIF3 is composed of five core proteins in *S. cerevisiae* (Hinnebusch et. al., 2004). Additional interactions with noncore components of eIF3 have been identified with Hcr1, eIF1, and eIF5 (Valasek et. al., 2001; Hinnebusch et. al., 2004; Asano et. al., 2001). The broad range of functions postulated for the eIF3 complex leads to the hypothesis that there are yet to be identified proteins interacting with the eIF3 complex. To test this hypothesis, I performed affinity purifications of the components of eIF3 and determined the optimal strategy for obtaining the largest yield of the eIF3 complex. I coupled the optimized purification strategy to high sensitivity mass spectrometry based proteomics to obtain an extensive list of proteins interacting with eIF3.

I determined, in agreement with the previous work on eIF3, that its core complex is composed of Rpg1, Nip1, Prt1, Tif34 and Tif35. I was also able to detect interactions of eIF3 with Hcr1, eIF1, and eIF5, consistent with previous studies. Utilizing normalized spectral counting to estimate the relative abundance of known interacting proteins, we were able to identify novel intermolecular interactions of eIF3 with Fun12 and Pab1. Reciprocal affinity purifications of Fun12 and Pab1 revealed that they also copurified with the core members of eIF3. Fun12 has been shown to facilitate the joining of the 40S and 60S ribosomal subunits in the terminal step of translation initiation (Pestova et.

al., 2000). In addition, *Δfun12* null strains have a slow growth phenotype and altered polysome profiles suggesting a defect in translation initiation (Choi et. al., 1998). eIF3 has been shown to interact with the 40S subunit in the assembly of the 48S pre-initiation complex (Hinnebusch et. al., 2004; Asano et. al., 2001). This led to the postulation that the interaction of eIF3 with Fun12 links the formation of the pre-initiation complex with the binding of the 60S ribosome and the termination of translation initiation.

The finding that Pab1 associates with eIF3 is consistent with the current model of its function in translation. Pab1 has been shown to facilitate the joining of the 5' and 3' ends of mRNA by binding the initiation scaffold protein eIF4G (Tarun and Sachs, 1996;Cosson et. al., 2002). eIF4G along with eIF4A and eIF4E form the eIF4F complex (Hernandez and Vazquez-Pianzola, 2005). eIF4F facilitates the interaction of the 43S pre-initiation complex with the 5' cap structure of the mRNA producing the 48S pre-initiation complex. Efficient formation of the 48S pre-initiation complex is also dependent on eIF3 (Hinnebusch et. al., 2004). Similar to Fun12, *Δpab1* deleted strains have decreased levels of translation initiation (Sachs and Davis, 1990). Our finding that PABP interacts with the eIF3 complex complements the previous findings and suggests a role in this interaction in the efficient formation of the 48S pre-initiation complex.

Model and Future Directions

These two findings, namely the interaction of eIF3 with both Fun12 and Pab1, allow us to expand upon the model of what is currently believed to happen in translation initiation. Upstream of the cooperation of eIF3 with Fun12 is where the significance of the interaction between eIF3 and Pab1 may occur. Pab1 functions to circularize mRNA to facilitate formation of the 48S complex, a process for which eIF3 is also necessary. A direct interaction between eIF3 and Pab1 could help to stabilize the circularization of mRNA and the subsequent formation of the 48S complex. Since eIF3 functions to recruit the 40S subunit to form the 48S preinitiation complex and Fun12 functions in the formation of the 80S ribosome, it seems the two operate synergistically and directly to begin translation elongation following the efforts of Pab1 to form the 48S pre-initiation complex.

Further investigations are warranted to probe the true nature of the interactions of eIF3 with Fun12 and Pab1. Dr. Alan Hinnebusch's laboratory has performed work to map domains in eIF3 that interact with other proteins and initiation factors. It is possible that some of the uncharacterized domains of components of eIF3 interact with either or both Fun12 and Pab1. Analyzing mutants lacking these domains or mutants lacking sections of Fun12 or Pab1 using mass spectrometry based approaches may result in an abolition of the interactions observed between eIF3 and these two proteins. Additionally, these domain mutants may harbor defects in translation initiation that would manifest in

growth defects, translation defects, drug sensitivities, or altered polysome profiles. It would be interesting to generate and test such mutants in an attempt to discern the true consequence of the observed interactions.

Part 2: The Phosphorylation State of eIF3

Protein phosphorylation is a dynamic posttranslational modification that is widespread within the eukaryotic proteome. This modification's affects range from stochastic to specifically defined and targeted. While investigating the interactome of the eIF3 complex, it was found that the Casein Kinase 2 (CK2) complex copurifies with eIF3. Reciprocal isolations of components of the CK2 complex also isolated components of eIF3. The observation that a protein kinase copurifies with eIF3 led me to postulate that one or several components of the eIF3 complex are phosphorylated *in vivo*.

To test this hypothesis, cell cultures containing TAP-Rpg1 were labeled with ATP containing ^{32}P. The resulting mixture was affinity purified, separated via SDS-PAGE, transferred to nitrocellulose, and exposed to film. This experiment revealed a prominent band in the molecular weight region corresponding to the Nip1 protein of the eIF3 complex. This result indicated that Nip1 is phosphorylated *in vivo*. This evidence, along with the previous results showing that CK2 copurifies with eIF3, raised the question as to whether CK2 specifically targets eIF3 for the phosphorylation of Nip1. An *in vitro* kinase assay was performed with a broad range of kinases found in yeast. This experiment revealed that CK2 had the ability to phosphorylate Nip1 *in vitro*. Interestingly, a

less prominent signal was observed for Prt1 indicating that CK2 also has the ability to phosphorylate this component of eIF3. One reason for observing the signal *in vitro* and not *in vivo* for Prt1 could be that the signal in the latter approach may be too weak to be detectable by autoradiography. Conversely, this observation could simply be an artifact of using an *in vitro* approach whereby one loses a cellular regulatory event that inhibits the phosphorylation of Prt1 *in vivo*.

The next step in determining the cellular consequences of the observed phosphorylations was to localize the modification to specific amino acid side-chains. The traditional biochemical approach to elucidating which S, T, or Y residues are phosphorylated is Edman degradation followed by thin layer chromatography. This approach is laborious, requires large amounts of material, and utilizes additional radioactivity. I chose a high throughput approach that takes advantage of the sensitivity of mass spectrometry. The strategy with this approach is to affinity purify eIF3 and then use proteomics to determine which sites on the proteins comprising eIF3 are phosphorylated. This set of experiments identified two sites on Prt1, S61 and T746, that are phosphorylated *in vivo*. However, no phosphoresidues were identified on sites in Nip1 with this approach. As previously discussed, this can be attributed to ion suppression by an unmodified form of Nip1 masking the signal from the phosphorylated form or β-elimination of phosphoric acid from phosphorylated Nip1 resulting in a loss of signal in the mass spectrometer.

A variety of techniques exist that allow for the specific enrichment of phosphopeptides that increase the likelihood of identifying them downstream using proteomic approaches. Of the available techniques, I chose to perform immobilized metal affinity chromatography (IMAC) to selectively enrich for phosphopeptides from affinity purified samples of the eIF3 complex. This approach allowed for the identification of a triply phosphorylated peptide containing S98, S99, and S103, from Nip1. Doubly phosphorylated forms of the same peptide were also detected with S99 being constitutively modified and the second phosphorylation event involving either S98 or S103. The previously identified singly phosphorylated peptides from Prt1 were not identified with the IMAC approach. This is a common limitation of IMAC in that it preferentially binds multiply phosphorylated peptides leading to the loss of singly phosphorylated species (Ficarro et al., 2002). The localization of the phosphorylation to this region of Nip1 is an interesting observation since this section of Nip1 is proposed to mediate its interaction with Prt1. It could be speculated that losing the phosphorylation events will greatly decrease the polarity in this particular region of Nip1. A loss of strong polar interactions between Prt1 and Nip1 could reduce the stability of the eIF3 complex. The net result would be a smaller pool of eIF3 available to perform its native biological functions. This could in turn cause a biological defect in cells that lack the ability to form the stabilizing interaction between Nip1 and Prt1.

I chose to focus on the observed sites in Nip1 for further investigation since they may play a role in the stability of the eIF3 complex. To determine if

there were any other sites of phosphorylation on Nip1, I performed an *in vitro* inhibitory kinase assay to see if the signal observed for Nip1 would be abolished. The inhibitor was a commercially synthesized peptide identical in sequence to the peptide identified via mass spectrometry. Upon introduction of the peptide inhibitor to the assay, the signal in the corresponding Nip1 region is markedly decreased but not completely abolished. This result could indicate that there are more sites of phosphorylation on the Nip1 protein that were not identified by either proteomic approach attempted. The next step was to investigate the *in vivo* consequences of losing the three phosphorylation sites identified on Nip1. To accomplish this, a mutant form of Nip1 (*nip1S98,99,101A*) was generated. Repeating the autoradiography experiments utilizing the *nip1S98,99,101A* strain revealed an approximately 41% reduction in the observed signal in the Nip1 region. This result is further evidence that there still exist unidentified sites of phosphorylation on Nip1 that require additional work to identify.

The Biological Significance of *nip1S98,99,101A*

Since the region of Nip1 that I identified as phosphorylated is speculated to be involved in stabilizing the formation of the eIF3 complex, I hypothesized that the mutant *nip1S98,99,101A* strain would have a measurable biological defect. Defects in factors involved in translation initiation often manifest in reduced overall rates of protein synthesis. However, ^{35}S-methionine incorporation experiments showed no measurable difference between the rate of translation between wild-type and *nip1S98,99,101A*. Strains harboring defects in

the translation machinery often show increased sensitivity to drugs such as rapamycin, paromycin or cyclohexamide. Again there were no detectable differences in the growth of cells exposed to these drugs and other stresses such as osmotic and temperature shock when comparing the wild-type and *nip1S98,99,101A* strains.

An interesting observation was made throughout the experiments that required liquid culturing of the mutant strain. Overnight cultures of *nip1S98,99,101A* consistently resulted in a smaller cell pellet following centrifugation when compared to the wild-type cells. This observation led to the speculation that perhaps the *nip1S98,99,101A* strain has a detectable defect in its growth rate. Cell counting based experiments were performed to investigate this observation. These investigations revealed that the wild-type strain doubled every 111 ± 12 min, within the normal range for *S. cerevisiae.* However, the *nip1S98,99,101A* mutant strain doubled every 148 min ± 10 min, a 33% increase (p-value = 0.00687). Complementing the mutant strain with a wild-type Nip1 plasmid results in a restoration of the doubling time to normal levels (112 min ±8 min).

Model and Future Directions

The largest component of eIF3, Rpg1, has been suggested to be essential for G1-S phase transition and to be involved in the growth control of yeast cells (Kovarik et. al., 1998). A separate study conducted in human cells found that reducing eIF3a (Rpg1) expression also reduced cell proliferation by elongating

the cell cycle without changing the cell cycle distribution (Dong, 2009). These studies highlight a link between the growth rate of cells and the concerted action of the proteins composing eIF3. The model that I propose follows these same lines in that the phosphorylation of Nip1 introduces a key structural element that is essential for the efficient formation of the eIF3 complex. Perhaps the increased polarity provided by the phosphorylations stabilizes interactions with the Prt1 protein as this region of Nip1 is suspected to be involved in Nip1-Prt1 contacts. The resulting depletion of the stable eIF3 complex decreases the growth rate of the cells as observed by Kovarik and coworkers for Rpg1 depletion (Kovarik et. al., 1998).

Additional work is necessary from what was observed during the above experiments. Prt1 was found to contain two sites of phosphorylation at S61 and T746. Generating mutants lacking either one or both of these sites and performing experiments analogous to those performed on the Nip1 mutant could generate interesting results that would lead to further insights into the role of eIF3. These strains could possibly have more pronounced defects in their biology than what was observed for the *nip1S98,99,101A* mutant. The autoradiography experiments done with *nip1S98,99,101A* revealed a modest reduction in the amount of ^{32}P incorporated onto Nip1. Experiments using an alternative enrichment strategy such as immunoaffinity purification or TiO_2 enrichment followed by mass spectrometry could reveal additional phosphopeptides from Nip1. The generation of phosphomimetic strains that are

incapable of being dephosphorylated could also reveal further insight into the significance of the identified modifications.

Part 3: Pulsed-Q Dissociation and iTRAQ

Quantitative mass spectrometry-based proteomic techniques are providing researchers with powerful tools to investigate cellular biology. Quantifying differences in the proteome under differential states can yield valuable information about disease and aberrant cellular processes. The utility of these approaches owes to the observation that measurable differences in the levels of proteins can be indicative of particular states within cells or tissues. The advent of iTRAQ reagents to quantify either the relative or absolute amounts of proteins in biological samples has become a widespread technique in proteomics. This provides a robust method simultaneously identifying proteins in complex mixture while yielding quantification data. However, ion trap mass spectrometers are typically not useful for iTRAQ analysis because the reporter ions generated from the fragmentation of the iTRAQ tags are lost along with the lower 1/3 of the MS/MS data.

To circumvent this caveat of ion trap collision induced dissociation (CID), Thermo Electron, Inc. introduced pulsed-Q dissociation (PQD). The process of PQD involves activating the ions within the mass spectrometer's ion trap at both high Q values to generate sequencing fragment ions and activation at the low Q values to trap low m/z fragments. To this end, I hypothesized that an ion trap mass spectrometer capable of PQD could successfully fragment peptide ions for

sequencing while still providing low *m/z* iTRAQ reporter ions for quantitative studies. The ultimate goal was to use the knowledge gained in this study and extent it to the study of the eIF3 complex. Namely, this technique could prove advantageous in determining the relative ratios of eIF3's core components with its interacting partners.

The first goal of the study to evaluate the utility of PQD with iTRAQ was to determine if sufficient fragmentation of the precursor peptide could be accomplished to yield detectable ions for sequencing. The percent Q was varied and compared with complex mixtures of proteins analyzed with CID. I determined that a PQD normalized percent collision energy of between 25-35% will yield the best fragmentation data for use in identifying proteins in a complex biological mixture. However, PQD fails to provide as many peptide identifications when spectra are searched as does typical CID. I speculate that this observation may be due to the time delay imparted by the pulse in PQD whereby the precursor ion can lose kinetic energy via routes other that collision energy as the Q is pulsed. The resulting spectrum would contain fewer fragmentation ions for sequencing as a result of the delay in PQD. The loss of kinetic energy during this delay could also lead to a reduction in signal observed for the iTRAQ reporter ion series. These finding was also observed by other investigators where PQD spectra were dominated by the unfragmented precursor ion indicating poor fragmentation efficiency and a resulting limited iTRAQ reporter ion intensity (Bantscheff et. al., 2008). However, at the time I attempted these experiments, this information was yet to be published.

Although fragmentation spectra resulted in a reduced amount of sequencing information as compared to CID, protein identifications still resulted from the PQD spectra. I believed that if reliable reporter ions could still be detected with PQD induced fragmentation, that PQD could still find utility in quantifying peptides with the iTRAQ approach. I found that between 25 and 35% PQD collision energy resulted in the optimum number of peptide identifications. I next wanted to investigate at which percent PQD I could reliably detect iTRAQ reporter ions. The six protein standard supplied with the iTRAQ kit was used to evaluate the ability of PQD to reliably detect iTRAQ reporter ions in the low m/z range (114-117). Little to no reporter ion signal was detected below 25% PQD. Reporter ion detection maxed out at 30% PQD and decreased with increasing percent PQD thereafter.

It is not sufficient to only be able to fragment and detect the reporter ions. Reliable quantitative data must be able to be obtained from the intensities of the signal observed for the reporter ions. However, when the intensities of reporter ions were compared, the expected 1:1 ratio was not observed. The patterns for reporter ions from the same peptide were inconsistent when compared to other peptides generated from the same sample. Similar results have since been reported by other investigators and raise concerns as to the wide spread use of this technique in quantitative proteomics (Griffen, 2007). These experiments were repeated with a complex, affinity purified sample of yeast eIF3, mixed in a 2:1 ratio, resulted in similarly inconsistent results. I reasoned that perhaps if the ratios of reporter ions could be averaged across proteins, more consistent

quantitative data may be obtained. However, this was beyond the scope of the study, and it was decided to abandon the approach of using PQD together with iTRAQ.

A limited number of researchers have published on the utility of using PQD with iTRAQ labeling with limited success (Kocher et. al., 2009; Yang and Wu, 2009; Bantscheff et. al., 2008). Some of these groups found best results were obtained when overly abundant proteins were removed from the complex mixtures (Zhang et. al., 2008). More recently, PQD has been replaced by utilizing higher energy c-trap dissociation (HCD). HCD in hybrid Orbitrap mass spectrometers takes advantage of the presence of a C-trap in their design. HCD allows for the retention of the low m/z region on the spectra where reporter ions are often encountered (Olsen et. al., 2007). Recent groups have proven the utility of combining CID with HCD activation modes in an Orbitrap for the precise identification of peptides as well as quantification (Dayon et. al., 2010).

REFERENCES

Ackermann, K., Waxmann, A., Glover, C. V. and Pyerin, W. (2001). Genes targeted by protein kinase CK2: a genome-wide expression array analysis in yeast. Mol Cell Biochem *227*, 59-66.

Aebersold, R. and Mann, M. (2003). Mass spectrometry-based proteomics. Nature *422*, 198-207.

Ahmed, N. and Thornalley, P. J. (2003). Quantitative screening of protein biomarkers of early glycation, advanced glycation, oxidation and nitrosation in cellular and extracellular proteins by tandem mass spectrometry multiple reaction monitoring. Biochem Soc Trans *31*, 1417-22.

Alberti, S., Gitler, A. D. and Lindquist, S. (2007). A suite of Gateway cloning vectors for high-throughput genetic analysis in Saccharomyces cerevisiae. Yeast *24*, 913-9.

Alkalaeva, E. Z., Pisarev, A. V., Frolova, L. Y., Kisselev, L. L. and Pestova, T. V. (2006). In vitro reconstitution of eukaryotic translation reveals cooperativity between release factors eRF1 and eRF3. Cell *125*, 1125-36.

Anderson, N. L. and Anderson, N. G. (1998). Proteome and proteomics: new technologies, new concepts, and new words. Electrophoresis *19*, 1853-61.

Andersson, L. and Porath, J. (1986). Isolation of phosphoproteins by immobilized metal (Fe3+) affinity chromatography. Anal Biochem *154*, 250-4.

Asano, K., Clayton, J., Shalev, A. and Hinnebusch, A. G. (2000). A multifactor complex of eukaryotic initiation factors, eIF1, eIF2, eIF3, eIF5, and initiator tRNA(Met) is an important translation initiation intermediate in vivo. Genes Dev *14*, 2534-46.

Asano, K., Phan, L., Valasek, L., Schoenfeld, L. W., Shalev, A., Clayton, J., Nielsen, K., Donahue, T. F. and Hinnebusch, A. G. (2001). A multifactor complex of eIF1, eIF2, eIF3, eIF5, and tRNA(i)Met promotes initiation complex assembly and couples GTP hydrolysis to AUG recognition. Cold Spring Harb Symp Quant Biol *66*, 403-15.

Bantscheff, M., Boesche, M., Eberhard, D., Matthieson, T., Sweetman, G. and Kuster, B. (2008). Robust and sensitive iTRAQ quantification on an LTQ Orbitrap mass spectrometer. Mol Cell Proteomics *7*, 1702-13.

Bantscheff, M., Schirle, M., Sweetman, G., Rick, J. and Kuster, B. (2007). Quantitative mass spectrometry in proteomics: a critical review. Anal Bioanal Chem *389*, 1017-31.

Beausoleil, S. A., Jedrychowski, M., Schwartz, D., Elias, J. E., Villen, J., Li, J., Cohn, M. A., Cantley, L. C. and Gygi, S. P. (2004). Large-scale characterization of HeLa cell nuclear phosphoproteins. Proc Natl Acad Sci U S A *101*, 12130-5.

Bennett, K. L., Stensballe, A., Podtelejnikov, A. V., Moniatte, M. and Jensen, O. N. (2002). Phosphopeptide detection and sequencing by matrix-assisted laser desorption/ionization quadrupole time-of-flight tandem mass spectrometry. J Mass Spectrom *37*, 179-90.

Beretta, L. (2004). Translational control in T lymphocytes. Int Rev Immunol *23*, 347-63.

Berger, S. L. (2007). The complex language of chromatin regulation during transcription. Nature *447*, 407-12.

Bidwai, A. P., Reed, J. C. and Glover, C. V. (1995). Cloning and disruption of CKB1, the gene encoding the 38-kDa beta subunit of Saccharomyces cerevisiae casein kinase II (CKII). Deletion of CKII regulatory subunits elicits a salt-sensitive phenotype. J Biol Chem *270*, 10395-404.

Bjornsti, M. A. and Houghton, P. J. (2004). Lost in translation: dysregulation of cap-dependent translation and cancer. Cancer Cell *5*, 519-23.

Blagoev, B., Ong, S. E., Kratchmarova, I. and Mann, M. (2004). Temporal analysis of phosphotyrosine-dependent signaling networks by quantitative proteomics. Nat Biotechnol *22*, 1139-45.

Blume-Jensen, P. and Hunter, T. (2001). Oncogenic kinase signalling. Nature *411*, 355-65.

Bodenmiller, B., Mueller, L. N., Pedrioli, P. G., Pflieger, D., Junger, M. A., Eng, J. K., Aebersold, R. and Tao, W. A. (2007). An integrated chemical, mass spectrometric and computational strategy for (quantitative) phosphoproteomics: application to Drosophila melanogaster Kc167 cells. Mol Biosyst *3*, 275-86.

Bodnar, W. M., Blackburn, R. K., Krise, J. M. and Moseley, M. A. (2003). Exploiting the complementary nature of LC/MALDI/MS/MS and LC/ESI/MS/MS for increased proteome coverage. J Am Soc Mass Spectrom *14*, 971-9.

Browning, K. S., Gallie, D. R., Hershey, J. W., Hinnebusch, A. G., Maitra, U., Merrick, W. C. and Norbury, C. (2001). Unified nomenclature for the subunits of eukaryotic initiation factor 3. Trends Biochem Sci *26*, 284.

Calkhoven, C. F., Muller, C. and Leutz, A. (2002). Translational control of gene expression and disease. Trends Mol Med *8*, 577-83.

Cantin, G. T., Shock, T. R., Park, S. K., Madhani, H. D. and Yates, J. R., 3rd (2007). Optimizing TiO2-based phosphopeptide enrichment for automated multidimensional liquid chromatography coupled to tandem mass spectrometry. Anal Chem *79*, 4666-73.

Carr, S. A., Huddleston, M. J. and Annan, R. S. (1996). Selective detection and sequencing of phosphopeptides at the femtomole level by mass spectrometry. Anal Biochem *239*, 180-92.

Chang, I. F. (2006). Mass spectrometry-based proteomic analysis of the epitope-tag affinity purified protein complexes in eukaryotes. Proteomics *6*, 6158-66.

Choi, S. K., Lee, J. H., Zoll, W. L., Merrick, W. C. and Dever, T. E. (1998). Promotion of met-tRNAiMet binding to ribosomes by yIF2, a bacterial IF2 homolog in yeast. Science *280*, 1757-60.

Cirulli, C., Chiappetta, G., Marino, G., Mauri, P. and Amoresano, A. (2008). Identification of free phosphopeptides in different biological fluids by a mass spectrometry approach. Anal Bioanal Chem *392*, 147-59.

Clemens, M. J. (2005). Translational control in virus-infected cells: models for cellular stress responses. Semin Cell Dev Biol *16*, 13-20.

Cohen, P. (2001). The role of protein phosphorylation in human health and disease. The Sir Hans Krebs Medal Lecture. Eur J Biochem *268*, 5001-10.

Coon, J. J., Syka, J. E. P., Schwartz, J. C., Shabanowitz, J. and Hunt, D. F. (2004). Anion dependence in the partitioning between proton and electron transfer in ion/ion reactions. International Journal of Mass Spectrometry *236*, 33–42.

Cosson, B., Berkova, N., Couturier, A., Chabelskaya, S., Philippe, M. and Zhouravleva, G. (2002). Poly(A)-binding protein and eRF3 are associated in vivo in human and Xenopus cells. Biol Cell *94*, 205-16.

Covey, T. R., Huang, E. C. and Henion, J. D. (1991). Structural characterization of protein tryptic peptides via liquid chromatography/mass spectrometry and

collision-induced dissociation of their doubly charged molecular ions. Anal Chem *63*, 1193-200.

Crick, F. (1970). Central dogma of molecular biology. Nature *227*, 561-3.

Crick, F. H. (1958). On protein synthesis. Symp Soc Exp Biol *12*, 138-63.

Cuchalova, L., Kouba, T., Herrmannova, A., Danyi, I., Chiu, W. L. and Valasek, L. (2010). The RNA recognition motif of eukaryotic translation initiation factor 3g (eIF3g) is required for resumption of scanning of posttermination ribosomes for reinitiation on GCN4 and together with eIF3i stimulates linear scanning. Mol Cell Biol *30*, 4671-86.

Cunningham, C., Jr., Glish, G. L. and Burinsky, D. J. (2006). High amplitude short time excitation: a method to form and detect low mass product ions in a quadrupole ion trap mass spectrometer. J Am Soc Mass Spectrom *17*, 81-4.

Das, S. and Maitra, U. (2001). Functional significance and mechanism of eIF5-promoted GTP hydrolysis in eukaryotic translation initiation. Prog Nucleic Acid Res Mol Biol *70*, 207-31.

Das, S. and Maitra, U. (2000). Mutational analysis of mammalian translation initiation factor 5 (eIF5): role of interaction between the beta subunit of eIF2 and eIF5 in eIF5 function in vitro and in vivo. Mol Cell Biol *20*, 3942-50.

Dayon, L., Pasquarello, C., Hoogland, C., Sanchez, J. C. and Scherl, A. Combining low- and high-energy tandem mass spectra for optimized peptide quantification with isobaric tags. J Proteomics *73*, 769-77.

Dayon, L., Turck, N., Kienle, S., Schulz-Knappe, P., Hochstrasser, D. F., Scherl, A. and Sanchez, J. C. Isobaric tagging-based selection and quantitation of cerebrospinal fluid tryptic peptides with reporter calibration curves. Anal Chem *82*, 848-58.

de Moor, C. H., Meijer, H. and Lissenden, S. (2005). Mechanisms of translational control by the 3' UTR in development and differentiation. Semin Cell Dev Biol *16*, 49-58.

Denman, R. B., Dolzhanskaya, N. and Sung, Y. J. (2004). Regulating a translational regulator: mechanisms cells use to control the activity of the fragile X mental retardation protein. Cell Mol Life Sci *61*, 1714-28.

Dinman, J. D. (2009). The eukaryotic ribosome: current status and challenges. J Biol Chem *284*, 11761-5.

Dongre, A. R., Jones, J. L., Somogyi, A. and Wysocki, V. H. (1996). Influence of peptide composition, gas-phase basicity, and chemical modification on fragmentation efficiency: Evidence for the mobile proton model. Journal of the American Chemical Society *118*, 8365-8374.

Farley, A. R., Powell, D. W., Weaver, C. M., Jennings, J. L. and Link, A. J. (2011) Assessing the components of the eIF3 complex and their phosphorylation status. J Proteome Res *10*, 1481-94.

Feng, L., Yoon, H. and Donahue, T. F. (1994). Casein kinase II mediates multiple phosphorylation of Saccharomyces cerevisiae eIF-2 alpha (encoded by SUI2), which is required for optimal eIF-2 function in S. cerevisiae. Mol Cell Biol *14*, 5139-53.

Ficarro, S. B., McCleland, M. L., Stukenberg, P. T., Burke, D. J., Ross, M. M., Shabanowitz, J., Hunt, D. F. and White, F. M. (2002). Phosphoproteome analysis by mass spectrometry and its application to Saccharomyces cerevisiae. Nat Biotechnol *20*, 301-5.

Fleischer, T. C., Weaver, C. M., McAfee, K. J., Jennings, J. L. and Link, A. J. (2006). Systematic identification and functional screens of uncharacterized proteins associated with eukaryotic ribosomal complexes. Genes Dev *20*, 1294-307.

Frolova, L. Y., Tsivkovskii, R. Y., Sivolobova, G. F., Oparina, N. Y., Serpinsky, O. I., Blinov, V. M., Tatkov, S. I. and Kisselev, L. L. (1999). Mutations in the highly conserved GGQ motif of class 1 polypeptide release factors abolish ability of human eRF1 to trigger peptidyl-tRNA hydrolysis. Rna *5*, 1014-20.

Fuchs, S. M., Laribee, R. N. and Strahl, B. D. (2009). Protein modifications in transcription elongation. Biochim Biophys Acta *1789*, 26-36.

Garcia, B. A., Shabanowitz, J. and Hunt, D. F. (2005). Analysis of protein phosphorylation by mass spectrometry. Methods *35*, 256-64.

Garcia, B. A., Shabanowitz, J. and Hunt, D. F. (2007). Characterization of histones and their post-translational modifications by mass spectrometry. Curr Opin Chem Biol *11*, 66-73.

Gatzka, M. and Walsh, C. M. (2007). Apoptotic signal transduction and T cell tolerance. Autoimmunity *40*, 442-52.

Gavin, A. C., Aloy, P., Grandi, P., Krause, R., Boesche, M., Marzioch, M., Rau, C., Jensen, L. J., Bastuck, S., Dumpelfeld, B., Edelmann, A., Heurtier, M. A., Hoffman, V., Hoefert, C., Klein, K., Hudak, M., Michon, A. M., Schelder, M.,

Schirle, M., Remor, M., Rudi, T., Hooper, S., Bauer, A., Bouwmeester, T., Casari, G., Drewes, G., Neubauer, G., Rick, J. M., Kuster, B., Bork, P., Russell, R. B. and Superti-Furga, G. (2006). Proteome survey reveals modularity of the yeast cell machinery. Nature

Gavin, A. C., Bosche, M., Krause, R., Grandi, P., Marzioch, M., Bauer, A., Schultz, J., Rick, J. M., Michon, A. M., Cruciat, C. M., Remor, M., Hofert, C., Schelder, M., Brajenovic, M., Ruffner, H., Merino, A., Klein, K., Hudak, M., Dickson, D., Rudi, T., Gnau, V., Bauch, A., Bastuck, S., Huhse, B., Leutwein, C., Heurtier, M. A., Copley, R. R., Edelmann, A., Querfurth, E., Rybin, V., Drewes, G., Raida, M., Bouwmeester, T., Bork, P., Seraphin, B., Kuster, B., Neubauer, G. and Superti-Furga, G. (2002). Functional organization of the yeast proteome by systematic analysis of protein complexes. Nature *415*, 141-7.

Ge, Y., Rybakova, I. N., Xu, Q. and Moss, R. L. (2009). Top-down high-resolution mass spectrometry of cardiac myosin binding protein C revealed that truncation alters protein phosphorylation state. Proc Natl Acad Sci U S A *106*, 12658-63.

Gebauer, F. and Hentze, M. W. (2004). Molecular mechanisms of translational control. Nat Rev Mol Cell Biol *5*, 827-35.

Gerber, S. A., Rush, J., Stemman, O., Kirschner, M. W. and Gygi, S. P. (2003). Absolute quantification of proteins and phosphoproteins from cell lysates by tandem MS. Proc Natl Acad Sci U S A *100*, 6940-5.

Ghaemmaghami, S., Huh, W. K., Bower, K., Howson, R. W., Belle, A., Dephoure, N., O'Shea, E. K. and Weissman, J. S. (2003). Global analysis of protein expression in yeast. Nature *425*, 737-41.

Gingras, A. C., Raught, B., Gygi, S. P., Niedzwiecka, A., Miron, M., Burley, S. K., Polakiewicz, R. D., Wyslouch-Cieszynska, A., Aebersold, R. and Sonenberg, N. (2001). Hierarchical phosphorylation of the translation inhibitor 4E-BP1. Genes Dev *15*, 2852-64.

Gingras, A. C., Raught, B. and Sonenberg, N. (1999). eIF4 initiation factors: effectors of mRNA recruitment to ribosomes and regulators of translation. Annu Rev Biochem *68*, 913-63.

Glover, C. V., 3rd (1998). On the physiological role of casein kinase II in Saccharomyces cerevisiae. Prog Nucleic Acid Res Mol Biol *59*, 95-133.

Gobom, J., Schuerenberg, M., Mueller, M., Theiss, D., Lehrach, H. and Nordhoff, E. (2001). Alpha-cyano-4-hydroxycinnamic acid affinity sample preparation. A protocol for MALDI-MS peptide analysis in proteomics. Anal Chem *73*, 434-8.

Godde, J. S. and Ura, K. (2008). Cracking the enigmatic linker histone code. J Biochem *143*, 287-93.

Good, D. M., Wirtala, M., McAlister, G. C. and Coon, J. J. (2007). Performance characteristics of electron transfer dissociation mass spectrometry. Mol Cell Proteomics *6*, 1942-51.

Goodlett, D. R., Keller, A., Watts, J. D., Newitt, R., Yi, E. C., Purvine, S., Eng, J. K., von Haller, P., Aebersold, R. and Kolker, E. (2001). Differential stable isotope labeling of peptides for quantitation and de novo sequence derivation. Rapid Commun Mass Spectrom *15*, 1214-21.

Goshe, M. B., Conrads, T. P., Panisko, E. A., Angell, N. H., Veenstra, T. D. and Smith, R. D. (2001). Phosphoprotein isotope-coded affinity tag approach for isolating and quantitating phosphopeptides in proteome-wide analyses. Anal Chem *73*, 2578-86.

Graves, P. R. and Haystead, T. A. (2002). Molecular biologist's guide to proteomics. Microbiol Mol Biol Rev *66*, 39-63; table of contents.

Gray, N. S., Wodicka, L., Thunnissen, A. M., Norman, T. C., Kwon, S., Espinoza, F. H., Morgan, D. O., Barnes, G., LeClerc, S., Meijer, L., Kim, S. H., Lockhart, D. J. and Schultz, P. G. (1998). Exploiting chemical libraries, structure, and genomics in the search for kinase inhibitors. Science *281*, 533-8.

Griffin, T. J., Xie, H., Bandhakavi, S., Popko, J., Mohan, A., Carlis, J. V. and Higgins, L. (2007). iTRAQ reagent-based quantitative proteomic analysis on a linear ion trap mass spectrometer. J Proteome Res *6*, 4200-9.

Gruhler, A., Olsen, J. V., Mohammed, S., Mortensen, P., Faergeman, N. J., Mann, M. and Jensen, O. N. (2005). Quantitative phosphoproteomics applied to the yeast pheromone signaling pathway. Mol Cell Proteomics *4*, 310-27.

Gu, Z., Moerschell, R. P., Sherman, F. and Goldfarb, D. S. (1992). NIP1, a gene required for nuclear transport in yeast. Proc Natl Acad Sci U S A *89*, 10355-9.

Gygi, S. P., Rist, B., Gerber, S. A., Turecek, F., Gelb, M. H. and Aebersold, R. (1999). Quantitative analysis of complex protein mixtures using isotope-coded affinity tags. Nat Biotechnol *17*, 994-9.

Hanic-Joyce, P. J., Singer, R. A. and Johnston, G. C. (1987). Molecular characterization of the yeast PRT1 gene in which mutations affect translation initiation and regulation of cell proliferation. J Biol Chem *262*, 2845-51.

Hayduk, E. J., Choe, L. H. and Lee, K. H. (2004). A two-dimensional electrophoresis map of Chinese hamster ovary cell proteins based on fluorescence staining. Electrophoresis *25*, 2545-56.

Hernandez, G. and Vazquez-Pianzola, P. (2005). Functional diversity of the eukaryotic translation initiation factors belonging to eIF4 families. Mech Dev *122*, 865-76.

Hinnebusch, A. G. (2005). Translational regulation of GCN4 and the general amino acid control of yeast. Annu Rev Microbiol *59*, 407-50.

Hinnebusch, A. G. (1997). Translational regulation of yeast GCN4. A window on factors that control initiator-trna binding to the ribosome. J Biol Chem *272*, 21661-4.

Hinnebusch, A. G., Asano, K., Olsen, D. S., Phan, L., Nielsen, K. H. and Valasek, L. (2004). Study of translational control of eukaryotic gene expression using yeast. Ann N Y Acad Sci *1038*, 60-74.

Ho, Y., Gruhler, A., Heilbut, A., Bader, G. D., Moore, L., Adams, S. L., Millar, A., Taylor, P., Bennett, K., Boutilier, K., Yang, L., Wolting, C., Donaldson, I., Schandorff, S., Shewnarane, J., Vo, M., Taggart, J., Goudreault, M., Muskat, B., Alfarano, C., Dewar, D., Lin, Z., Michalickova, K., Willems, A. R., Sassi, H., Nielsen, P. A., Rasmussen, K. J., Andersen, J. R., Johansen, L. E., Hansen, L. H., Jespersen, H., Podtelejnikov, A., Nielsen, E., Crawford, J., Poulsen, V., Sorensen, B. D., Matthiesen, J., Hendrickson, R. C., Gleeson, F., Pawson, T., Moran, M. F., Durocher, D., Mann, M., Hogue, C. W., Figeys, D. and Tyers, M. (2002). Systematic identification of protein complexes in Saccharomyces cerevisiae by mass spectrometry. Nature *415*, 180-3.

Holcik, M. and Sonenberg, N. (2005). Translational control in stress and apoptosis. Nat Rev Mol Cell Biol *6*, 318-27.

Huang, Y., Triscari, J. M., Tseng, G. C., Pasa-Tolic, L., Lipton, M. S., Smith, R. D. and Wysocki, V. H. (2005). Statistical characterization of the charge state and residue dependence of low-energy CID peptide dissociation patterns. Anal Chem *77*, 5800-13.

Hubbard, M. J. and Cohen, P. (1993). On target with a new mechanism for the regulation of protein phosphorylation. Trends Biochem Sci *18*, 172-7.

Hunt, D. F., Zhu, N. Z. and Shabanowitz, J. (1989). Oligopeptide sequence analysis by collision-activated dissociation of multiply charged ions. Rapid Commun Mass Spectrom *3*, 122-4.

Ishii, T. M., Zerr, P., Xia, X. M., Bond, C. T., Maylie, J. and Adelman, J. P. (1998). Site-directed mutagenesis. Methods Enzymol *293*, 53-71.

Issad, T. and Kuo, M. (2008). O-GlcNAc modification of transcription factors, glucose sensing and glucotoxicity. Trends Endocrinol Metab *19*, 380-9.

Ito, K., Ebihara, K. and Nakamura, Y. (1998). The stretch of C-terminal acidic amino acids of translational release factor eRF1 is a primary binding site for eRF3 of fission yeast. Rna *4*, 958-72.

Jackson, R. J., Hellen, C. U. and Pestova, T. V. (2010). The mechanism of eukaryotic translation initiation and principles of its regulation. Nat Rev Mol Cell Biol *11*, 113-27.

Jenuwein, T. and Allis, C. D. (2001). Translating the histone code. Science *293*, 1074-80.

Jivotovskaya, A. V., Valasek, L., Hinnebusch, A. G. and Nielsen, K. H. (2006). Eukaryotic translation initiation factor 3 (eIF3) and eIF2 can promote mRNA binding to 40S subunits independently of eIF4G in yeast. Mol Cell Biol *26*, 1355-72.

Kimball, S. R. (1999). Eukaryotic initiation factor eIF2. Int J Biochem Cell Biol *31*, 25-9.

Kisselev, L., Ehrenberg, M. and Frolova, L. (2003). Termination of translation: interplay of mRNA, rRNAs and release factors? Embo J *22*, 175-82.

Klann, E. and Dever, T. E. (2004). Biochemical mechanisms for translational regulation in synaptic plasticity. Nat Rev Neurosci *5*, 931-42.

Knippschild, U., Milne, D. M., Campbell, L. E., DeMaggio, A. J., Christenson, E., Hoekstra, M. F. and Meek, D. W. (1997). p53 is phosphorylated in vitro and in vivo by the delta and epsilon isoforms of casein kinase 1 and enhances the level of casein kinase 1 delta in response to topoisomerase-directed drugs. Oncogene *15*, 1727-36.

Kocher, T., Pichler, P., Schutzbier, M., Stingl, C., Kaul, A., Teucher, N., Hasenfuss, G., Penninger, J. M. and Mechtler, K. (2009). High precision quantitative proteomics using iTRAQ on an LTQ Orbitrap: a new mass spectrometric method combining the benefits of all. J Proteome Res *8*, 4743-52.

Kovarik, P., Hasek, J., Valasek, L. and Ruis, H. (1998). RPG1: an essential gene of saccharomyces cerevisiae encoding a 110-kDa protein required for passage through the G1 phase. Curr Genet *33*, 100-9.

Krogan, N. J., Peng, W. T., Cagney, G., Robinson, M. D., Haw, R., Zhong, G., Guo, X., Zhang, X., Canadien, V., Richards, D. P., Beattie, B. K., Lalev, A., Zhang, W., Davierwala, A. P., Mnaimneh, S., Starostine, A., Tikuisis, A. P., Grigull, J., Datta, N., Bray, J. E., Hughes, T. R., Emili, A. and Greenblatt, J. F. (2004). High-definition macromolecular composition of yeast RNA-processing complexes. Mol Cell *13*, 225-39.

Kuersten, S. and Goodwin, E. B. (2003). The power of the 3' UTR: translational control and development. Nat Rev Genet *4*, 626-37.

Larsen, M. R., Thingholm, T. E., Jensen, O. N., Roepstorff, P. and Jorgensen, T. J. (2005). Highly selective enrichment of phosphorylated peptides from peptide mixtures using titanium dioxide microcolumns. Mol Cell Proteomics *4*, 873-86.

Lee, C. H., McComb, M. E., Bromirski, M., Jilkine, A., Ens, W., Standing, K. G. and Perreault, H. (2001). On-membrane digestion of beta-casein for determination of phosphorylation sites by matrix-assisted laser desorption/ionization quadrupole/time-of-flight mass spectrometry. Rapid Commun Mass Spectrom *15*, 191-202.

Lee, I., Date, S. V., Adai, A. T. and Marcotte, E. M. (2004). A probabilistic functional network of yeast genes. Science *306*, 1555-8.

Lim, K. B. and Kassel, D. B. (2006). Phosphopeptides enrichment using on-line two-dimensional strong cation exchange followed by reversed-phase liquid chromatography/mass spectrometry. Anal Biochem *354*, 213-9.

Lindemann, S. W., Weyrich, A. S. and Zimmerman, G. A. (2005). Signaling to translational control pathways: diversity in gene regulation in inflammatory and vascular cells. Trends Cardiovasc Med *15*, 9-17.

Link, A. J., Eng, J., Schieltz, D. M., Carmack, E., Mize, G. J., Morris, D. R., Garvik, B. M. and Yates, J. R., 3rd (1999). Direct analysis of protein complexes using mass spectrometry. Nat Biotechnol *17*, 676-82.

Link, A. J., Fleischer, T. C., Weaver, C. M., Gerbasi, V. R. and Jennings, J. L. (2005). Purifying protein complexes for mass spectrometry: applications to protein translation. Methods *35*, 274-90.

Lu, B., Motoyama, A., Ruse, C., Venable, J. and Yates, J. R., 3rd (2008). Improving protein identification sensitivity by combining MS and MS/MS

information for shotgun proteomics using LTQ-Orbitrap high mass accuracy data. Anal Chem *80*, 2018-25.

Ma, Y., Lu, Y., Zeng, H., Ron, D., Mo, W. and Neubert, T. A. (2001). Characterization of phosphopeptides from protein digests using matrix-assisted laser desorption/ionization time-of-flight mass spectrometry and nanoelectrospray quadrupole time-of-flight mass spectrometry. Rapid Commun Mass Spectrom *15*, 1693-700.

Maag, D., Fekete, C. A., Gryczynski, Z. and Lorsch, J. R. (2005). A conformational change in the eukaryotic translation preinitiation complex and release of eIF1 signal recognition of the start codon. Mol Cell *17*, 265-75.

MacCoss, M. J., McDonald, W. H., Saraf, A., Sadygov, R., Clark, J. M., Tasto, J. J., Gould, K. L., Wolters, D., Washburn, M., Weiss, A., Clark, J. I. and Yates, J. R., 3rd (2002). Shotgun identification of protein modifications from protein complexes and lens tissue. Proc Natl Acad Sci U S A *99*, 7900-5.

Makarov, A., Denisov, E., Kholomeev, A., Balschun, W., Lange, O., Strupat, K. and Horning, S. (2006). Performance evaluation of a hybrid linear ion trap/orbitrap mass spectrometer. Anal Chem *78*, 2113-20.

Mann, M., Ong, S. E., Gronborg, M., Steen, H., Jensen, O. N. and Pandey, A. (2002). Analysis of protein phosphorylation using mass spectrometry: deciphering the phosphoproteome. Trends Biotechnol *20*, 261-8.

McAfee, K. J., Duncan, D. T., Assink, M. and Link, A. J. (2006). Analyzing proteomes and protein function using graphical comparative analysis of tandem mass spectrometry results. Mol Cell Proteomics *5*, 1497-513.

McLachlin, D. T. and Chait, B. T. (2001). Analysis of phosphorylated proteins and peptides by mass spectrometry. Curr Opin Chem Biol *5*, 591-602.

McLachlin, D. T. and Chait, B. T. (2003). Improved beta-elimination-based affinity purification strategy for enrichment of phosphopeptides. Anal Chem *75*, 6826-36.

Meric, F. and Hunt, K. K. (2002). Translation initiation in cancer: a novel target for therapy. Mol Cancer Ther *1*, 971-9.

Mikesh, L. M., Ueberheide, B., Chi, A., Coon, J. J., Syka, J. E., Shabanowitz, J. and Hunt, D. F. (2006). The utility of ETD mass spectrometry in proteomic analysis. Biochim Biophys Acta *1764*, 1811-22.

Mirgorodskaya, E., Wanker, E., Otto, A., Lehrach, H. and Gobom, J. (2005). Method for qualitative comparisons of protein mixtures based on enzyme-catalyzed stable-isotope incorporation. J Proteome Res *4*, 2109-16.

Moser, K. and White, F. M. (2006). Phosphoproteomic analysis of rat liver by high capacity IMAC and LC-MS/MS. J Proteome Res *5*, 98-104.

Nagaraj, N., Lu, A., Mann, M. and Wisniewski, J. R. (2008). Detergent-Based but Gel-Free Method Allows Identification of Several Hundred Membrane Proteins in Single LC-MS Runs. J Proteome Res *7*, 5028-32.

Nielsen, K. H., Szamecz, B., Valasek, L., Jivotovskaya, A., Shin, B. S. and Hinnebusch, A. G. (2004). Functions of eIF3 downstream of 48S assembly impact AUG recognition and GCN4 translational control. Embo J *23*, 1166-77.

Nielsen, K. H., Valasek, L., Sykes, C., Jivotovskaya, A. and Hinnebusch, A. G. (2006). Interaction of the RNP1 motif in PRT1 with HCR1 promotes 40S binding of eukaryotic initiation factor 3 in yeast. Mol Cell Biol *26*, 2984-98.

Obenauer, J. C., Cantley, L. C. and Yaffe, M. B. (2003). Scansite 2.0: Proteome-wide prediction of cell signaling interactions using short sequence motifs. Nucleic Acids Res *31*, 3635-41.

Oda, Y., Huang, K., Cross, F. R., Cowburn, D. and Chait, B. T. (1999). Accurate quantitation of protein expression and site-specific phosphorylation. Proc Natl Acad Sci U S A *96*, 6591-6.

Oda, Y., Nagasu, T. and Chait, B. T. (2001). Enrichment analysis of phosphorylated proteins as a tool for probing the phosphoproteome. Nat Biotechnol *19*, 379-82.

Old, W. M., Meyer-Arendt, K., Aveline-Wolf, L., Pierce, K. G., Mendoza, A., Sevinsky, J. R., Resing, K. A. and Ahn, N. G. (2005). Comparison of label-free methods for quantifying human proteins by shotgun proteomics. Mol Cell Proteomics *4*, 1487-502.

Olsen, D. S., Savner, E. M., Mathew, A., Zhang, F., Krishnamoorthy, T., Phan, L. and Hinnebusch, A. G. (2003). Domains of eIF1A that mediate binding to eIF2, eIF3 and eIF5B and promote ternary complex recruitment in vivo. Embo J *22*, 193-204.

Olsen, J. V., Blagoev, B., Gnad, F., Macek, B., Kumar, C., Mortensen, P. and Mann, M. (2006). Global, in vivo, and site-specific phosphorylation dynamics in signaling networks. Cell *127*, 635-48.

Olsen, J. V., Macek, B., Lange, O., Makarov, A., Horning, S. and Mann, M. (2007). Higher-energy C-trap dissociation for peptide modification analysis. Nat Methods *4*, 709-12.

Olsen, J. V. and Mann, M. (2004). Improved peptide identification in proteomics by two consecutive stages of mass spectrometric fragmentation. Proc Natl Acad Sci U S A *101*, 13417-22.

Olsson, A., Manzl, C., Strasser, A. and Villunger, A. (2007). How important are post-translational modifications in p53 for selectivity in target-gene transcription and tumour suppression? Cell Death Differ *14*, 1561-75.

Ong, S. E., Blagoev, B., Kratchmarova, I., Kristensen, D. B., Steen, H., Pandey, A. and Mann, M. (2002). Stable isotope labeling by amino acids in cell culture, SILAC, as a simple and accurate approach to expression proteomics. Mol Cell Proteomics *1*, 376-86.

Ong, S. E. and Mann, M. (2005). Mass spectrometry-based proteomics turns quantitative. Nat Chem Biol *1*, 252-62.

Ong, S. E., Mittler, G. and Mann, M. (2004). Identifying and quantifying in vivo methylation sites by heavy methyl SILAC. Nat Methods *1*, 119-26.

Padmanabha, R., Chen-Wu, J. L., Hanna, D. E. and Glover, C. V. (1990). Isolation, sequencing, and disruption of the yeast CKA2 gene: casein kinase II is essential for viability in Saccharomyces cerevisiae. Mol Cell Biol *10*, 4089-99.

Pagano, M. A., Poletto, G., Di Maira, G., Cozza, G., Ruzzene, M., Sarno, S., Bain, J., Elliott, M., Moro, S., Zagotto, G., Meggio, F. and Pinna, L. A. (2007). Tetrabromocinnamic acid (TBCA) and related compounds represent a new class of specific protein kinase CK2 inhibitors. Chembiochem *8*, 129-39.

Pan, C., Gnad, F., Olsen, J. V. and Mann, M. (2008). Quantitative phosphoproteome analysis of a mouse liver cell line reveals specificity of phosphatase inhibitors. Proteomics *8*, 4534-46.

Pandey, A. and Mann, M. (2000). Proteomics to study genes and genomes. Nature *405*, 837-46.

Paoletti, A. C. and Washburn, M. P. (2006). Quantitation in proteomic experiments utilizing mass spectrometry. Biotechnol Genet Eng Rev *22*, 1-19.

Parsa, A. T. and Holland, E. C. (2004). Cooperative translational control of gene expression by Ras and Akt in cancer. Trends Mol Med *10*, 607-13.

Patton, W. F. (2002). Detection technologies in proteome analysis. J Chromatogr B Analyt Technol Biomed Life Sci *771*, 3-31.

Pestova, T. V., Lomakin, I. B., Lee, J. H., Choi, S. K., Dever, T. E. and Hellen, C. U. (2000). The joining of ribosomal subunits in eukaryotes requires eIF5B. Nature *403*, 332-5.

Phan, L., Zhang, X., Asano, K., Anderson, J., Vornlocher, H. P., Greenberg, J. R., Qin, J. and Hinnebusch, A. G. (1998). Identification of a translation initiation factor 3 (eIF3) core complex, conserved in yeast and mammals, that interacts with eIF5. Mol Cell Biol *18*, 4935-46.

Pinkse, M. W., Uitto, P. M., Hilhorst, M. J., Ooms, B. and Heck, A. J. (2004). Selective isolation at the femtomole level of phosphopeptides from proteolytic digests using 2D-NanoLC-ESI-MS/MS and titanium oxide precolumns. Anal Chem *76*, 3935-43.

Pinna, L. A. (2002). Protein kinase CK2: a challenge to canons. J Cell Sci *115*, 3873-8.

Pitteri, S. J., Chrisman, P. A., Hogan, J. M. and McLuckey, S. A. (2005). Electron transfer ion/ion reactions in a three-dimensional quadrupole ion trap: reactions of doubly and triply protonated peptides with SO2*. Anal Chem *77*, 1831-9.

Poole, A., Poore, T., Bandhakavi, S., McCann, R. O., Hanna, D. E. and Glover, C. V. (2005). A global view of CK2 function and regulation. Mol Cell Biochem *274*, 163-70.

Powell, D. W., Rane, M. J., Joughin, B. A., Kalmukova, R., Hong, J. H., Tidor, B., Dean, W. L., Pierce, W. M., Klein, J. B., Yaffe, M. B. and McLeish, K. R. (2003). Proteomic identification of 14-3-3zeta as a mitogen-activated protein kinase-activated protein kinase 2 substrate: role in dimer formation and ligand binding. Mol Cell Biol *23*, 5376-87.

Powell, D. W., Weaver, C. M., Jennings, J. L., McAfee, K. J., He, Y., Weil, P. A. and Link, A. J. (2004). Cluster analysis of mass spectrometry data reveals a novel component of SAGA. Mol Cell Biol *24*, 7249-59.

Pyronnet, S., Imataka, H., Gingras, A. C., Fukunaga, R., Hunter, T. and Sonenberg, N. (1999). Human eukaryotic translation initiation factor 4G (eIF4G) recruits mnk1 to phosphorylate eIF4E. Embo J *18*, 270-9.

Qoronfleh, M. W. (2006). Role and challenges of proteomics in pharma and biotech: technical, scientific and commercial perspective. Expert Rev Proteomics *3*, 179-95.

Reid, G., Gallais, R. and Metivier, R. (2009). Marking time: the dynamic role of chromatin and covalent modification in transcription. Int J Biochem Cell Biol *41*, 155-63.

Rigaut, G., Shevchenko, A., Rutz, B., Wilm, M., Mann, M. and Seraphin, B. (1999). A generic protein purification method for protein complex characterization and proteome exploration. Nat Biotechnol *17*, 1030-2.

Ross, P. L., Huang, Y. N., Marchese, J. N., Williamson, B., Parker, K., Hattan, S., Khainovski, N., Pillai, S., Dey, S., Daniels, S., Purkayastha, S., Juhasz, P., Martin, S., Bartlet-Jones, M., He, F., Jacobson, A. and Pappin, D. J. (2004). Multiplexed protein quantitation in Saccharomyces cerevisiae using amine-reactive isobaric tagging reagents. Mol Cell Proteomics *3*, 1154-69.

Roth, S. Y., Denu, J. M. and Allis, C. D. (2001). Histone acetyltransferases. Annu Rev Biochem *70*, 81-120.

Rucker, R. B. and McGee, C. (1993). Chemical modifications of proteins in vivo: selected examples important to cellular regulation. J Nutr *123*, 977-90.

Ruggero, D. and Sonenberg, N. (2005). The Akt of translational control. Oncogene *24*, 7426-34.

Rush, J., Moritz, A., Lee, K. A., Guo, A., Goss, V. L., Spek, E. J., Zhang, H., Zha, X. M., Polakiewicz, R. D. and Comb, M. J. (2005). Immunoaffinity profiling of tyrosine phosphorylation in cancer cells. Nat Biotechnol *23*, 94-101.

Sachs, A. and Davis, R. (1990). The poly(A)-binding protein is required for translation initiation and poly(A) tail shortening. Mol Biol Rep *14*, 73.

Sadygov, R. G., Eng, J., Durr, E., Saraf, A., McDonald, H., MacCoss, M. J. and Yates, J. R., 3rd (2002). Code developments to improve the efficiency of automated MS/MS spectra interpretation. J Proteome Res *1*, 211-5.

Sanders, S. L., Jennings, J., Canutescu, A., Link, A. J. and Weil, P. A. (2002). Proteomics of the Eukaryotic Transcription Machinery: Identification of Proteins Associated with Components of Yeast TFIID by Multidimensional Mass Spectrometry. Mol Cell Biol *22*, 4723-38.

Scheper, G. C., Morrice, N. A., Kleijn, M. and Proud, C. G. (2001). The mitogen-activated protein kinase signal-integrating kinase Mnk2 is a eukaryotic initiation factor 4E kinase with high levels of basal activity in mammalian cells. Mol Cell Biol *21*, 743-54.

Schlosser, A. and Lehmann, W. D. (2000). Five-membered ring formation in unimolecular reactions of peptides: a key structural element controlling low-energy collision-induced dissociation of peptides. J Mass Spectrom *35*, 1382-90.

Schmidt, A., Kellermann, J. and Lottspeich, F. (2005). A novel strategy for quantitative proteomics using isotope-coded protein labels. Proteomics *5*, 4-15.

Schroeder, M. J., Shabanowitz, J., Schwartz, J. C., Hunt, D. F. and Coon, J. J. (2004). A neutral loss activation method for improved phosphopeptide sequence analysis by quadrupole ion trap mass spectrometry. Anal Chem *76*, 3590-8.

Schulenberg, B., Aggeler, R., Beechem, J. M., Capaldi, R. A. and Patton, W. F. (2003). Analysis of steady-state protein phosphorylation in mitochondria using a novel fluorescent phosphosensor dye. J Biol Chem *278*, 27251-5.

Schulenberg, B., Beechem, J. M. and Patton, W. F. (2003). Mapping glycosylation changes related to cancer using the Multiplexed Proteomics technology: a protein differential display approach. J Chromatogr B Analyt Technol Biomed Life Sci *793*, 127-39.

Schulenberg, B., Goodman, T. N., Aggeler, R., Capaldi, R. A. and Patton, W. F. (2004). Characterization of dynamic and steady-state protein phosphorylation using a fluorescent phosphoprotein gel stain and mass spectrometry. Electrophoresis *25*, 2526-32.

Scigelova, M. and Makarov, A. (2006). Orbitrap mass analyzer--overview and applications in proteomics. Proteomics *6 Suppl 2*, 16-21.

Shmulevitz, M., Marcato, P. and Lee, P. W. (2005). Unshackling the links between reovirus oncolysis, Ras signaling, translational control and cancer. Oncogene *24*, 7720-8.

Singh, C. R., Curtis, C., Yamamoto, Y., Hall, N. S., Kruse, D. S., He, H., Hannig, E. M. and Asano, K. (2005). Eukaryotic translation initiation factor 5 is critical for integrity of the scanning preinitiation complex and accurate control of GCN4 translation. Mol Cell Biol *25*, 5480-91.

Sirard, J. C., Vignal, C., Dessein, R. and Chamaillard, M. (2007). Nod-like receptors: cytosolic watchdogs for immunity against pathogens. PLoS Pathog *3*, e152.

Sonenberg, N. (1997). Research on mRNA translation into protein. Methods *11*, 331.

Song, H., Mugnier, P., Das, A. K., Webb, H. M., Evans, D. R., Tuite, M. F., Hemmings, B. A. and Barford, D. (2000). The crystal structure of human eukaryotic release factor eRF1--mechanism of stop codon recognition and peptidyl-tRNA hydrolysis. Cell *100*, 311-21.

Soufi, B., Gnad, F., Jensen, P. R., Petranovic, D., Mann, M., Mijakovic, I. and Macek, B. (2008). The Ser/Thr/Tyr phosphoproteome of Lactococcus lactis IL1403 reveals multiply phosphorylated proteins. Proteomics *8*, 3486-93.

Steinberg, T. H., Agnew, B. J., Gee, K. R., Leung, W. Y., Goodman, T., Schulenberg, B., Hendrickson, J., Beechem, J. M., Haugland, R. P. and Patton, W. F. (2003). Global quantitative phosphoprotein analysis using Multiplexed Proteomics technology. Proteomics *3*, 1128-44.

Steinberg, T. H., Pretty On Top, K., Berggren, K. N., Kemper, C., Jones, L., Diwu, Z., Haugland, R. P. and Patton, W. F. (2001). Rapid and simple single nanogram detection of glycoproteins in polyacrylamide gels and on electroblots. Proteomics *1*, 841-55.

Strahl, B. D. and Allis, C. D. (2000). The language of covalent histone modifications. Nature *403*, 41-5.

Sudhakar, A., Ramachandran, A., Ghosh, S., Hasnain, S. E., Kaufman, R. J. and Ramaiah, K. V. (2000). Phosphorylation of serine 51 in initiation factor 2 alpha (eIF2 alpha) promotes complex formation between eIF2 alpha(P) and eIF2B and causes inhibition in the guanine nucleotide exchange activity of eIF2B. Biochemistry *39*, 12929-38.

Sutton, M. A. and Schuman, E. M. (2005). Local translational control in dendrites and its role in long-term synaptic plasticity. J Neurobiol *64*, 116-31.

Swaney, D. L., McAlister, G. C. and Coon, J. J. (2008). Decision tree-driven tandem mass spectrometry for shotgun proteomics. Nat Methods *5*, 959-64.

Swaney, D. L., McAlister, G. C., Wirtala, M., Schwartz, J. C., Syka, J. E. and Coon, J. J. (2007). Supplemental activation method for high-efficiency electron-transfer dissociation of doubly protonated peptide precursors. Anal Chem *79*, 477-85.

Syka, J. E., Coon, J. J., Schroeder, M. J., Shabanowitz, J. and Hunt, D. F. (2004). Peptide and protein sequence analysis by electron transfer dissociation mass spectrometry. Proc Natl Acad Sci U S A *101*, 9528-33.

Sykora, C., Hoffmann, R. and Hoffmann, P. (2007). Enrichment of multiphosphorylated peptides by immobilized metal affinity chromatography using Ga(III)- and Fe(III)-complexes. Protein Pept Lett *14*, 489-96.

Taniguchi, C. M., Emanuelli, B. and Kahn, C. R. (2006). Critical nodes in signalling pathways: insights into insulin action. Nat Rev Mol Cell Biol *7*, 85-96.

Tarun, S. Z., Jr. and Sachs, A. B. (1996). Association of the yeast poly(A) tail binding protein with translation initiation factor eIF-4G. Embo J *15*, 7168-77.

Tee, A. R. and Blenis, J. (2005). mTOR, translational control and human disease. Semin Cell Dev Biol *16*, 29-37.

Thingholm, T. E., Jorgensen, T. J., Jensen, O. N. and Larsen, M. R. (2006). Highly selective enrichment of phosphorylated peptides using titanium dioxide. Nat Protoc *1*, 1929-35.

Thompson, A., Schafer, J., Kuhn, K., Kienle, S., Schwarz, J., Schmidt, G., Neumann, T., Johnstone, R., Mohammed, A. K. and Hamon, C. (2003). Tandem mass tags: a novel quantification strategy for comparative analysis of complex protein mixtures by MS/MS. Anal Chem *75*, 1895-904.

Tsaprailis, G., Nair, H., Somogyi, A., Wysocki, V. H., Zhong, W., Futrell, J. H., Summerfield, S. G. and Gaskell, S. J. (1999). Influence of secondary structure on the fragmentation of protonated peptides. J. Am. Chem. Soc. *121*, 5142-5154.

Udeshi, N. D., Shabanowitz, J., Hunt, D. F. and Rose, K. L. (2007). Analysis of proteins and peptides on a chromatographic timescale by electron-transfer dissociation MS. Febs J *274*, 6269-76.

Ulintz, P. J., Yocum, A. K., Bodenmiller, B., Aebersold, R., Andrews, P. C. and Nesvizhskii, A. I. (2009). Comparison of MS(2)-only, MSA, and MS(2)/MS(3) methodologies for phosphopeptide identification. J Proteome Res *8*, 887-99.

Unbehaun, A., Borukhov, S. I., Hellen, C. U. and Pestova, T. V. (2004). Release of initiation factors from 48S complexes during ribosomal subunit joining and the link between establishment of codon-anticodon base-pairing and hydrolysis of eIF2-bound GTP. Genes Dev *18*, 3078-93.

Valasek, L., Hasek, J., Nielsen, K. H. and Hinnebusch, A. G. (2001). Dual function of eIF3j/Hcr1p in processing 20 S pre-rRNA and translation initiation. J Biol Chem *276*, 43351-60.

Valasek, L., Hasek, J., Trachsel, H., Imre, E. M. and Ruis, H. (1999). The Saccharomyces cerevisiae HCR1 gene encoding a homologue of the p35

subunit of human translation initiation factor 3 (eIF3) is a high copy suppressor of a temperature-sensitive mutation in the Rpg1p subunit of yeast eIF3. J Biol Chem *274*, 27567-72.

Valasek, L., Mathew, A. A., Shin, B. S., Nielsen, K. H., Szamecz, B. and Hinnebusch, A. G. (2003). The yeast eIF3 subunits TIF32/a, NIP1/c, and eIF5 make critical connections with the 40S ribosome in vivo. Genes Dev *17*, 786-99.

Valasek, L., Nielsen, K. H. and Hinnebusch, A. G. (2002). Direct eIF2-eIF3 contact in the multifactor complex is important for translation initiation in vivo. Embo J *21*, 5886-98.

Valasek, L., Nielsen, K. H., Zhang, F., Fekete, C. A. and Hinnebusch, A. G. (2004). Interactions of eukaryotic translation initiation factor 3 (eIF3) subunit NIP1/c with eIF1 and eIF5 promote preinitiation complex assembly and regulate start codon selection. Mol Cell Biol *24*, 9437-55.

Valasek, L., Phan, L., Schoenfeld, L. W., Valaskova, V. and Hinnebusch, A. G. (2001). Related eIF3 subunits TIF32 and HCR1 interact with an RNA recognition motif in PRT1 required for eIF3 integrity and ribosome binding. Embo J *20*, 891-904.

Van Der Kelen, K., Beyaert, R., Inze, D. and De Veylder, L. (2009). Translational control of eukaryotic gene expression. Crit Rev Biochem Mol Biol *44*, 143-68.

Washburn, M. P., Wolters, D. and Yates, J. R., 3rd (2001). Large-scale analysis of the yeast proteome by multidimensional protein identification technology. Nat Biotechnol *19*, 242-7.

Waskiewicz, A. J., Johnson, J. C., Penn, B., Mahalingam, M., Kimball, S. R. and Cooper, J. A. (1999). Phosphorylation of the cap-binding protein eukaryotic translation initiation factor 4E by protein kinase Mnk1 in vivo. Mol Cell Biol *19*, 1871-80.

White, F. M. (2008). Quantitative phosphoproteomic analysis of signaling network dynamics. Curr Opin Biotechnol *19*, 404-9.

Wilkins, M. R., Pasquali, C., Appel, R. D., Ou, K., Golaz, O., Sanchez, J. C., Yan, J. X., Gooley, A. A., Hughes, G., Humphery-Smith, I., Williams, K. L. and Hochstrasser, D. F. (1996). From proteins to proteomes: large scale protein identification by two- dimensional electrophoresis and amino acid analysis. Biotechnology (N Y) *14*, 61-5.

Witze, E. S., Old, W. M., Resing, K. A. and Ahn, N. G. (2007). Mapping protein post-translational modifications with mass spectrometry. Nat Methods *4*, 798-806.

Wysocki, V. H., Tsaprailis, G., Smith, L. L. and Breci, L. A. (2000). Mobile and localized protons: a framework for understanding peptide dissociation. J Mass Spectrom *35*, 1399-406.

Yang, F., Wu, S., Stenoien, D. L., Zhao, R., Monroe, M. E., Gritsenko, M. A., Purvine, S. O., Polpitiya, A. D., Tolic, N., Zhang, Q., Norbeck, A. D., Orton, D. J., Moore, R. J., Tang, K., Anderson, G. A., Pasa-Tolic, L., Camp, D. G., 2nd and Smith, R. D. (2009). Combined pulsed-Q dissociation and electron transfer dissociation for identification and quantification of iTRAQ-labeled phosphopeptides. Anal Chem *81*, 4137-43.

Yates, J. R., 3rd, Eng, J. K. and McCormack, A. L. (1995). Mining genomes: correlating tandem mass spectra of modified and unmodified peptides to sequences in nucleotide databases. Anal Chem *67*, 3202-10.

Zanchin, N. I. and McCarthy, J. E. (1995). Characterization of the in vivo phosphorylation sites of the mRNA.cap-binding complex proteins eukaryotic initiation factor-4E and p20 in Saccharomyces cerevisiae. J Biol Chem *270*, 26505-10.

Zappacosta, F., Collingwood, T. S., Huddleston, M. J. and Annan, R. S. (2006). A quantitative results-driven approach to analyzing multisite protein phosphorylation: the phosphate-dependent phosphorylation profile of the transcription factor Pho4. Mol Cell Proteomics *5*, 2019-30.

Zhang, H., Li, X. J., Martin, D. B. and Aebersold, R. (2003). Identification and quantification of N-linked glycoproteins using hydrazide chemistry, stable isotope labeling and mass spectrometry. Nat Biotechnol *21*, 660-6.

Zhang, K., Williams, K. E., Huang, L., Yau, P., Siino, J. S., Bradbury, E. M., Jones, P. R., Minch, M. J. and Burlingame, A. L. (2002). Histone acetylation and deacetylation: identification of acetylation and methylation sites of HeLa histone H4 by mass spectrometry. Mol Cell Proteomics *1*, 500-8.

Zhang, K., Yau, P. M., Chandrasekhar, B., New, R., Kondrat, R., Imai, B. S. and Bradbury, M. E. (2004). Differentiation between peptides containing acetylated or tri-methylated lysines by mass spectrometry: an application for determining lysine 9 acetylation and methylation of histone H3. Proteomics *4*, 1-10.

Zhang, L., Jiang, J., Arellano, M., Yan, X., Wong, D. T. and Hu, S. (2008). Quantification of Serum Proteins of Metastatic Oral Cancer Patients Using LC-MS/MS and iTRAQ Labeling. Open Proteomics J *1*, 72-78.

Zhang, R. and Regnier, F. E. (2002). Minimizing resolution of isotopically coded peptides in comparative proteomics. J Proteome Res *1*, 139-47.

Zhang, Y., Wolf-Yadlin, A., Ross, P. L., Pappin, D. J., Rush, J., Lauffenburger, D. A. and White, F. M. (2005). Time-resolved mass spectrometry of tyrosine phosphorylation sites in the epidermal growth factor receptor signaling network reveals dynamic modules. Mol Cell Proteomics *4*, 1240-50.

Zhen, Y., Xu, N., Richardson, B., Becklin, R., Savage, J. R., Blake, K. and Peltier, J. M. (2004). Development of an LC-MALDI method for the analysis of protein complexes. J Am Soc Mass Spectrom *15*, 803-22.

Zhou, F. and Johnston, M. V. (2004). Protein characterization by on-line capillary isoelectric focusing, reversed-phase liquid chromatography, and mass spectrometry. Anal Chem *76*, 2734-40.